STUDIA

UNIVERSITATIS BABEŞ-BOLYAI

CHEMIA

1

1986

CLUJ-NAPOCA

ANUL XXXI 1986

STUDIA

UNIVERSITATIS BABEŞ-BOLYAI

CHEMIA

1

Redacţia: 3400 CLUJ-NAPOCA, str. M. Kogălniceanu, 1 ● Telefon 1 61 01

SUMAR — CONTENTS — SOMMAIRE — INHALT

Cronică — Cronicle — Chronique — Chronik

Recenzii — Book Reviews — Comptes rendus — Buchbesprechungen

STUDIA UNIV. BABEŞ—BOLYAI, CHEMIA, XXXI, 1, 1986

SEPARATION OF p-NITROPHENOL FROM o-NITROPHENOL THROUGH MOLECULAR COMPLEX FORMATION WITH HEXAMETHYLENETETRAMINE

MARIA VAGAONESCU*, ION COCREAN, LETIŢIA GHIZDAVU* and ANIKÓ TATÁR***

Received: Aprili 16, 1984

ABSTRACT. — Separation of p-nitrophenol from its o-isomer by complexation with hexamethylelenetetramine, followed by acid splitting of the obtained molecular complex. A thermogravimetric analysis on the complex is also undertaken.

In previous papers the molecular complexes of nitrophenols with hexamethylenetetramine (HMT) have been studied [1, 2, 3].

The fact that p-nitrophenol (pNP) in contrast with o-nitrophenol (oNP) forms with HMT a stable molecular complex, which can be isolated [1], enabled us to separate pNP from the mixture with its isomer, oNP [4]. In the present paper we have followed the formation of this molecular complex as well as its splitting in components.

The experimental data have led us to conclude that the molecular complex formation and its decomposition practically occur quantitative ($\mu = 99\%$). The separation of pNP from its isomer has been carried out by steam distillation of oNP, followed by molecular complex formation with HMT and by its splitting in components. As the mixture of pNP and oNP, obtained by phenol nitration, is usually in acid medium, we have followed the separation at acid pH. From the experimental data a maximum yield (95%) results, in separating pNP at pH=3. After nitration of phenol under literature mentioned conditions [5], the oNP has been separated by steam distillation, and then the pNP — by adding HMT and splitting the formed molecular complex with 2N hydrochloric acid. Two ways for separation and purification of pNP, after steam distillation of oNP, are mentioned [6]. One method is based on the natrium salt formation of pNP and then separation by acidifying with hydrochloric acid. As mentioned, it is not advisable to treat the crude pNP with natrium hydroxide solution because alkali causes extensive resinification. The other way of separating pNP consists in cooling the residue of pNP, after steam distillation of oNP, in ice for 2.5 hours. Then the crude pNP is boiled with 2% hydrochloric acid together with decolourising charcoal, for 10 minutes. After a new filtration the filtrate is allowed to crystallise overnight and the pure pNP is

* *University of Cluj-Napoca, Faculty of Chemical Technology, Department of Physical, Organic, and Technologic Chemistry, 3400 Cluj-Napoca, Romania*
** *Enterprise „Vidra" — Orăştie, Alba County, Romania*

obtained. Although this method yields pure pNP, it presents the disadvantage to be hard-working and it takes too much time.

In our method of separating pNP through complex formation, the working time has been much reduced, from 24 h to 30 min.

From analytical and IR spectral data of the molecular complex of pNP with HMT a molar ratio 2:1 (pNP : HMT) and a hydrogen bonding (H.b.) structure results [2]:

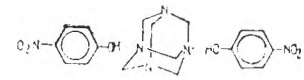

the molecular complex HMT-dipNP.

In order to get more information concerning the structure of this complex and its thermal behaviour, a thermal analysis for the complex and its components has been carried out. The thermal analysis has been achieved in the temperature range of 20°—1000°C. The recorded thermal curves point out chemical modifications accompanied by weight loss in the TG and DTG curves, as well as physical transformations such as the melting point of the complex and of the components. The recorded thermal curves of the complex (Fig. 1) of pNP and HMT show, on the differential curve, an endothermic effect, corresponding to the melting of the studied compounds, followed by endo- and exothermic effects, due to the thermal decomposition reactions in the components and to the final pyrrolysis (Tab. 1). It is noticed that the recorded derivative thermogravimetric curve for HMT does not show the endothermic effect corresponding to melting, because as it s nown, HMT decomposes without melting. The thermal stability of the studied compounds, determined through temperature t_d, at which the first decomposition reaction begins, is shown in Table 2.

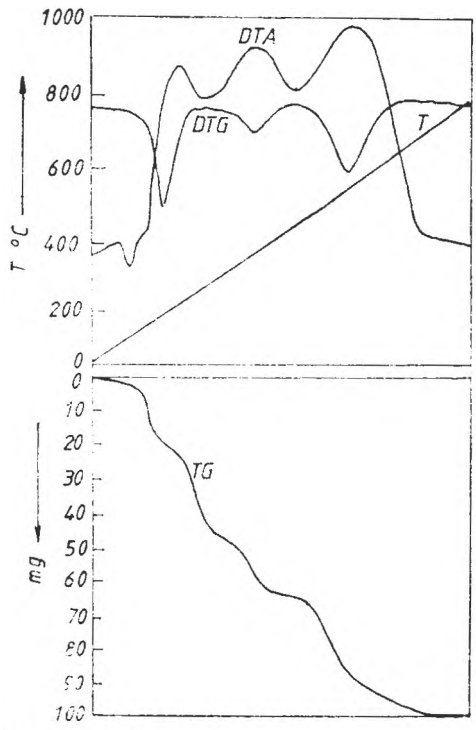

Fig. 1. The thermal curves of complex HMT-dipNP at a heating rate of 14°/min

Kinetic parameters have been determined for the first decomposition process (Table 2) after chemical equation:

$$\left.\begin{matrix} O_2N-C_6H_4-OH \\ O_2N-C_6H_4-OH \end{matrix}\right\rangle N_4(CH_2)_6 \rightarrow$$

$$\rightarrow 2HOC_6H_4NO_2 + (CH_2)_6N_4$$

Table 1

Temperatures (K) of DTA peaks and melting of the compounds

Samples	Melting temperature*	Temperature of DTA peaks	
		endothermic	exother.
pNP	386	533 ; 648	753 ; 831
HMT	—	471 ; 573	793
complex	414	453 ; 506 ; 698	593 ; 843

* As reported in the literature [7]

Table 2

The thermal stability and kinetic parameters for first decomposition process of the compounds

Nr.	Compound	t_d K	E_a kJ·mol^{-1}	n
1	complex	435	215.45	2.15
2	pNP	463	201.13	2.50
3	HMT	450	162.82	1.33

using the Freeman-Carroll method [6], based on the relation :

$$\Delta \lg \frac{dW_t}{dt} = n\Delta \lg W_r - \frac{E_a}{2{,}303\,R} \cdot \Delta\left(\frac{1}{T}\right)$$

where :

W_t — weight loss at the t moment $= W_\infty - W_r$;
W_∞ — weight loss at the end of the reaction ;
W_r — the quantity of residual substance at the t moment ;

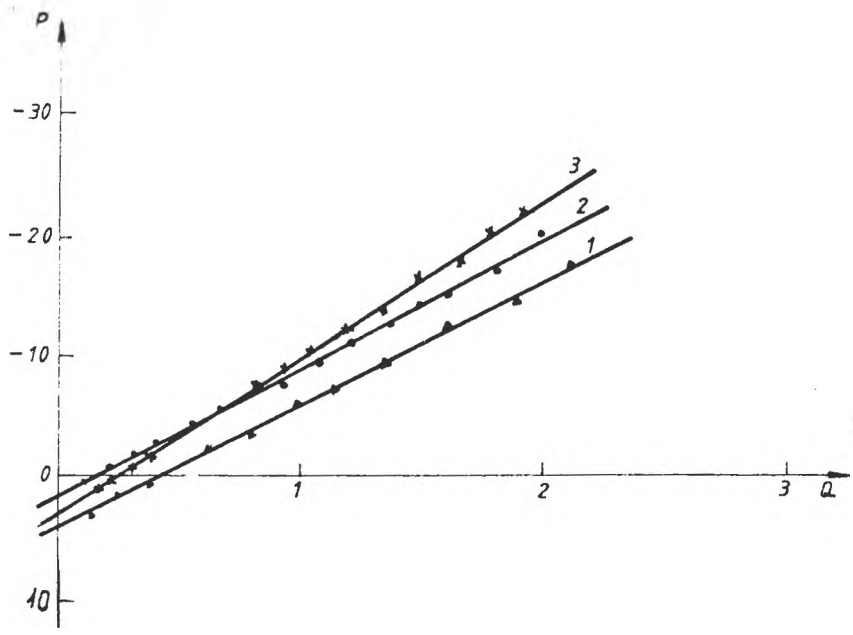

Fig. 2. Kinetic of thermal decomposition : 1 — complex ; 2 — pNP ;3 — HMT

$\frac{dW_t}{dt}$ — reaction velocity;

E_a — activation energy;

T — absolute temperature.

From the Freeman-Carroll graph representing $P = -\frac{\Delta \lg W_t}{\Delta \lg W_r}$ versus $Q = \frac{\Delta(T^{-1}) \cdot 10^3}{\Delta \lg W_r}$, $E_a = 4{,}575 \cdot \operatorname{tg} \alpha$ and n which is the origin ordinate (Fig. 2) have been determined.

The higher value of E_a for the complex as compared to that of pNP can be explained through the thermal decomposition of the complex, which first includes the H.b. splitting, followed by the HMT decomposition [7]. This statement may be proved through the weight loss value, of 34.5%, in agreement with the theoretical participation of HMT at the complex formation. It is to be mentioned that the heterogeneous kinetics is only a formal application of the homogeneous kinetics, namely E_a and n do not represent the real values in the classic kinetics, but only the apparent values which do characterise the thermal decomposition process.

Conclusions. 1. Separation of pNP from a mixture with oNP has been achieved by means of molecular complex formation with HMT.

2. The formation of the complex and its splitting in components practically occur quantitative.

3. The proposed separation method presents the following advantages: it reduces working-time, avoids resinous compound formation by using HMT, instead of NaOH, and it leads to yielding pure pNP.

4. Thermal analysis investigations of the complex and its components point to their thermal stability as well as their kinetic parameters.

Experimental. *Preparation of molecular complex HMT-dipNP.* 0.5 g of pNP and 0.5 g HMT with 1 ml H_2O are heated on water bath for 30 min. After cooling, the crystallised pNP is filtered through a G_3 filtrant crucible, then it is dried and weighed. The yield of the complex is 0.7425 g ($\mu = 99\%$) and it melts at 138—140°C.

Splitting of molecular complex. The complex is boiled with 2N hydrochloric acid, it is filtered and the solution is cooled. The crystallysed pNP is filtered through a G_3 crucible and after drying it is weighed ($\mu = 99\%$).

Separation of a mixture of pure oNP and pNP. To a mixture formed of 2 g pure oNP and 2 g pure pNP dil. HNO_3 is added until pH = 3. The oNP is separated by steam distillation and to the remaining solution, which contains pNP, 1,5 g HMT is added. The formed complex is isolated by filtration, then it is boiled with 2N HCl and, after cooling, the pure pNP crystallyses. The yield in pNP is 1,90g ($\mu = 95\%$).

REFERENCES

1. M. Vagaonescu, M. Ionescu, *Rev. Roumaine Chim.*, **16**, 105 (1971).
2. M. Vagaonescu, S. Mager, L. Munteanu, *Rev. Roumaine Chim.*, **23**,, 63 (1978).
3. M. Vagaonescu, L. Stoicescu, L. Aldea Pomărac, *Stud. Univ. Babeş—Bolyai, Chem.*, **25**, (2), 66 (1980).
4. M. Ionescu, M. Vagaonescu, R.S.R. Pat., 60505 (1965).
5. A. I. Vogel, *„Practical Organic Chemistry"*, Longmans Green and Co LTD, London, 1964,p. 665, 677.
6. E. S. Freeman, B. Carroll, *J. Phys. Chem.*, **62**, 394 (1958).
7. V. K. Pogorelîi, *Uspekhi Khim.*, **XLVI**, 602 (1977).

STUDIA UNIV. BABEŞ—BOLYAI, CHEMIA, XXXI, 1, 1986

CYCLIC VOLTAMMETRY OF THE $K_3[Fe(CN)_6]/K_4[Fe(CN)_6]$ SYSTEM AT SnO_2 ELECTRODES

LADISLAU KÉKEDY* and FIAMETTA KORMOS**

Received: May 24, 1985

ABSTRACT. — Electroanalytical chemists show an ever growing interest in doped tin oxide films as electrode materials due to their favourable properties. The present paper deals with study of the reversibility of $K_3[Fe(CN)_6]/K_4[Fe(CN)_6]$ (further Feic/Feoc) system at SnO_2 electrodes as a function of doping level (Sb^{3+} 1.7; 4.4 and 7 mole %, respectively, in the spray solution used for preparation of the SnO_2 film) and of pretreatment of the electrodes. It has been stated by cyclic voltammetry that reversibility of the system increases with the increase of the number of charge carriers in the electrode film, as well as with concentration of the depolarizer. Pretreatment with conc. HNO_3 increased the reversibility, too.

The Feic/Feoc redox couple has been extensively investigated, being a monoelectronic fast system. Voltammetric studies showed that the system is reversible at Pt [1—5], Au [3—4] and at vitreous carbon [6] electrodes, respectively, but at B_4C_3 [4] and graphite [5] electrodes it is only quasireversible. Literature data indicate that at SnO_2 electrodes [5,7—9] both reversible and quasireversible behaviour has been observed, depending on concentration of the redox couple and the metod of investigation used (Table 1). The present cyclic vol-

Table 1

Kinetic parameters of the Feic/Feoc system at different electrodes

Electrode	Experimental method	Concentr. of the redox syst.	Supporting electrolyte	k cm/s	α	Bibliography
Pt, wire			KCl 1 M	8×10^{-3}	0.50	1
Pt, rotating disc	voltammetry	10^{-3} M	KCl 1 M	5×10^{-3}	0.60	2
Pt, Au, wire	voltammetry	5 mM	K_2SO_4 0.5 M	2×10^{-3}	0.50	3
Pt, Au, tubular	voltammetry	0.1 mM	phosphate 0.1 M	1.4×10^{-2}	0.40	4
Pt, rotating disc	voltammetry	0.5 mM	$NaClO_4$ 1 M	1.3×10^{-2}	0.50	5
graphite, rot. disc	voltammetry	0.5 mM	$NaClO_4$ 1 M	5.8×10^{-4}	0.47	5
B_4C_3, rot. disc	voltammetry	0.1 mM	phosphate 0.1 M	3.3×10^{-4}	0.65	4
glassy carbon	voltammetry	0.1 μM	phosphate 0.1 M	5×10^{-3}	0.69	6
SnO_2 plate	chronopotentiom.	0.2 M	KCl 1 M	reversible		8
SnO_2 plate	chronopotentiom.		KCl 0.16 M	reversible		7
SnO_2 plate	spectroelectrochem.	5 mM	pH = 7	4.6×10^{-4}	0.32	9
SnO_2 plate	chronocoulom.	5 mM	pH = 7	4×10^{-4}	0.32	9
SnO_2, rot. nisc	voltammetry	0.5 mM	$NaClO_4$ 1 M	1.7×10^{-3}	0.31	5

* University of Cluj-Napoca, Department of Inorganic and Analytical Chemistry, 3400 Cluj-Napoca, Romania
** Institute of Chemistry, 3400 Cluj-Napoca, Romania

tammetric study deals with influence of the doping level and petreatment of SnO_2 film on the reversibility of the Feic/Feoc system at SnO_2 electrode.

Experimental. The experimental setup is represented in Fig. 1. It consists of a potentiostat (1), a variable resistor (2), an electrochemical cell with a cylindrical stationary working electrode (r = = 0.15 cm; l = 0.5 cm), a Pt auxiliary electrode (4) and a SCE reference electrode (5), of an XY recorder (7) and a digital millivoltmeter (3). Cyclic voltammograms of air-free 1×10^{-2}; 5×10^{-3} and $1 \cdot 10^{-3}$ M $K_3[Fe(CN)_6]$ solutions in 10^{-1} M KCl supporting electrolyte have been recorded. Analytical grade reagents and bidistilled water were used. A symmetrical triangular potential sweep between −1.0 and +1.0 volts vs. ESC was applied. Different sweep rates (v) were used, the potential sweep being reversed automatically. Differently doped (with Sb^{3+}) SnO_2 working electrodes were used, namely: I: with 1.7% Sb^{3+}; II: with 4,4% Sb^{3+}, and III: with 7.0% Sb^{3+} (in mole % of the spray solutions used for the preparation of the SnO_2 film). Two differently pretreated electrode types were used: electrodes I and II were dipped in conc. HNO_3 for 60 s; other two electrodes I and II were soaked with a $FeSO_4$ solution (0.5 M in 2 N H_2SO_4) for 60 s.

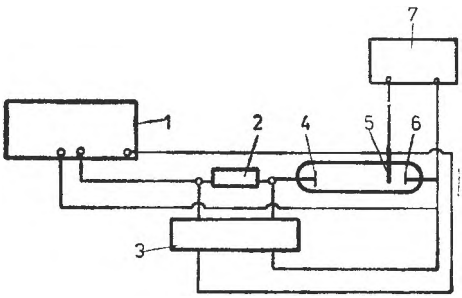

Fig. 1. Scheme of equipment used for cyclic voltammetry.

Results and Discussion. The current values observed were corrected for the residual current, the potential values for the ohmic potential drop ($\pm iR$) through the cell [10, 11]. The residual current was determined considering the cyclic voltammogram in 0.1M KCl solution. The cell resistance was determined by the method of Kuwana [7]. The degree of reversibility of the electrode process was estimated considering the following criteria: a) The $E_{p_a} - E_{p_c}$ difference on the cyclic voltammograms [11, 12], E_{p_a} being the anodic peak potential, E_{p_a} the cathodic one, according to the theory, in the case of a monoelectronic reversible reaction $E_{p_a} - E_{p_c} = 68$ mV; b) The value of the ratio i'_{p_a}/i'_{p_c} [13]:

$$\frac{i'_{p_a}}{i'_{p_c}} = \frac{i_{p_a}}{i_{p_c}} + \frac{0.485\, i_{sw}}{i_{p_c}} + 0.086 \qquad (1)$$

where i_{p_a} and i_{p_c} are the anodic and the cathodic peak currents, i_{sw} is the current value at the potential sweep reversal. In the case of reversible processes the value of the ratio i'_{p_a}/i'_{p_c} is equal to unity or near it, regardless of the value of the potential sweep; c) Considering the value of the heterogeneous rate constant (k), a system is considered as being reversible if $k > 10^{-3}$ cm/s, and an irreversible one, if $k < 10^{-3}$ cm/s. In our case k has been calculated considering the equation of the peak current [14]:

$$i_p = 0.227nFAC_0k \exp(-\alpha nF/RT)\,(E_p - E^\circ) \qquad (2)$$

n being the number of electrons associated with the electrode reaction, F is the faraday, A the electrode area, C_0 the concentration of the depolarizer, E_p the peak potential, E° the formal redox potential of the system, α the transfer

coefficient. According to Nicholson [15], equation (2) is valid for cylindrical electrodes, too, if the condition:

$$D/tr^2 \leqslant 3 \cdot 10^{-3} \tag{3}$$

is fulfilled, where D is the diffusion coefficient of the depolarizer, t the duration of the electrolysis, r the electrode radius. In the case of the cylindrical SnO_2 electrode used by us, the corresponding values were: $r = 0.15$ cm; $t = 120$ s, and $D = 7.26 \times 10^{-6}$ cm^2s^{-1} [16], thus $D/tr^2 = 1.3 \times 10^{-6}$, condition (3) being satisfied. α and k were calculated from the plot of $\log i_{p_c}/0.227nFAC_0$ vs. $0.43(E_p - E^\circ)$. The slope of the straight line obtained is equal to $\alpha nF/RT$, and the intercept with lg k.

1. *The influence of the doping level.* The characteristic parameters of the electrode reversibility in accordance with the above mentioned criteria have been calculated from the cyclic voltammograms (Figs. 2, 3, 4). It has been stated

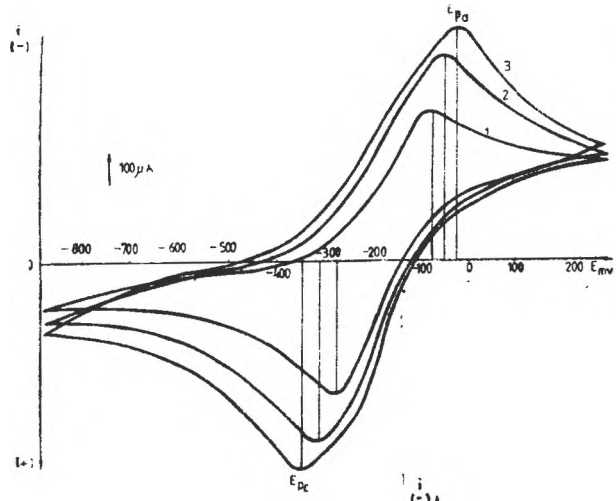

Fig. 2. Cyclic voltammetry of 10^{-2} M Feic in 10^{-1} M KCl at SnO_2 II electrode. Sweep rates (mV/s): 1—13; 2—25; 3—38

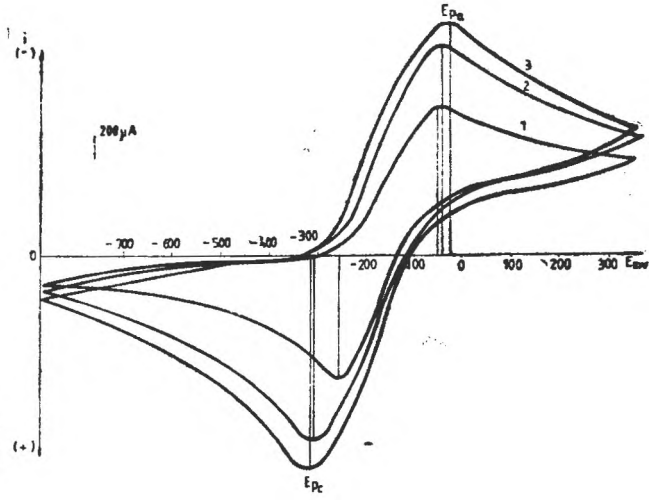

Fig. 3. Cyclic voltammetry of 5×10^{-3} M Feic in 10^{-1} M KCl at SnO_2 II electrode. Sweep rates (mV/S): 1—17; 2—30; 3—38

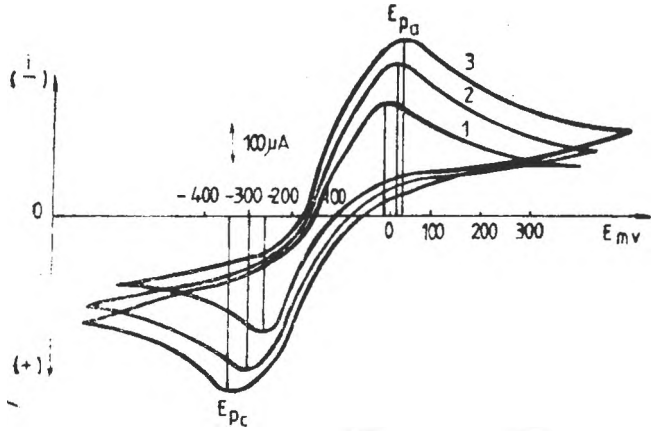

Fig. 4. Cyclic voltammetry of 10^{-3} M Feic in 10^{-1} M KCl at SnO_2 II electrode. Sweep rates (mV/s): 1—10; 2—23; 3—37

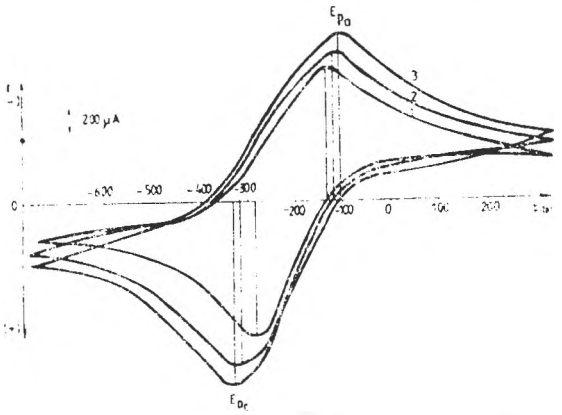

Fig. 5. Cyclic voltammetry of 10^{-3} M Feic in 10^{-1} M KCl at SnO_2 II electrode pretreated with conc. HNO_3. Sweep rates (mV/s): 1—16; 2—28; 3—37

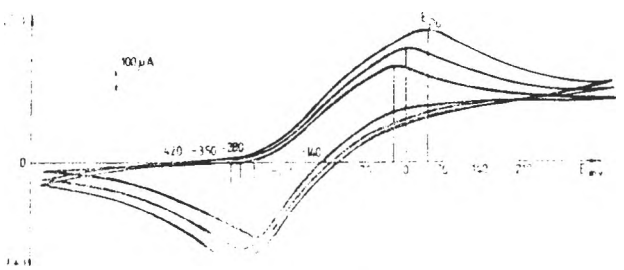

Fig. 6. Cyclic voltammetry of 10^{-3} M Feic in 10^{-1} M KCl at SnO_2 II electrode pretreated with $FeSO_4$. Sweep rates (mV/s): 1—20; 2—27; 3—37

that, at constant doping level, the potential differences $E_{p_a} - E_{p_c}$ increase with the decrease of concentration of the depolarizer, indicating an increased reversibility of the system. According to Elliot and coworkers [8] the reversibility can be correlated with the number of charge carriers in the SnO_2 film so that if this number is higher than $10^{21}/cm^3$ the electrode process is reversible. If the number of the charge carriers is about 10^{19}—$10^{20}/cm^3$, the electrode process is less reversible, and below 10^{18} carriers/cm^3 it is quite irreversible. The same conclusion can be drawn from the values of the ratio i'_{p_a}/i'_{p_c}, which approaches to unity only in the case of electrode SnO_2 (see Table 2) and if the concentration of the Feic was 10^{-2} M. The values of the rate constants account for a quasireversible process in all cases, except when electrode SnO_2 II was used and 10^{-2}M Feic, when the system behaved as reversible.

2. The influence of the pretreatment. The characteristic data calculated from the cyclic voltammograms (Figs. 5, 6) recorded with SnO_2 electrodes pretreated

Table 2

Characteristic parameters of the reduction of Feic of different concentrations at SnO_2 electrodes

C mol/l	SnO_2 film type	V mV/sec	$E_{p_a} - E_{p_c}$ mV	$i'_{p_a} - i'_{p_c}$	k cm/sec	α
10^{-2}	I	39	200	1,32	$3,5 \cdot 10^{-4}$	0,43
		34	180	1,37		
		26	167	1,31		
	II	38	55	1,13	10^{-3}	0,60
		25	55	1,14		
		13	50	1,06		
	III	39	404	2,68	$2,8 \cdot 10^{-5}$	0,70
		25	408	2,80		
		13	356	3,08		
$5 \cdot 10^{-3}$	I	38	300	1,25	$7 \cdot 10^{-5}$	0,62
		30	288	1,24		
		22	290	1,22		
	II	38	200	1,34	$8,9 \cdot 10^{-4}$	0,58
		30	165	1,36		
		17	132	1,41		
10^{-3}	I	38	332	1,28	$5 \cdot 10^{-5}$	0,75
		26	315	1,30		
		15	267	1,31		
	II	37	280	1,35	$6,4 \cdot 10^{-4}$	0,72
		23	270	1,29		
		10	200	1,28		

with conc. HNO_3 or $FeSO_4$ are summarized in Table 3. From these data it can be seen that in the case of the electrodes pretreated with cc. HNO_3 the $E_{p_a} - E_{p_c}$ differences were below 68 mV, the values of the ratio i'_{p_a}/i'_{p_c} approached much to unity, and the values of the rate constants were greater than 10^{-3} cm/s, all indicating the reversibility of the process. Consequently, the pretreatment

Table 3

Characteristic parameters of the reduction of 10^{-2} M Feic at pretreated SnO_2 electrodes

Pretreatment	SnO_2 film type	V mV/sec	$E_{p_a} - E_{p_c}$ mV	i'_{p_a}/i'_{p_c}	k cm/sec	α
HNO_3	I	39	36	1,17	10^{-3}	0,53
		30	25	1,13		
		17	1	1,10		
	II	37	43	1,15	$5 \cdot 10^{-3}$	0,45
		28	25	1,10		
		16	5	1,05		
$FeSO_4$	I	36	270	1,60	$8 \cdot 10^{-5}$	0,70
		26	256	1,54		
		17	240	1,53		
	II	37	288	1,51	$4,5 \cdot 10^{-4}$	0,53
		27	250	1,43		
		20	202	1,36		

with HNO_3 increased the reversibility both at electrodes SnO_2 II and SnO_2 I. On the contrary, the pretreatment with $FeSO_4$ yielded a decrease in reversibility.

In conclusion, the Feic/Feoc system at stationary, cylindrical SnO_2 electrodes behaved as quasireversible in accordance with the literature data. The degree of reversibility increased with the increase of the concentration of the depolarizer, the number of charge carriers in the SnO_2 film, as well as with the pretreatment with HNO_3.

REFERENCES

1. J. Jordan, R. A. Jawick, *Electrochim, Acta*, **6**, 22 (1962).
2. W. Vielstich, D. Jahn, *J. Electrochim. Soc.*, **109**, 849 (1962).
3. D. H. Angell, T. Dickinson, *J. Electroanal. Chem.*, **35**, 55 (1972).
4. W. J. Bladel, G. W. Schieffer, *J. Electroanal. Chem.*, **80**, 259 (1977).
5. K. H. Heckner, I.F. Müller, Z. *Phys Chem.*, **261**, 585 (1980).
6. W. J. Bladel, R. C. Engstrom, *Analyt. Chem.*, **50**, 476 (1978).
7. T. Kuwana, R.K. Darlington, D. W. Leedy, *Analyt. Chem.*, **36**, 2023 (1964).
8. O. Elliot, O.L. Zellmer, H. A. Laitinen, *J. Electrochem. Soc.*, **117**, 1343 (1970).
9. D. E. Albertson, H. N. Blount, *Analyt. Chem.*, **51**, 556 (1979).
10. H. A. Laitinen, W. J. Subcasky, *J. Amer. Chem. Soc.*, **80**, 2623 (1958).
11. Z. Kublik, *J. Electroanal. Chem.*, **5**, 450 (1963).
12. P. Frankental, I. Shain, *J. Amer. Chem. Soc.*, **78**, 2969 (1956).
13. I. Shain, R. S. Nicholson, *Analyt. Chem.*, **38**, 1406 (1966).
14. R. S. Nicholson, I. Shain, *Analyt. Chem.*, **36**, 706 (1964).
15. M. M. Nicholson, *J. Amer. Chem. Soc.*, **76**, 2539 (1954).
16. S. J. Kanopka, B. McDuffie, *Analyt. Chem.*, **42**, 1748 (1970).

STUDIA UNIV. BABEŞ—BOLYAI, CHEMIA, XXXI, 1, 1986

PERFORMANCE OF GLASS POWDER IMPREGNATED WITH POLYAMIDE AT STATIONARY PHASE IN THIN LAYER CHROMATOGRAPHY

SIMION GOCAN* and CRISTINE KONNERT*

Received: June 4, 1984

ABSTRACT. — The impregnation degree of a glass powder (10—50 μm) with polyamide content ranging between 0.5—20% was investigated by microscope analyses. The polyamide content was correlated to a number of chromatographic parameters (R_f, spot expansion and separating resolution). A regression equation of the form: $\log hR_f = a - b \log X_A$ was determined for the variation of hR_f values *vs.* polyamide content X_A. The resolution values increase and turn superunitary for all pairs of components starting with a polyamide content of 15%, which corresponds to an impregnation degree of 0.5.

The polyamide powder was used in mixtures with other absorbents for obtaining stationary phases: polyamide-cellulose [1—2], polyamide — Kieselguhr [3] and polyamide-silica gel [4—6].

By impregnation with polyamide (Nylon 66) of a glass powder (10—50 μm) a new stationary phase for thin layer chromatography was obtained, which can be used for the separation of polar compounds. The obtained thin layers of this adsorbent are very resistant. The eluent migration velocity is high and the separation time will be relatively short.

Because the chromatographic properties of these stationary phases depend on the amount of the active compound, it was necessary to study the opzimization of the impregnation degree.

Experimental. The neutral glass powder (10—50 μm) was impregnated with 0.5; 2.5; 5.0; 7,5; 10.0; 15.0 and 20.0 weight percent of polyamide. The impregnation was carried out by dissolving the polyamide in warm formic acid and methanol [7]. The thin layers on glass plates were obtained by using 3% carboxymethyl-cellulose as a binding agent.

The impregnated powder was examined by an optic microscope (40 × 10) to assess the uniformity of the polyamide film on the glass particles.

The chromatographic properties of the layers with various contents of polyamide were tested by separating a mixture of polyphenols, namely, phenol, pyrocatechol, resorcinol, pyrogallol and phloroglucinol (each in 0.05% concentration).

A ternary mixture of benzene + methanol + acetic acid (80 : 13 : 7, v/v) was used as eluent.

The developing was carried out ascendingly, in an S-chamber, at room temperature, on glass plates (10 × 14 cm), with layers of 0.25 mm thick. The average migration time was 25 min. and was not significantly influenced by the increase of the polyamide content of the layer.

The detection of components was effected by spraying with diazotized p-nitoaniline followed by a spraying with 10% NaOH [8].

Results and discussion. By examining under the microscope the powder obtained by impregnating glass with polyamide, a very non-uniform coating is observed. Not all of the glass grains are impregnated with the polyamide

* *University of Cluj-Napoca, Faculty of Chemical Technology, Department of Inorganic and Analytical Chemistry, 3400 Cluj-Napoca, Romania*

and there is a distinct preference for larger grains. A uniform layer of polyamide on the surface of the glass particles was not obtained even when using small concentrations of polyamide By increasing the polyamide content of the system, a preferential deposition on already existing layers is observed, and large particles, or even aggregates are formed by binding several glass grains together.

By counting the number of impregnated paticles and the total number of particles in the microscope field, a degree of impregnation, G, (the ratio of impregnated particles to the total number of particles) could be determined. The value of G was determined by counting the paticles in 20 different microscopic fields for each polyamide concentration X_A (Table 1). An increase of G is observed, up

Table

Degree of impregnation values, G, *vs.* the polyamide content of the layer, X_A

X_A%	0.5	2.5	5.0	7.5	10.0	12.5	15.0	20.0
G	0.25	0.26	0.27	0.28	0.31	0.40	0.50	0.37

to 15% polyamide, where a value of 0.5 is reached. At larger concentrations of polyamide, *e.g.* 20%, the degree of impregnation is only 0.37, because under these conditions larger aggregates prevail, and many small glass grains are left uncoated.

Prey and Scherz [9] reported that in the case of mixed layers, consisting of an adsorption active component and an inert one, the hR_f is a function of the layer composition, namely, it decreases with increasing content in the active component of the layer, a hyperbolic dependence being observed.

A plot of log hR_f *vs.* the logarithm of the polyamide content points to the existence of a linear corelation of these parameters (Fig. 1). These straight lines present a change both in the slope and intercept for concentrations of polyamide larger than 10%.

These obsevations, not as yet reported by other workers in the field [9, 10] are probably due to the more complex character of the chromatographic systems with polyamide as the active component, since in such systems the separation process incorporates not only the contribution of adsorption, but also that of the partition in the polyamide gel.

As long as the polyamide content of the layer is small, the deciding part in the separation process is played by the adsorbtion of proton-donating molecules at the carbonyl groups of the polyamide, these groups behaving as active centers. The NH groups are also contributing to the adsorbtive properties, but to a lesser extent, as indicated by some literature data [11]. At the same time, the solvation of carbonyl groups by the solvent molecules (methanol, acetic acid) may occur, so that the adsorbtion of the phenols will take place in a competition with the solvent molecules, thus migrating to higher hR_f values.

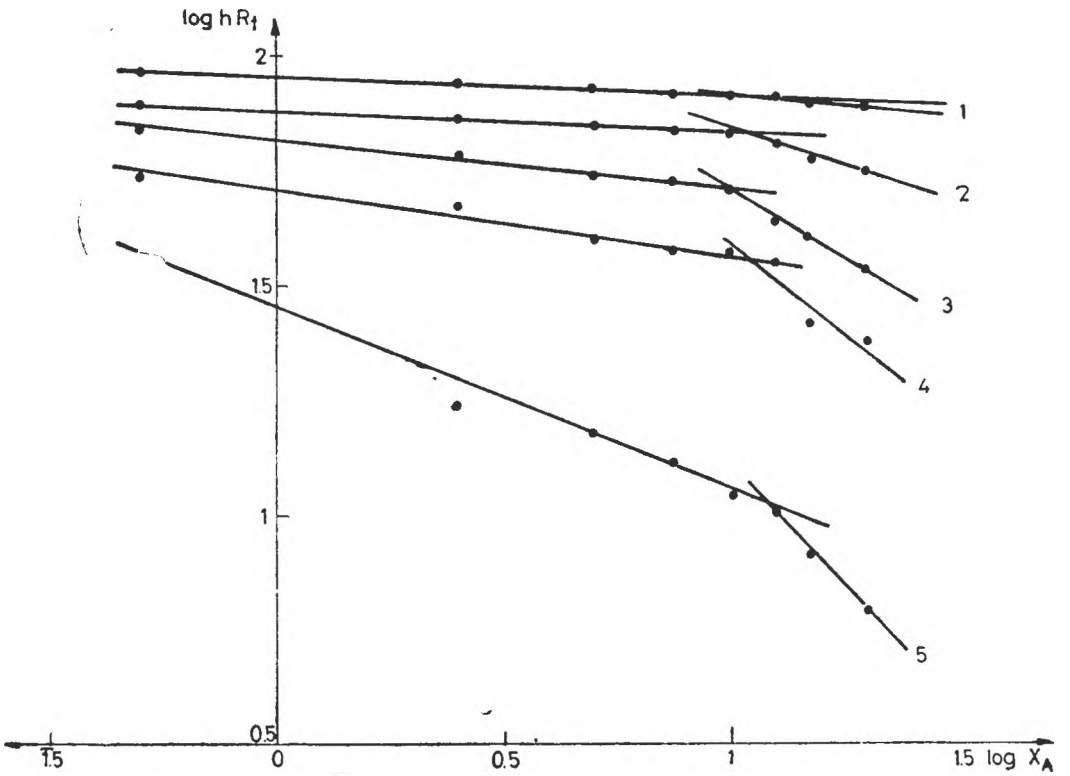

Fig. 1. Plot of log hR *vs.* the logarithm fo the polyamide content of the layer X_A.
Eluent: benzene + methanol + acetic acid (80 : 13 : 7, v/v).
Compounds: 1 — phenol, 2— pyrocatechol, 3—resorcinol, 4— pyrogallol and 5 — phloroglucinol.

By means of partial regression equations for the range of polyamide concentrations 0.5—10.1% (Table 2, column 1) the calculated hR_f values are obtained, which are in a very good agreement with the experimental hR_f values (Table 3).

Table 2

Regression equations of the hR *vs.* the polyamide content of the layer for the separation of some polyphenols

Compound	Range of polyamide concentration	
	0.5—10%	12.5—20.0%
Phenol	$\log hR_f = 1.9566 - 0.0365 \log X_A$	$\log hR_f = 2.0509 - 0.1242 \log X_A$
Pyrocatechol	$\log hR_f = 1.8696 - 0.0606 \log X_A$	$\log hR_f = 2.1034 - 0.2756 \log X_A$
Resorcinol	$\log hR_f = 1.7574 - 0.1090 \log X_A$	$\log hR_f = 2.2473 - 0.5498 \log X_A$
Pyrogallol	$\log hR_f = 1.7110 - 0.1440 \log X_A$	$\log hR_f = 2.3451 - 0.7544 \log X_A$
Phloroglucinol	$\log hR_f = 1.2260 - 0.3890 \log X_A$	$\log hR_f = 2.1740 - 1.0740 \log X_A$

Table 3

$hR_{fexp.}$ and $hR_{fcalc.}$ values of some phenols *vs.* the polyamide content of the layer, X_A

Polyamide content X_A%	Phenol hR_f		Pyrocatechol hR_f		Resorcinol hR_f		Pyrogallol hR_f		Phloroglucinol hR_f	
	exp.	calc.	exp.	calc.	exp.	calc.	exp.	clac.	exp.	calc.
0.5	92	92	78	76	70	71	56	57	37	36
2.5	87	87	72	72	60	60	47	46	17	19
5.0	84	85	70	71	55	55	40	41	15	15
7.5	83	83	69	70	53	53	38	38	13	13
10.0	83	83	68	69	50	51	37	37	11	11
12.5	83	82	64	64	44	44	35	33	10	10
15.0	79	80	59	60	40	40	26	29	8	9
20.0	78	78	56	56	34	34	24	23	6	7

The increase of the polyamide content entails increasing chances for the formation of a polyamide gel. The use of the nonaqueous solvent, which contains acetic acid, facilitates the formation of the gel, produces an optimal swelling of the polyamide and a sufficent break-up of its structure; this fact results in a high capacity of the layer, as well as in a rapid equilibration of the mobile and stationary phase [11]. The larger agglomerations of polyamide in this concentration range will favour the formation of the gel phase. The separation will therefore be the result of both adsorption of the polyphenols and their repartition between the mobile and stationry phase (the polyamide gel). Consequently, the parameters from the regression equations will have other values for the 12.5—20.0% (Table 2, column 2). By examining these results a good agreement was found between the experimental values and the values calculated by means of the regression equations (Table 3).

The larger the number of polar groups, the steeper are the slopes of the curves log hR_f *vs.* log X_A (Table 2) and, consequently the higher the polarity of the molecules, the faster will decrease the hR_f values.

With pyrocatechol the slope is smaller than with resorcinol, which is also a dihidroxilic compound. Probably that is due to the neighbouring positions of the OH groups, the pyrocatechol is able to form intermolecular hydrogen bonds [12]. This explains the fact that the slope value for the pyrocatechol is to be found between the values for mono- and dihydroxylic compounds. The same situation is also met in the case of pyrogallol when the slope has intermediary values between those of the di- and trihydroxylic compounds.

By plotting the size of the spot (Fig. 2) in hR_f units, as a function of the polyamide content of the layer, a longitudinal narrowing of the spot becomes evident, simultaneously with the increasing content in active component and therefore an enhancement in the separation capacity of the layer.

Table 4 gives the resolution values for a series of polyphenols as function of the polyamide content of the layer. By examining this table it has been established that, starting with a 15% polyamide content, a supraunitary resolution for all the pairs of the components is obtained. An increase in polyamide concentration above this value does not lead to significant modifications in the chromatograhpic properties of the layer.

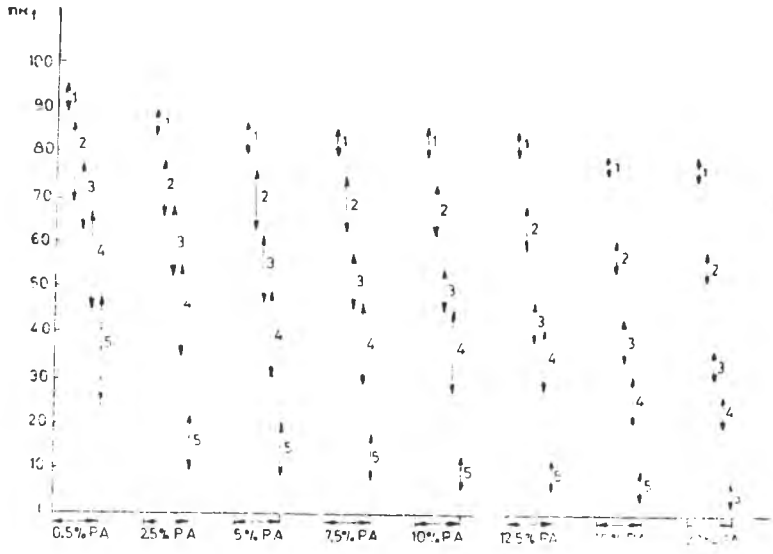

Fig. 2. Plot of the longitudinal size of the spot in hR_f units *vs.* the polyamide content of the layer X_A.
Eluent: benzene + methanol + acetic acid (80 : 13 : 7, v/v).
Compounds: 1 — phenol, 2 — pyrocatechol, 3 — resorcinol, 4 — pyrogallol and 5 — phloroglucinol.

Table 4

Resolution values, R_f, of some phenols *vs.* the polyamide content of the layer, X_A

Polyamide content of the layer X_A(%)	Phenol-Pyrocatechol	Pyrocatechol-Resorcinol	Resorcinol-Pyrogallol	Pyrogallol-Phloroglucinol
0.5	1.08	0.47	0.78	0.83
2.5	1.36	0.80	0.77	1.88
5.0	1.40	1.07	0.88	1.56
7.5	1.75	1.39	0.97	1.72
10.0	1.77	1.64	0.90	1.93
12.5	2.53	2.22	0.82	2.27
15.0	3.64	2.38	1.40	2.00
20.0	4.00	2.93	1.18	2.25

The correlation of the microscopic data with the chromatographic parameters leads to the conclusion that the optimal degree of impregnation of the glass powder with polyamide is 0.5 and corresponds to a content of 15% polyamide.

REFERENCES

1. K. Egger, M. Keil, Z. *Analyt, Chem.*, **210,** 201 (1965).
2. L. S. Bark, R. J. T. Graham, J. *Chromatog.*, **27,** 109 (1967).
3. H. C. Chiang, T. M. Chiang, *J. Chromatog.*, **47,** 128 (1970).
4. H. C. Chiang, *J. Chromatog.*, **40,** 189 (1969).
5. H. C. Chiang, Y. Lin, Y. C. Wu, *J. Chromatog.*, **45,** 161 (1969).
6. S. Gocan, C. Konnert. *Stud. Univ. „Babeș—Bolyai", Chem.*, **22** (2), 39 (1977).
7. S. Gocan, C. Liteanu, C. Konnert, *Patent R.S.R., no* 63244 (1977).
8. L. Krauss, D. Dupokova, *Pharmazie,* **19,** 41 (1964).
9. V. Pery, H. Scherz, E. Bancher, *Mikrochim. Acta,* **1963,** 567.
10. D. C. Abbot, H. Egon, E. W. Hammond, J. Thomson, *Analyst,* **89,** 480 (1964)
11. E. Soczewinski, G. Golkiewicz, H. Szumilo, J. Chromatog., **45,** 1 (1969).
12. H. Szumilo, E. Soczewinski, *J. Chromatog.*, **124,** 394 (1974).

STUDIA UNIV. BABEŞ—BOLYAI, CHEMIA, XXXI, 1, 1986

CONTRIBUŢII LA STUDIUL ACTIVITĂŢII CATALITICE A UNOR SISTEME $nSiO_2 \cdot mAl_2O_3 \cdot xH_2O$ ÎN REACŢIA DE DESCOMPUNERE A HIDROPEROXIDULUI DE CUMEN[1]

XI. Viaţa catalizatorului

AUGUSTIN POP şi LIVIU CORMOŞ*

Received: October 19, 1984

ABSTRACT. — Contribution to the Study of Catalytic Activity of Some $nSiO_2 \cdot mAl_2O_3 \cdot xH_2O$ Systems in the Decomposition Reaction of Cumene Hydroperoxide. The life of synthethic aluminosilicate catalyzers in the decomposition reaction of cumene hydroperoxide was studied. It was found that the synthetic aluminosilicates used in the process display constant catalytic activity for over 200 hrs of continuing operation, without regeneration. Also, the selectivity and productivity of these catalyzers was followed.

Într-o serie de lucrări [1—8] noi am studiat descompunerea hidroperoxidului de cumen (HPC) în cataliză eterogenă, utilizînd drept catalizatori aluminosilicaţi sintetici. Procesul a fost urmărit în reactor discontinuu cu amestecare perfectă, în reactor continuu cu strat fix de catalizator şi în reactor cu strat fluidizat.

În prezenta lucrare am urmărit modul în care aceşti catalizatori corespund condiţiilor ce se cer unui catalizator industrial [9], în ceea ce priveşte viaţa catalizatorului, capacitatea de producţie şi selectivitatea.

Partea experimentală. Pentru a obţine aluminosilicaţi sintetici cît mai lipsiţi de cationi străini, am preparat aceste sisteme prin coprecipitarea gelurilor mixte, pornind de la soluţii de acid silicic liber şi azotat de aluminiu. Coprecipitarea s-a efectuat la pH = 5 în prezenţa unei soluţii de carbonat de amoniu. Am studiat influenţa concentraţiei iniţiale a soluţiei de azotat de aluminiu asupra activităţii catalizatorilor obţinuţi, în reacţia de descompunere a HPC. Datele obţinute sînt prezentate în Tabelul 1.

Rezultate şi discuţii. Se constată că se obţin conversii ceva mai ridicate şi mai reproductibile, cu cît soluţia de azotat de aluminiu folosită este mai diluată. Pentru prepararea soluţiilor s-a folosit apă deionizată pe coloane cu schimbători de ioni. În soluţia de acid silicic am lăsat să picure, sub puternică agitare, soluţia de azotat de aluminiu, concomitent cu adăugarea soluţiei de carbonat de amoniu. Utilizarea acidului silicic liber în locul silicatului de sodiu este mai avantajoasă deoarece catalizatorul obţinut nu mai trebuie spălat prea mult pentru eliminarea ionilor de sodiu, ioni care dezactivează centrii mai puternic acizi ai catalizatorului. Analizele prin flamfotometrie a sodiului, arată că în toate probele conţinutul în sodiu este sub 0,05%. Utilizarea azota-

[1] Nota 8: L. Cormoş, [A. Pop], *Buletinul Institutului de Învăţămînt Superior Suceava*, 1985, sub tipar.

* *Universitatea din Cluj-Napoca, Facultatea de Tehnologie Chimică, Catedra de chimie fizică, organică şi tehnologie 3400 Cluj-Napoca, Romania*

Tabel 1

Influenţa concentraţiei de azotat de aluminiu asupra activităţii catalitice a catalizatorului

Cantitatea de sol. de azotat, g	Conc. sol. de azotat de aluminiu	Cantitatea de sol. de acid silicic, 3%, g.	Conţinutul procentual fără apă în:		Conversia după acelaşi timp de reacţie, %
			SiO_2	Al_2O_3	
50	10%	100	61,09	38,91	9,37 9,62 9,14
25	20%	100	61,09	38,91	11,90 11,82 11,86
100	5%	100	61,09	38,91	12,42 12,38 12,35

tului de aluminiu în locul sulfatului de aluminiu prezintă avantajul că, în final, îndepărtarea ionului azotat se face mult mai uşor decît a ionului sulfat.

Gelurile mixte voluminoase obţinute prin coprecipitare la 20°C, au fost lăsate să se matureze 48 ore la temperatura camerei, apoi se filtrează, se spală cu apă deionizată, se usucă în atmosferă, iar în final se usucă în etuvă la 105°C. Catalizatorii obţinuţi se granulează, se clasează şi se supun tratamentului termic. În prezenta lucrare s-au utilizat sisteme calcinate la 580°C, temperatură la care cea mai mare parte a apei legate a fost deja îndepărtată, iar pierderea de apă din sistem devine constantă [1].

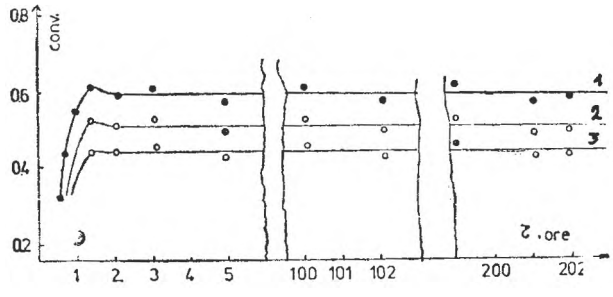

Fig. 1. Viaţa catalizatorului. 1 la 30 °C; 2 la 40 °C şi 3 la 50 °C.

Utilizînd un reactor cu deplasare totală în strat fluidizat [8] s-a urmărit viaţa catalizatorului. În Figura 1 este prezentată activitatea catalitică a sistemului cu 33% Al_2O_3.

Din Figura 1 se constată că apare o scurtă perioadă de inducţie de circa 30 de minute, după care are loc o creştere a activităţii catalitice la un maxim şi o revenire rapidă la o valoare constantă. Această valoare constantă a conversiei în proces se menţine peste 200 ore de funcţionare neîntreruptă a catalizatorului. S-a lucrat cu soluţii de 30% HPC în cumen, la conversii parţiale în jur de 60%, la temperaturile de lucru de 30,40 şi 50°C, cu separarea produşilor de reacţie în afara reactorului.

Pentru comparație s-a urmărit și viața catalizatorului S industrial de cracare catalitică, în acest proces, care are 10% Al_2O_3 (Fig. 2).

Se constată că activitatea catalitică a catalizatorului de cracare este mai mică decît a catalizatorului sintetizat de noi.

Pentru a putea urmări selectivitatea și productivitatea catalizatorului, s-a efectuat o descompunere totală a soluției de 70% HPC în cumen. Selectivitatea cataclizatorului S sereferă la produsul principal al reacției, în acest caz fenolul, și este dată de relația:

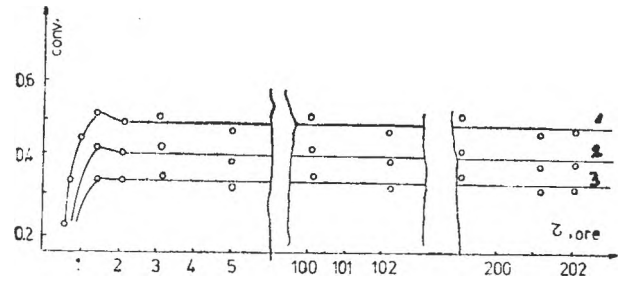

Fig. 2. Viața catalizatorului industrial de cracare. 1 la 30 °C; 2 la 40 °C și 3 la 50 °C.

$$S\% = \frac{\text{nr. moli fenol rezultat}}{\text{nr. moli HPC transformați}}$$

Pentru determinarea practică a selectivității s-a pornit de la 1000 g soluție 70% HPC în cumen și s-a colectat din reactor un amestec de reacție în cantitate de 998,2 g. Se constată că în proces au loc pierderi de 1,8 g ceea ce reprezintă 0,18%. În amestecul de reacție s-a dozat prin metoda bromat-bromură fenolul existent, obținîndu-se valoarea de 42,77%. Acetona s-a dozat cu clorhidrat de hidroxil-amină, obținîndu-se valoarea de 26,47%. Pe baza analizei s-a calculat cantitatea de fenol obținută și anume 4,5292 moli. Cantitatea de HPC existentă în materia primă supusă descompunerii (cele 1000 g soluție 70% HPC în cumen) este de 4,6054 moli. Ca urmare putem calcula selectivitatea S:

$$S\% = \frac{4,5292}{4,6054} \cdot 100 = 98,34\ \%$$

Masa de reacție rezultată se supune unei distilări fracționate într-o coloană cu umplutură de 16,9 talere teoretice, în raport cu CCl_4. În urma fracționării s-au colectat trei fracții principale: fracția acetonică, fracția de hidrocarburi și fracția fenolică. Între fracția acetonică și cea de hidrocarburi s-a colectat și o fracție intermediară de 2,18 g. Fracția acetonică s-a colectat la 57 °C temperatura la vîrful coloanei, iar temperatura în blaz s-a urcat pînă la 146,5 °C. Alimentarea coloanei s-a făcut cu 500 g amestec de reacție. Masa fracției acetonice a fost de 132,3 g. S-a controlat tot timpul indicele de refracție al acetonei, care se menține la 1,3600 față de cel din literatură de 1,3597. Aceasta ne dovedește că fracția acetonică nu conține nici metanol și nici apă. Aceste produse apar în proces atunci cînd se realizează descompunerea în cataliză omogenă. Astfel, se trage concluzia că în cazul nostru nu se petrec acele reacții secundare ce conduc la formarea metanolului și a apei. Această concluzie este confirmată de faptul că la analiza cromatografică a fenolului obținut nu se

identifică prezența α-metilstirenului, produs ce apare concomitent cu apariția apei.

Fracția intermediară de 2,18 g s-a colectat la temperaturi la vîrful coloanei pînă la 120°C, iar în blaz pînă la 161°C. Între temperatura de 120 și 151°C la vîrful coloanei, nu se colectează nimic, iar la 151°C începe colectarea cumenului. În blaz temperatura a urcat pînă la 182°C. Cantitatea fracției de hidrocarbură a fost de 148,8 g.

Ultima fracție rezultată este cea din blaz, fracția fenolică, de 313,32 g.

În tabelul 2 este prezentat bilanțul de materiale al procesului de fracționare și stabilirea pierderilor în proces.

Tabel 2

Bilanțul de materie al procesului de fracționare

INTRAT		IEȘIT	
1. Amestec de reacție 500 g		1. Fenol	213,32 g
		2. Acetonă	132,30 g
		3. Cumen	148,80 g
		4. Fracție intermediară	2,18 g
		5. Pierderi	3,40 g
Total intrat:	500 g	Total ieșit:	500 g

Din datele de bilanț, ținînd seama de raportul reactant/catalizator utilizat, se poate calcula productivitatea catalizatorului, deci cantitatea de fenol obținut de unitatea de masă de catalizator, în unitate de timp. Efectuaînd experiențele cu un debit de 5 ml/minut, cu soluții de 70% HPC în cumen și la un raport masic între catalizator și reactant de 1 : 5, în cele 200 de ore cît s-a urmărit viața catalizatorului, găsim prin calcul că prin reactor trec 6000 ml soluție, ceea ce corespunde la o concentrație de 4,60 moli/l. Rezultă că un gram de catalizator poate produce în 200 ore 81,76 g fenol, iar într-o oră produce 0,4083 g fenol. Un litru de catalizator (1 g = 0,9 ml) produce într-o oră 408,8 g fenol. Se știe că industrial nu se pot utiliza catalizatori cu o capacitate de producție raportată la produs final, sub 20 g/l.h. [9]. În cazul nostru această valoare este mult depășită, obținîndu-se 408,8 g/l.h.

Ținînd seama de cei 4,6054 moli HPC introduși în reactor, de cantitatea de fenol obținută de 4,5292 moli și de pierderile de 0,18%, putem calcula randamentul procesului:

$$\% = \frac{4{,}5210}{4{,}6054} \cdot 100 = 98{,}10$$

Concluzii. Se studiază viața catalizatorului dovedindu-se că el poate funcționa, fără regenerare, peste 200 ore. De asemenea, s-a urmărit selectivitatea catalizatorului și randamentul acestuia în proces. Productivitatea catalizatorului este de asemenea foarte bună, fapt ce ne îndreptățește să considerăm o posibilă utilizare industrială a lui.

BIBLIOGRAFIE

1. A. Pop, P. Krőbl, L. Cormoş. Gh. Lengyel, *Stud. Univ. Babeş—Bolyai, Chem.*, **12** (2), 89 (1967).
2. A. Pop, L. Cormoş, *Stud. Univ. Babeş—Bolyai, Chem.*, **16** (1), 61 (1971).
3. A. Pop, L. Cormoş, *Stud. Univ. Babeş—Bolyai, Chem.*, **16** (2), 101 (1971).
4. L. Cormoş, S. Popica, *Stud. Univ. Babeş—Bolyai, Chem.*, **19** (1), 19 (1974).
5. L. Cormoş, A. Pop, L. Orbu, *Rev. Roumaine Chim.*, **23** (2), 225 (1978)
6. L. Cormoş, A. Pop, M. Stanca, C. Orbai, *Rev. Chim.*, **30** (9), 868 (1979).
7. A. Pop, L. Cormoş, *Stud. Univ. Babeş—Bolyai, Chem.*, **30** (1985).
8. L. Cormoş. A. Pop, Buletinul Institutului de Invăţămînt Superior Suceava, 1985.
9. I. I. Ioffe, L. M. Pismen, Cataliza eterogenă în ingineria chimică", Ed. Tehnică, Bucureşti, 1967, p. 273.

STUDIA UNIV. BABEŞ—BOLYAI, CHEMIA, XXXI, 1, 1986

L'OPTIMISATION EN PHASE DE LABORATOIRE DE L'OXIDATION DU p-NITROTOLUÈNE À ACIDE p-NITROBENZOÏQUE

VICTOR LITEANU*, MIRCEA FODOREAN*, IOAN BĂTIU* et MARINELA PRIPAS*

Received: November 27, 1984

ABSTRACT. — Laboratory Phase Optimization. This paper deals with an operational researchwork lying in a central factorial experiment 2^3 (experiment planning matrix, statistical processing, polynominal mathematical model adjustment and model optimization, conclusions) leading to an increase of the yield in p-nitrobenzoic acid, as a result of oxidation with manganese dioxide at a ratio from 41—65% to over 75%, in a laboratory installation.

On sait que la réactivité des groupements méthyle liés au noyau aromatique diminue en présence des groupements nitro. Leur oxydation dans cette situation a constitué l'objet des recherches relativement récentes [1], à la suite desquelles on a opté pour l'oxydation à MnO_2 en présence de H_2SO_4 de concentration supérieure à 60%.

Puisque les rendements en acide p-nitrobenzoïque [1] étaient d'environ 40% et les plus récents [2] d'environ 65%, on a considéré opportune l'étude opérationnelle du processus pour trouver les conditions d'un rendement supérieur. Celle-ci a consisté dans l'adaptation de la méthodologie d'un expériment factoriel central, à deux niveaux, en trois variables indépendantes, 2^3 [3].

L'organisation de l'expériment. Les variables choisies ont été: la température de réaction, la durée de la réaction et la quantité de MnO_2. Le niveau de départ et les domaines de variation admissibles pour les trois variables ont été établis à:

$$Z_0 = \begin{bmatrix} 140\ ^\circ C \\ 3{,}5\ \text{heures} \\ 60\ \text{g}\ MnO_2 \end{bmatrix} \pm \begin{matrix} 20\ ^\circ C \\ 1\ \text{heure} \\ 11{,}9\ \text{g}\ MnO_2 \end{matrix}$$

À ceux-ci correspondent (Tableau 1) la matrice de planification de l'expériment 2^3 dans des coordonnées naturelles (°C, heures, g MnO_2) et en coordonnées conventionnelles (± 1, 0), aux réponses y de l'installation (les rendements in % d'acide p-nitrobenzoïque) et à six essais supplémentaires sur le niveau de départ, pour tester la reproductibilité des expériments.

L'ajustement du modèle mathématique. Aux données du tableau 1 on a ajusté, conformément à la procédure de l'expériment factoriel [3], par la méthode des moindres carrés, le modèle polynomial, facile à travailler statistiquement et à optimiser

$$\hat{y}(X) = a_0 + a_1 \cdot x_1 + a_2 \cdot x_2 + a_3 \cdot x_3 + a_{12} \cdot x_1x_2 + a_{13} \cdot x_1x_3 + a_{23} \cdot x_2x_3 + a_{123} \cdot x_1x_2x_3$$

* *Université de Cluj-Napoca, Departement de Chemie Inorganique et Analytique, 3400 Cluj-Napoca, Romania*

Tableau 1

La matrice de planification de l'expériment 2^3 et les résultats obtenus

No. cour.	Z_1, °C	X_1	Z_2, heures	X_2	Z_3, g MnO_2	X_3	Y, %
1	160	1	4,5	1	71,9	1	53,34
2	120	−1	2,5	−1	71,9	1	61,55
3	160	1	2,5	−1	48,1	−1	30,36
4	120	−1	4,5	1	48,1	−1	71,80
5	160	1	4,5	1	71,9	1	41,03
6	120	−1	4,5	1	71,9	1	75,50
7	160	1	2,5	−1	48,1	−1	47,10
8	120	−1	2,5	−1	48,1	−1	55,39
9	140	0	3,5	0	60,0	0	62,78
10	140	0	3,5	0	60,0	0	65,65
11	140	0	3,5	0	60,0	0	64,01
12	140	0	3,5	0	60,0	0	61,55
13	140	0	3,5	0	60,0	0	63,60
14	140	0	3,5	0	60,0	0	67,70

où

$$a_0 = \bar{y} = \frac{1}{8}\sum_{k=1}^{8} y_k \qquad a_i = \frac{1}{8}\sum_{k=1}^{8} x_{k,i} \cdot y_k$$

$$a_{ij} = \frac{1}{8}\sum_{k=1}^{8} x_{k,i} \cdot x_{k,j} \cdot y_k \qquad a_{123} = \frac{1}{8}\sum_{k=1}^{8} x_{k,1} \cdot x_{k,2} \cdot x_{k,3} \cdot y_k$$

de sorte que

$$\hat{y}(X) = 54{,}509 - 11{,}551 \cdot x_1 + 7{,}426 \cdot x_2 + 3{,}346 \cdot x_3 - 0{,}164 \cdot x_1x_2 + \\ + 0{,}881 \cdot x_1x_3 - 0{,}861 \cdot x_2x_3 - 0{,}246 \cdot x_1x_2x_3$$

L'analyse statistique du modèle. En calculant la variance de la reproductibilité :

$$s^2_{repr} = \frac{\sum_{i=1}^{6} (y_{i,0} - \bar{y}_0)^2}{6 - 1} = 4{,}757,$$

l'écart standard des coefficients :

$$s_a = \sqrt{\frac{s^2_{repr}}{N}} = \sqrt{\frac{4{,}757}{8}} = 0{,}771,$$

et les valeurs $t_{exp} = [a]/s_a$, par le test de Student ($P = 95\%$ et $t_{95}(6 - 1) = 2{,}771$ [4]) en éliminant les coefficients pour lesquels $t_{exp} < t_{tab} = 2{,}771$, on trouve significatifs les coefficients du modèle simplifié :

$$\hat{y}(X) \cong 54{,}509 - 11{,}551 \cdot x_1 + 7{,}426 \cdot x_2 + 3{,}346 \cdot x_3$$

Ensuite on a vérifié si le modèle est adéquat par le test de Fisher pour sanoir si le modèle ajusté et simplifié décrit de manière satisfaisante (à $P = 95\%$) la réponse de l'installation dans le domaine expérimental considéré et si optimisation doit avoir donc lieu.

On a calculé donc la variance résiduelle :

$$s^2_{res} = \frac{\sum_{i=1}^{N} [y_i - \hat{y}(X^i)]^2}{N - \text{nr. coeff. modèle}} = \frac{12{,}846}{8 - 4} = 3{,}212$$

Puisque

$$F_{exp} = \frac{s^2_{repr}}{s^2_{res}} = 1{,}481 < F_{tab} = F_{95}(5\,;\,4) = 6{,}26 \ [5]$$

il résulte que le modèle linéaire est adéquat, a un coefficient de corrélation multiple [6] $R_{yX} = 0{,}993$ qui, étant très proche de l'unité, dénote la dépendence linéaire pratiquement fonctionnelle [7].

L'optimisation du modèle ajusté. Ceci a consisté dans la maximisation du rendement estimé $\hat{y}(X)$, dans le domaine admissible $-1 \leqslant X \leqslant 1$.

$\hat{y}_{max}$ peut être trouvé immédiatement en observant que $\hat{y}(X)$ devient maximum pour l'X pour lequel le membre droit est une somme de termes positifs de valeurs maximales. Ceci se réalise pour la sixième valeur de X de la matrice d'expérimentation, X^6 :

$$y_{max} = y(X_{max}) = y(X^6) = \max_{-1 \leqslant X \leqslant 1} y(X) = 76{,}83\%$$

On sait du tableau 1 que le meilleur rendement, 75,50% est obtenu pour X^6. Or c'est justement la confirmation pratique nécessaire pour le résultat antérieur.

Avec ce qu'on a montré ci-dessus, on a mis en évidence que dans les conditions de travail adoptées, $y_{max} = 75{,}50\%$ est le maximum global du rendement dans le domaine admissible ou la meilleure valeur du rendement dans les conditions des restrictions existentes.

Conclusions. L'avantage de la méthode adoptée par comparaison à l'analyse dispersionnelle est évident. Celle-ci, par un même effort de calcul aurait mis en évidence les facteurs qui influencent le rendement, mais le modèle manquant, ne permet pas de trouver les conditions de l'optimum.

X_{max} trouvé peut constituer le nouveau niveau de départ dans un autre expériment factoriel, le cas échéant plus restreint si c'était plus convenable.

Par la startégie expérimentale adoptée, on a trouvé les conditions pour obtenir en laboratoire, une importante augmentation du rendement en acide p-nitrobenzoïque.

BIBIOGRAPHIE

1. N. J. Mruk, P. Boro, *US* 3, 775, 473/1973.
2. M. Fodorean, *Ouvrage non-publié*, Université de Cluj-Napoca, 1983.
3. V. Kafarov, „Méthodes cybernétiques et technologie chimique, Mir, Moscou, 1974, pp. 205—211.
4. C. Liteanu, I. Rîcă, „Statistical Theory and Methodology of Trace Analysis", Ellis Horwood Limited, Chichester, 1980, p. 430, 431.
5. A. Glück, „Metode matematice în industria chimică", Ed. Tehnică, București, 1971, pp. 138—139, 196.

STUDIA UNIV. BABEŞ—BOLYAI, CHEMIA, XXXI, 1, 1986

STUDY OF Cd-Zn SEPARATION USING VIONIT CS-3-TYPE ION-EXCHANGE RESIN

GHEORGHE MARCU*, LIVIA CRIVEI and NICOLAE PASCU****

Received: December 8, 1984

ABSTRACT. — The behaviour on adsorption from sulphate solutions of Cd^{2+} and Zn^{2+} ions, on strongly acid cation-exchange resin — Vionit CS—3 (Romanian made) — and elution in sodium chloride medium were investigated. Separation of Cd from Zn and the accompanying elements from residual solutions resulted from Zn and Pb metallurgy was obtained.

Introduction. Chromatographic separation methods, through ion-exchange, have ever more gained ground of late, imposing themselves thanks to their simplicity and efficiency.

In ion-exchange chromatography, separations were often obtained in the presence of complexing reagents. The complexing action of hydrochloric acid and alkaline chlorides [1—3] was employed to separate cadmium from zinc, by ion-exchange.

The difference in the distribution coefficients [4] of the elements between the resin and solution, as well as the stability difference of the complexes formed between the ions of the separate and eluents — which are also complexing reagents [5] — constituted the basis of some ion-exchange separation approaches.

In this paper Cd^{2+} and Zn^{2+} ion distribution between Vionit CS—3 resin and sodium chloride solutions of varied concentrations is followed, to the end of stating some optimum separation conditions. The sulphuric aqueous solutions resulted from lye washing of volatile powders in zinc and lead metallurgy lie at the basis of our investigations.

Experimental. *Ion-Exchange Resin.* Indigenous, ion-exchange resin strongly acid cationit Vionit CS—3 (styrene copolymer of 8% divinylbenzene with sulphonic groups) of 50—100 mesh granulation, of the form R—H and R—Na was used.

The H^+ type cationit (delivery form) was purified by washing in 10% HCl solution, in column, to remove iron traces, then washed in distilled water spout until the effluent gave negative reaction for Cl^- ion (with Ag^+). The resin was converted under Na^+ form with 10% NaCl solution, washed in distilled water and dried in air at room temperature (~25°C).

The bulk difference between the R—H and R—Na forms was 6.5%. The water content, determined by drying to constant weight at 110°C, was found to be 24.18% with R—H and 23.78% with R—Na form respectively. The ion-exchange capacity, determined by acid-basic titration (STAS 9475/7—74) for the H^+ form, was of 4.25 mVal/g dried resin[1] and 1.90 mVal/ml damp resin.

The Ion-Exchange Column. A 1.7 bore glass column was used. To the end of preparing the resin layer, a suspension of the resin in water was poured in the water-filled column, till the layer reached to 22.7 cm high.

* *University of Cluj-Napoca, Department of Anorganic and Analytic Chemistry, 3400 Cluj-Napoca, Romania*
** *Institute of Chemistry, 3400 Cluj-Napoca, Romania*
[1] The weight of dried resin was derived from the weight of the resin dried in air (25°C) and the water content.

Metallic Ion Solutions. The solutions of the metallic ions were prepared by dissolving the respective sulphates (Cd, Zn) in distilled water. To avoid hydrolysis, a minimum amount of sulphuric acid was added. The metallic ions were determined by titration with Complexon III solution, using Erio T as indicator [6].

Distribution Coefficient Measurements. Adsorbability of the elements was expressed in distribution coefficients, determined by series equilibration. The measured amounts of H^+ and Na^+ form resin (1.0 g) were stirred with known quantities of sodium chloride (50 ml) of varied concentrations, containing approximately 1 mmol of each studied metal. The samples were being stirred for 24 hs. at room temperature. After filtration of the resin particles, the liquid phase-element concentration was determined [6]. By difference as to initial concentration, the amount of element retained by the resin was determined.

The distribution coefficients were calculated with the following relation:

$$K_d = \frac{\text{amount of metal/gram of dry resin}}{\text{amount of metal/ml of solution}}$$

The adsorbtion was achieved under a ratio q [7] of resin loading:

$$q = \frac{\text{total amount of cations (in equivalents)}}{\text{total amount of the resin (in equivalents)}} = 0.4$$

Results and Discussion. In aqueous chloride solutions, Cd and Zn form various types of chloro-complexes, as a function of the complexing agent concentration [8].

Of the data given in Table 1, it appears that, in NaCl solutions, Zn^{2+} is strongly adsorbed by the cationit, and the distribution coefficient increases with the decrease of sodium chloride concentration, attaining a maximum at NaCl 0.1 N.

As for Cd^{2+}, the distribution coefficient increases with the decrease of NaCl concentration; it is noticed that Cd adsorbability is low at NaCl concentration values higher than 0.2 N, because of $CdCl_3^-$ chloro-complex formation, unretained by the cationic resin. In contrast, Zn — existing as a positive ion — is strongly retained by the resin, it being completely desorbed at concentrations of NaCl $\geqslant$ 2N.

Table 1

Cd^{2+} and Zn^{2+} distribution coefficients in NaCl solutions of various concentrations*, and R—H and R—Na—form resin (q = 0.4)

NaCl (N) concentration	R—H resin		R—Na resin	
	Cd^{2+}	Zn^{2+}	Cd^{2+}	Zn^{2+}
0.1	222.87	575.22	126.69	286.94
0.2	40.73	147.44	39.25	99.94
0.3	14.15	74.40	10.45	56.71
0.4	14.54	50.70	10.48	37.44
0.5	5.66	34.10	7.87	32.35
0.8	2.78	13.70	2.52	12.86
1.0	2.58	10.22	2.44	11.85
2.0	2.10	6.49	0.92	1.60
3.0	2.17	2.84	1.50	1.41
4.0	2.28	1.28	0.36	1.66

* Each value is a double-determination mean.

Table 2

Cd^{2+} and Zn^{2+} distribution coefficients in NaCl solutions and R—Na—form resin (q = 0.1)

NaCl (N) concentration	Cd^{2+}	Zn^{2+}
0.1	170.91	325.17
0.2	59.08	199.30
0.4	4.73	82.75
0.5	3.96	31.87
0.8	4.27	11.03
1.0	4.68	11.03
2.0	4.36	0
3.0	4.41	0
4.0	0.36	0

Of the values of Cd and Zn adsorbability on resin in R-H and R-Na form, it is to be noted that both Cd and Zn are stronger retained by the R-H — form resin, the differences between the distribution coefficients being higher at low NaCl concentrations.

Lowering the resin loading ratio to q = 0.1, we observe (Table 2) that, at small values of K_d, the loading effect is little, while at high K_d values, the loading diminution leads to an increase of the distribution coefficients.

Consequenty, elution curves for each element were plotted (Fig. 1) by adsorbtion of a known Cd or Zn amount and elution with 0.2 N NaCl solution.

The column supply rate was of 0.5—0.8 ml/min. Cadmium and zinc were retained by the resin in a ratio of 95—97%. The elution rate was of 1.3 ml/min.

Portions of 10 ml were collected and the amount of element in each fraction was determined by the known method.

On Fig. 1, it is noticed that upon loading the column with cadmium (q = 0.68), this latter was completely eluted with 1560 ml 0.2 N NaCl solution.

While loading the column with zinc (q = 0.54), the zinc elution curve is superposed over the elution curve of cadmium, because zinc occurs in the effluent after 375 ml 0.2 N NaCl solution was flowed up in the column.

Separation Method Set up. Of the adsorbtion data given in Table 1, it clearly appears that zinc is adsorbed by the resin in NaCl concentration ranges of 0.2—0.5 N, while cadmium is less so (or not at all adsorbed).

On the basis of the difference between the distribution coefficients, an attempt was made to separate Cd from Zn on Vionit CS—3, using for cadmium 0.2 N NaCl as eluent, and 2.0 N NaCl as eluent for zinc.

In Fig.2, two examples of separation of cadmium from zinc are given, at various ratios and elution rates.

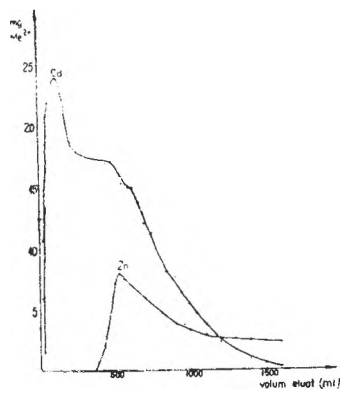

Fig. 1. Cd and Zn elution curves using 0.2 N NaCl solution as eluent: *resin (Na^+—form) : 50—100 mesh; 22.7 cm × 1.7 cm column; adsorbtion rate 0.6 ml/min; elution rate 1.3 ml/min; column loading; q = 0.68 for Cd and, q = 0.54 for Zn.*

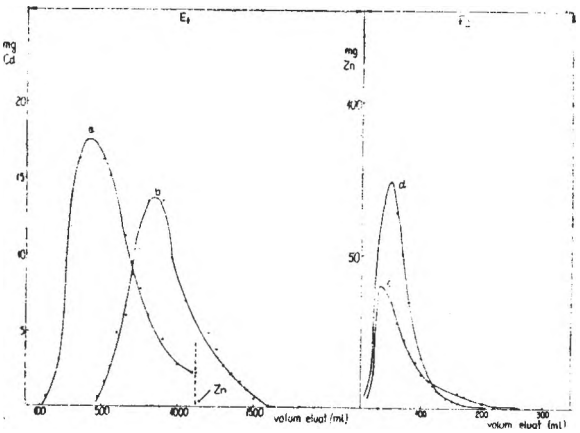

Fig. 2. Separation of Cd from Zn on Vionit CS—3-*resin (Na^+-form) 50—100 mesh; 22.7 cm × 1.7 cm column; adsorbtion rate 0.5—0.8 ml/min.; elution rate 5 ml/min.; curve (a) Cd adsorbed: 0,824 g, curve (c) Zn adsorbed: 0,329 g; elution rate 1.3 ml/min. curve (b) Cd adsorbed: 0.687 g, curve (d) Zn adsorbed 0.415 g.; E_1 = 0.2 N NaCl solution; E_2 = 2.0 N NaCl solution.*

It is to be noticed that, when the column loading is low, cadmium will occur in the effluent later:

— at a loading ratio of q = 0.22, cadmium will occur after 120 ml eluent amount;

— at a loading ratio of q = 0.10, cadmium occurs after 480 ml eluent amount.

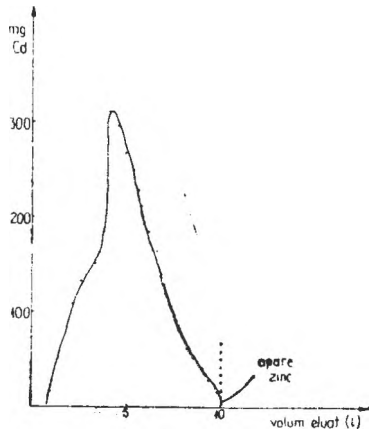

Fig. 3. Selective elution of cadmium from industrial solutions, on Vionit CS—3: *resin (Na^+-form); 50 — 100 mesh; 31.3 cm × 78.1 cm column; adsorbtion rate 6.4 ml/min.; elution rate 14.5 ml/min.; amounts adsorbed: Cd = 13.64 g, Zn = 5.39 g.*

At elution of cadmium with 0.2 N NaCl solution, at an elution rate of 5 ml/min., zinc occurs in the effluent after 1120 ml eluted amount, impurifying cadmium.

Upon elution of cadmium with NaCl 0.2 N NaCl solution at an elution rate of 1.3 ml/min., zinc does not occur in the effluent, even after 1560 ml eluent solution, amount in which about 96% cadmium has been desorbed.

Zinc was eluted with 2 N NaCl solution, 200—250 ml being enough for complete desorbtion of zinc.

The separation of the two elements is better when column loading is smaller and the elution rate is low.

The procedure was applied with good results in separation of cadmium from zinc (Figure 3) and other accompanying elements (Table 3) in sulphuric aqueons solutions, resulted from lye washing of volatile powders in lead zinc metallurgy.

Cadmium adsorbed on the resin was almost completely eluted (Table 4) with about 10 l 0.2 N NaCl solution; final Cd concentration of the solution resulted on elution was of 1.4 g/l.

Table 3

Mean chemical composition of cadmium solution resulted from oxidant acid lye washing of volatile powders determined by atomic absorbtion spectrophotometry*

Ion	Cd^{2+}	Zn^{2+}	Fe^{2+}	Pb^{2+}	Mg^{2+}	Mn^{2+}	Ni^{2+}	Co^{2+}	Na^{+}	K^{+}	Cr^{3+}	Ca^{2+}	Al^{3+}
Concentration g/l	2.2	0.870	0.1165	0.0081	0.027	0.0016	0.0007	0.0003	0.109	0.170	0.001	0.141	0.002

* Perkin Elmer Model 300 Atomic Absorbtion Spectrophotometer.

Table 4

Ion-exchange separation of cadmium from industrial solutions (determinations were performed by atomic absorbtion spectrophotometry)*

Ion	Loaded amount (g)	Eluted amount (g)
Cd^{2+}	13.64	13.47

* Perkin Elmer Model 300 Atomic Absorbtion Spectrophotometer.

It was only after 10 l eluent that zinc was traced.

The resin column was regenerated with a solution of 10% sodium chloride, when all metals adsorbed on resin were eluted.

Conclusions. The separation of cadmium from zinc in sulphuric aqueous solutions, resulted from lye washing of volatile powders in lead and zinc metallurgy, was studied.

The separation of cadmium from zinc and other accompanying elements, with Vionit CS-3 (strongly acid cation exchange resin) was realized, by selective elution with aqueous 0.2 N NaCl solution.

In view of establishing the separation conditions, distribution coefficients in aqueous NaCl solutions were determined.

REFERENCES

1. R. Wickbold, *Z. analyt. Chem.*, **132**, 401 (1951).
2. Ch. K. Mann, Ch. L. Swanson. *Analyt. Chem.*, **33**, 459 (1961).
3. F. Nelson, T. Murase. K. A. Kraus, *J. Chromatog*, **13**, 503 (1964).
4. F. W. Strelow, *Analyt. Chem.*, **32**, 1185 (1960).
5. I. Yoshino, M. Kojima, *Japan Analyst*, **4**, 311 (1955).
6. C. Liteanu, „Analiza chimică cantitativă-volumetria", Ed. Didactică şi pedagogică, Bucureşti, 1964, p. 596 şi p. 597.
7. T. W. Strelow, R. Rethemeyer, C.J.C. Bothma, *Analyt. Chem.*, **37**, 106 (1965).
8. D. S. Sklyapnikov, *Eksp. Issled. Protsessov Mineralobrazol*, **41**, 50 (1970).

STUDIA UNIV. BABEŞ—BOLYAI, CHEMIA, XXXI, 1, 1986

ÜBER DIOXIMINKOMPLEXE DER ÜBERGANGSMETALLE[1] LXVIII. die wasserstoff-dinitro-bis-octoximino-rhodiat (III)

CSABA VÁRHELYI*, FERENC MÁNOK*, NICOLAE ALMÁSI* und ILONA NAGY*

Eingegagen am 21 Januar 1985

ABSTRACT. — **On Dioximine Complexes of Transition Metals (LXVIII).** *Hydrogen-Dinitro-Bis-Octoximino-Rhodiat (III).* A new monobasic complex acid of rhodium (III): H [Rh (Octox. H_2 $(NO_2)_2$] has been obtained by a substitution reaction at $Na_3[Rh(NO_2)_6]$ with) 1,2-cyclo-octane dione dioxime (Octox. H_2). The complex is characterized by a series of double exchange reactions (17 new ammonium and cobalt (III)-amine salts) as well as by pH-metric measurements and UV and IR spectra, respectively.

Einleitung. Im Gegensatz zum Kobalt (III) entstehen die Rhodium(III)-dioximinchelate ohne Verwendung von Oxidationsmitteln. Das Rh(II) katalysiert die Bildung von Rh(III)-komplexen und deshalb ist es zweckmässig kleine Mengen Reduktionsmittel (z.B. Unterphoshorige Säure, Hydrazin, Alkohol) dem Reaktionsgemisch hinzufügen [1]. Die ersten Dioximinchelate des Rhodiums wurden von Chugaev und Lebedinskii erhalten [2]. Später haben Lebedinskii und Fedorov [3], Dwyer und Nyholm [4], bzw. Malatesta und Turner [5] einige Derivate der wichtigsten Komplextypen mit Dimethylglyoxim und Furyldioxim beschrieben. Ebenso haben Syrzova und Bolgar [6] die Kinetik der Hydrolyse einiger gemischten Sulfito-säuren von Typ $H_2[Rh(DH)_2X(SO_3)]$ (X = Cl, Br, I) untersucht. Weber und Schrauzer [7] haben einige Organyl-rhodoxime hergestellt und eine weitgehende Analogie mit den Kobaloximen vom chemischen und biochemischen Standpunkt ausbetrachtet, gefunden. Rhodium(III) Chelate wurden mit den höheren homologen der alycyclischen Dioximen nicht erhalten.

Resultate und Diskusrsion. In Fortsetzung unserer Untersuchungen über Dioximinchelate berichten wir in vorliegender Arbeit über die Bildung und Eigenschaften einer neuen monobasischen Komplexsäure des Rhodiums(III) mit 1,2-Cyclooctandiondioxim (Octoxim).

Das Hexanitro-rhodat(III)-Ion dient als Ausgangssubstanz für eine Reihe von Substitutionsreaktionen mit Aminen, Phosphinen, substituierten Oximen, Schiff'schen Basen, usw. Die Reaktion mit Octoxim (Octox.H_2) läuft nach folgender Gleichung ab:

$$Na_3[Rh(NO_2)_6] + 2\ Octox.H_2 = Na[Rh(Octox.H)_2(NO_2)_2] + 2\ NaNO_2 + 2HNO_2$$

[1] LXVII. Mitt. Cs. Várhelyi, J. Zsako, G. Liptay, M. Somay, *Rev. Roumaine Chim., 30,* 695 (1985

* *Universität Cluj—Napoca, Facultät für Chemie, 3400 Cluj-Napoca, Romania*

Aus wässriger Lösung kann die Komplexsäure mit kalter, verdünnter Schwefelsäure in Freiheit gesetzt werden.

Beim Erwärmen mit 1,5 Mol verd. Schwefelsäure tritt eine Aquotisierungsreaktion auf:

$$H[Rh(Octox.H)_2(NO_2)_2] + H_2O = [Rh(Octox.H)_2(H_2O)(NO_2)] + HNO_2$$

$H[Rh(Octox.H)_2(NO_2)_2]$ ist eine mittelstarke monobasische Säure. Die Dissoziationskonstante $K = 5 \cdot 10^{-3}$ (aus pH- metrischen Messungen [8]). Diese setzt CO_2 aus $NaHCO_3$ in Freiheit, und gibt eine Reihe Ammoniumsalze mit den Chlordydraten einiger heterocyclischen Aminen und Alkaloiden. Einige neue Ammoniumsalze sind in Tabelle 1 charakterisiert.

Tabelle 1

Neue Ammoniumsalze von Typ Amin. $H[Rh(Octox.H)_2(NO_2)_2]$

Formel	Mol. Gew. ber.	Charakteristik		Analyse Ber.	Analyse Gef.
o-Phenanthrolin·HA	714,5	Hellgelbe, kleine unregelmäss. Krist.	C	47,07	46,90
			H	4,94	5,18
			N	15,68	15,03
o-Oxy-chinolein·HA	680,3	Gelbe Würfeln	C	44,14	43,90
			H	5,03	5,25
			N	14,41	14,70
Benzimidazol·HA	653,3	Gelbe mikrokrist. Masse	C	42,28	42,00
			H	5,09	5,34
			N	17,15	17,50

A = $[Rh(C_8H_{13}H_2O_2)_2(NO_2)_2]$

Die einwertigen Übergangsmetallkationen, wie z.B. Ag^+, Tl^+ und Cu^+, sowie die Komlexkationen des Diacido-tetramin Typs bilden mit der obenerwähnten Dinitro-säure schwerlösliche Salze.

Sehr charakteristisch sind die binären Komplexsalze vom Typ $[Co(Diox.H)_2(Amin)_2] \cdot [Rh(Octox.H)_2(NO_2)_2]$. Die physikalischchemischen Eigenschaften dieser Komplexverbindungen ähneln mit denjenigen der analogen Kobalt(III)-derivaten:
$[Co(Diox.H)_2(Amin)_2] \cdot [Co(Diox.H)_2^x(NO_2)_2]$. Es ist bemerkenswert, dass die zwei- und dreiwertigen hydratisierten Metallionen ($M^{II} = 3d^5 - 3d^{10}$ Metalle, M^{III} = Fe, Al, Cr, Lanthaniden), die Hexammine $[M(NH_3)_6]^{3+}$, $[M(en)_3]^{3+}$ usw.) und die Monoacidopentammine $[M(NH_3)_5X]^{2+}$ $[M(en)_2X(Amin)]^{2+}$ keine Fällungsreaktionen mit $[Rh(Octox.H)_2(NO_2)_2]^-$ geben.

In den Ultraratspektren der $H[Rh(Octox.H)_2(NO_2)_2]$ und $Ag[Rh(Octox.H)_2(NO_2)_2]$ erscheinen die $^{v}N-OH$ und $^{v}N-O$ — Frequenzen bei 1330 (1325) (s.s.), bzw. bei 1425 cm^{-1} (s.s.) und die δONO — Deformationsschwingungsfrequenzen bei 830 cm^{-1} (s). Aus dieser Erscheinung geht hervor, dass die

Tabelle 2

Metall- und Metallamin-Salze der $H[Rh(Octox.H)_2(NO_2)_2]$ – Säure

No.	Formel	Mol. Gew. ber.	Charakteristik		Analyse Ber.	Analyse Gef.
1.	trans-$[Co(en)_2Br_2] \cdot A$	872,3	Gelbgrüne, kleine Prismen	C H N	27,54 4,86 16,05	28,45 5,04 15,57
2	trans-$[Co(pn)_2Cl_2] \cdot A$	811,5	Gelbe, kurze Prismen	C H N	32,60 5,32 17,26	33,20 5,85 16,80
3	trans-$[Co(en)_2Cl_2] \cdot A$	784	Gelbgrüne Nadeln	C H	30,64 5,40	30,30 5,15
4	cis-$[Co(en)_2Cl_2] \cdot A$	784	Braune Prismen	N	17,86	17,60
5	$Ag \cdot A$	642	Gelbe, mikrokrist. Masse	C H	29,94 4,08	29,50 4,40
6	$Tl \cdot A$	738,5	Gelbe, mikrokrist. Masse	C H	26,02 3,54	25,15 3,19

HgA_2 (Gelbe mikrokrist. Masse) (nicht analysiert)

PdA_2 (Gelbbraune mikrokrist. Masse)

Tabelle 3

Neue binäre Komplexsalze von Typ $[Co(DH)_2(Amin)_2][Rh(Octox \cdot H)_2(NO_2)_2]$

No.	Formel	Mol. Gew. ber.	Charakteristik		Analyse Ber.	Analyse Gef.
1	$[Co(DH)_2(Anilin_2] \cdot A$	1008,7	Braune Würfel	C H N	42,87 5,39 16,66	42,56 5,71 16,27
2	$[Co(DH)_2(p\text{-Äthyl-anilin})_2] \cdot A$	1064,8	Gelbbraune, dünne Nadeln	C H N	45,11 5,86 15,78	44,70 6,18 15,11
3	$[Co(DH)_2(NH_3)_2] \cdot A$	857,3	Quadratische, gelbe Platten	C H	33,63 5,40	33,10 5,10
4	$[Co(DH)_2(Thioharnstoff)_2] \cdot A$	975,5	Unregelmäss. kleine, braune Krist.	N	20,10	20,25
5	$[Co(DH)_2(m\text{-Amino-phenol})_2] \cdot A$	1040,7	Gelbbraune Nadeln	C H N	42,51 5,25 16,15	42,10 5,65 15,90
6	$[Co(DH)_2(m\text{-Toluidin})_2] \cdot A$	1037,6	Braune Prismen	C H	43,97 5,63	43,10 5,20
7	$[Co(DH)_2(o\text{-Anisidin})_2] \cdot A$	1068,8	Kleine, braune Plättchen	C H N	42,70 5,47 15,73	41,80 5,39 15,36
	$[Co(DH)_2(p\text{-Phenetidin})_2] \cdot A$	1096,8	Lange, dunkelbraune Platten	C H N	43,80 5,69 15,32	44,25 5,85 14,70

DH = $C_4H_7N_2O_2$ (deprotoniertes Dimethylglyoxim)

Rh-Nitro-Bindung, im Gegensatz zu den Nitrito-Komplexen (M-ONO), durch das Stickstoffatom verwirklicht wird. Die bei 1545 (1560) cm^{-1} (s.s.), 1245 (s.s.), 1100 cm^{-1} (s.s.) auftretenden Banden können den koordinierten Octoximliganden zugeordnet werden. Die $\nu C-H$ und δCH_2 — Frequenzen des Octoxims erscheinen bei 2950 (2940) (s) und 2880 (2875) cm^{-1} (s), bzw. bei 1470 und 1380 (1385) cm^{-1} (m) und werden durch den Koordinationseffekt nicht beeinflusst. Bei 2550—2585 cm^{-1} tritt eine breite mittlere Bande auf, welche im Falle des analogen $H[Rh(DH)_2Cl_2]$ von Gillard und Mitarbeiter [9] zu den intramolekularen O—H..O Wasserstoffbrückenbindungen zugeordnet wurde. Diese O—H..O Bindung ist länger und schwächer im Vergleich mit derjenigen des Kobalt(III) — Analoga ($\nu O-H$: 2250 — 2280 cm^{-1} (m)) und stabilisiert die $Rh(Octox.H)_2$ koplanare Atomgruppe (siehe Abb. 1.)

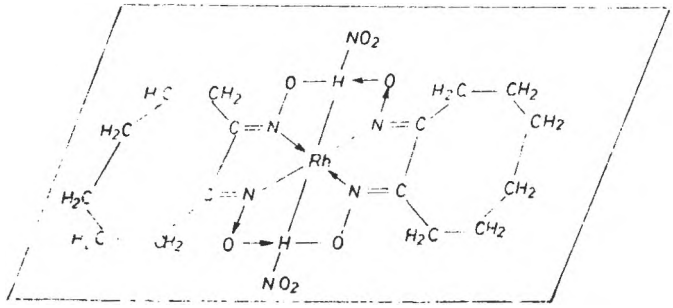

Abb. 1 Die Struktur der $Rh(Octox.H)_2(NO_2)_2[$ — Atmogruppe

Die Lichtabsorption der $H[Rh(Octox.H)_2(NO_2)_2]$ — Säure wurde in Methanol untersucht. Die Absorptionskurve zeigt keine d—d Übergansbande im sichtbaren Bereiche. Im UV-Gebiete tritt nur eine Ladungsüberführungsbande bei 36—38 kK. ($\log \varepsilon = 4{,}2$) auf. Die analoge Bande bei den Kobalt(III)-Dioximinen ist bei 40—40,4 kK erkennbar. Siehe Abb. 2.)

Experimenteller Teil. *1,2-Cyclooctandiondioxim* wurde aus Cyclooctanon (BDH) durch selektive Oxydation mit SeO_2 in absolutem Athanol und nachfolgender Oximierung des destillierten 1,2-Cyclooctan

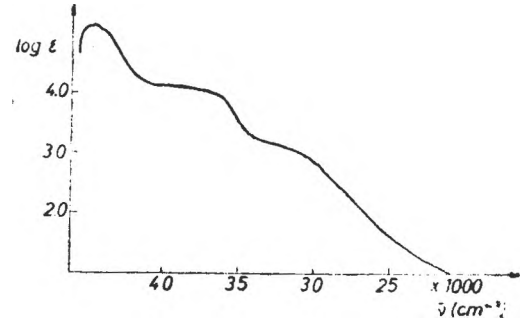

Abb. 2. Lichtabsorption von $H[Rh(Octox\cdot H)_2(NO_2)_2]$

dions (Siedepunkt$^{12\ mm}$; 100—105°) mit Hydroxyl-aminhydrochlorid in Pyridin erhalten. Das Rohprodukt wurde aus heissem Wasser umkristallisiert. Schmelzpunkt: 230°C (Zers.) [10].
$Na[Rh(Octox.H)_2(NO_2)_2]$ — *Lösung.* 0,02 Mol $RhCl_3 \cdot 3H_2O$ werden in einem mit Rückflusskühler versehenen Kolben mit 0,12 Mol $NaNO_2$ in 50—60 ml Wasser 2—3 Stunden gekocht. Die anfangs rotviolette Farbe des $RhCl_3$ tritt langsam in eine blassgelbe über ($Na_3[Rh(NO_2)_6]$. Dann werden 0,04 Mol Octoxim in 20—25 ml Athanol hinzugefügt und die Mischung noch 5—6 Stunden erhitzt. Die gelbe Lösung wird dann abfiltriert und zur doppelten Umsetzungsreaktionen verwendet.
$H[Rh(Octox.H)_2(NO_3)_2] \cdot H_2O \cdot 2mMolNa[Rh(Octox.H)_2(MO_2)_2]$
in 15—20 ml wässriger Lösung werden mit 2—3 ml 20%-iger Schwefelsäure behandelt. Die Dinitro-säure scheidet sich nach 15—20 Min. Stehenlassen in Form von hellgelben, dünnen Nadeln ab. $H[Rh(C_8H_{13}N_2O_2)_2(NO_2)_2] \cdot H_2O$ (Mol · Gew. 552,3); C ber 34,80, gef. 35,40, H ber. 5,29, gef. 5,47, N ber. 15,21, gef. 15,03.
Amin · $H[Rh(Octox.H)_2(NO_2)_2]$ und Kation. $[Rh\ (Octox.\ H)_2(NO_2)_2]$
Für die doppelten Umsetzungsreaktionen wurden je 10—15 mMol Amin. HCl, bzw. Komplexsalze in 20—30 ml Wasser oder verd. Äthanol und je 1—1,5 mMol $Na[Rh(Octox.H)_2(NO_2)_2]$ in 10—15 ml Wasser verwendet. Die entstehenden kristallinen Niederschläge wurden nach 15—30 Min. Stehenlassen abfiltriert, mit Wasser gewaschen und an der Luft getrocknet.

LITERATUR

1. R. D. Gillard, J. A. Osborn, G. Wilkinson, J. *Chem. Soc.*, **1965,** 1951.
2. L. A. Ciugaev, L. L. Lebedinskii, *Z. anorg. allg. Chem.*, **83,** 1 (1913).
3. V.V. Lebedinskii, I. A. Fedorov, *Izv. Sektova Platiny, Akad. Nauk SSSR,* **15,** 19 (1938); **17,** 81 (1940); **21,** 157 (1948); **22,** 158 (1948).
4. F.P. Dwyer, R. S. Nyholm, *J. Proc. Roy. Soc. N.S. Wales,* **77,** 256 (1944); **79,** 126 (1946).
5. L. Malatesta, F. Turner, *Gazz. chim. Ital.*, **72,** 489 (1942).
6. G. P. Syrzova, T. S. Bolgar, *Zhur. neorg. Khim.*, **14,** 2425 (1969); **16,** 2478 (1971); **17,** 455, 2719 (1972); **18,** 2156, 2706 (1973).
7. J. H. Weber, G. N. Schrauzer, *J. Amer. Chem. Soc.*, **92,** 726 (1970).
8. Cs, Várhelyi, Z. Finta, *Magy. Tud. Akad. Kém. Oszt. Közl.*, **45,** 79 (1976).
9. R. D. Gillard, G. Wilkinson, *J. Chem. Soc.*, **1963,** 6041.
10. J. Zsakó, J. Horák, Z. Finta Cs. Várhelyi, I. Mitrache, *Mikrochim. Acta,* **1979 I,** 405.

STUDIA UNIV. BABEŞ—BOLYAI, CHEMIA, XXXI, 1, 1986

STUDIEREA DESORBŢIEI SO_3 ŞI SO_2 DIN DIFERIŢI ABSORBANŢI

J. VODNÁR*

Intrat în redacţie: 6 februarie 1985

ABSTRACT. — **The Study of SO_3 and SO_2 Desorption from Different Absorbents.** The paper presents the results obtained by desorption of SO_3 from some absorbents composed of NMP (N-methylpyrrolidone) and water or E6 (ethylene glycol), fatty alcohols with C_{14}—C_{16} in their molecules and the desorption of SO_2 from NMP. The best absorbent for desorption of SO_3 is that composed of 75 vol. % NMP and 25 vol. % E6 and for the desorption of SO_2 is that composed of 75 vol. % NMP and 25 vol. % E6 and for desorption of SO_2 that composed of pure NMP. In the first case total desorption takes place at 80 °C, and in the second case at 65 °C.

În scopul de a se putea recupera şi valorifica trioxidul şi dioxidul de sulf din gazele emanate de fabricile de acid sulfuric, de instalaţiile metalurgice de prăjire, topire şi rafinare, de termocentralele care utilizează drept combustibil diferite varietăţi de cărbune (şi care emană în atmosferă gaze de ardere ce conţin 0,08—0,25% vol. SO_2, SO_3, H_2S şi debitul de emanare poate să ajungă la 1 mil. m^3/h) etc., a devenit necesară studierea absorbţiei şi desorbţiei acestor substanţe, utilizînd în acest scop diferiţi absorbanţi şi aparate cu peliculă de lichid turbulentă ascendentă brevetate de autor [1—7].

În această lucrare se descriu rezultatele obţinute la studierea desorbţiei SO_3 şi SO_2 dintr-o serie de absorbanţi, dintre care unii s-au dovedit a fi mai eficace decît orice alt absorbant utilizat în acest scop [7].

Partea experimentală. Trioxidul de sulf necesar obţinerii probelor destinate desorbţiei a fost obţinut prin oxidarea dioxidului de sulf pe un catalizator de pentoxid de vanadiu, utilizînd ca agent de oxidare oxigenul tehnic. În calitate de absorbanţi s-au utilizat amestecuri de NMP (N-metilpirolidonă) şi apă, de NMP şi EG (etilenglicol), NMP şi EG pur şi un amestec de alcooli graşi cu C_{14}—C_{16} în moleculă. Desorbţia SO_2 s-a studiat numai din NMP.

Desorbţia a fost efectuată cu o balanţă termogravimetrică echipată cu un cuptor electric în care probele supuse desorbţiei au putu fi menţinute la temperaturi constante.

Interpretarea rezultatelor. În prima serie de experienţe s-a studiat gradul de saturare al unor absorbanţi. În cazul absorbanţilor cu conţinut de NMP gradul de saturare maxim (100%) s-a considerat că se realizează dacă unui mol de NMP îi revine un mol de SO_3, iar în cazul EG şi alcoolilor graşi cu C_{14}—C_{16} în moleculă s-a considerat că unui mol de substanţă îi revine un mol de SO_3. Rezultatele obţinute la saturarea unor absorbanţi cu SO_3 se prezintă în graficul din Figura 1 în care sînt redate gradele de saturare ale diferiţilor absorbanţi exprimate în procente de masă.

Se poate vedea că cel mai înalt grad de saturare cu SO_3 se obţine în cazul probei de alcooli graşi (98%). În schimb, desorbţia SO_3 la aceste probe nu s-a

* *Universitatea din Cluj-Napoca, Facultatea de Ştiinţe economice, 3400 Cluj-Napoca, Romania*

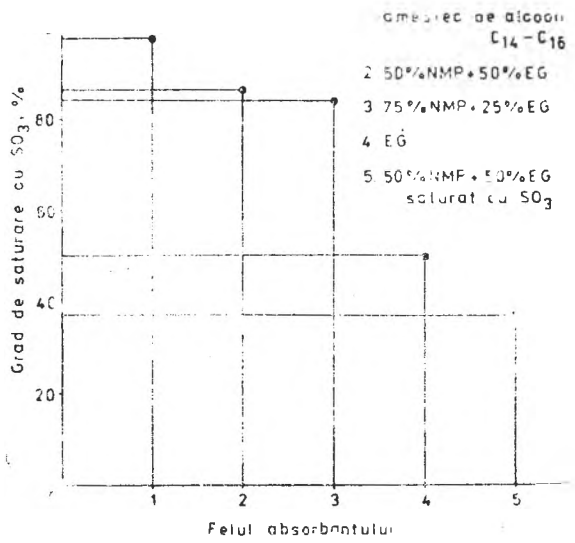

Fig. 1. Gradul de saturare cu SO_3 (%) al unor absorbanţi utilizaţi.

putut studia, deoarece ea a fost însoţită de un fenomen de descompunere şi de carbonizare a probelor.

Probele cu conţinut de 75% vol. NMP şi 25% vol. apă saturate cu SO_3 au fost supuse desorbţiei la mai multe temperaturi şi s-a constatat că la 67,5°C gradul de desorbţie ajunge la 100%. În schimb, aceşti solvenţi absorb cantităţi mici de SO_3 (cca 5 g în 20 ml). În Figura 2 este ilustrată variaţia gradului de desorbţie (%) al unei asemenea probe, în funcţie de temperatura de desorbţie.

Rezultate mai bune s-au obţinut cu amestecuri de 50% vol. NMP şi 50% vol. EG, care absorb cantităţi mai mari de SO_3 şi desorbţia se petrece la temperaturi cuprinse între 60 şi 150°C. În Figura 3 este redat graficul care ilustrează cinetica desorbţiei SO_3 dintr-o astfel de probă la 120°C. Se poate vedea că viteza de desorbţie la această temperatură nu este suficient de mare pentru a satisface cerinţele practice industriale.

Astfel, dintr-o probă de 0,6 g la 120°C în timp de 10 ore se desorb doar 0,11 g SO_3, ceea ce reprezintă un grad de desorbţie de 72,69%. Desorbţia totală se poate realiza la 140—150°C cu o durată de 3—4 ore. Variaţia gradului de desorbţie a SO_3 din aceste probe (%), în funcţie de temperatură, este ilustrat în Figura 4. Din grafic reiese că la temperaturi care depăşesc 120°C, se ajuhge la grade de desorbţie mai mari de 100%, ceea ce ne arată că la asemenea temperaturi se produc deja şi pierderi de solvent măsurabile (care în aplicaţiile industriale sînt totuşi, în general inevitabile).

Rezultatele de desorbţie a SO_3 cele mai promiţătoare din punct de vedere practic s-au obţinut în cazul probelor la care drept absorbant s-a utilizat un amestec de 75% vol. NMP şi 25% vol. EG. În Figura 5 este redată curba cinetică a desorbţiei SO_3 dintr-o astfel de probă la 60°C. Tot acolo apare şi curba cinetică înregistrată în cazul unei probe martor (M) care este compusă doar din absorbantul respectiv, neconţinînd şi SO_3 absorbit.

Se poate constata că desorbţia SO_3 din această probă are loc cu viteză mai mare (0,41 mg/min), chiar şi la numai 60°C, decît în cazul probei ilustrate în Figura 3 (0,21 mg/min), deşi în acest caz din urmă desorbţia s-a executat la temperatură de două ori mai mare, 120°C. În acelaşi timp, curba cinetică a probei martor (M) ne arată că la 60°C solventul are o tensiune de vapori foarte mică, pierderile de greutate fiind nesemnificative, ele producîndu-se cu viteza de 0,027 mg/min).

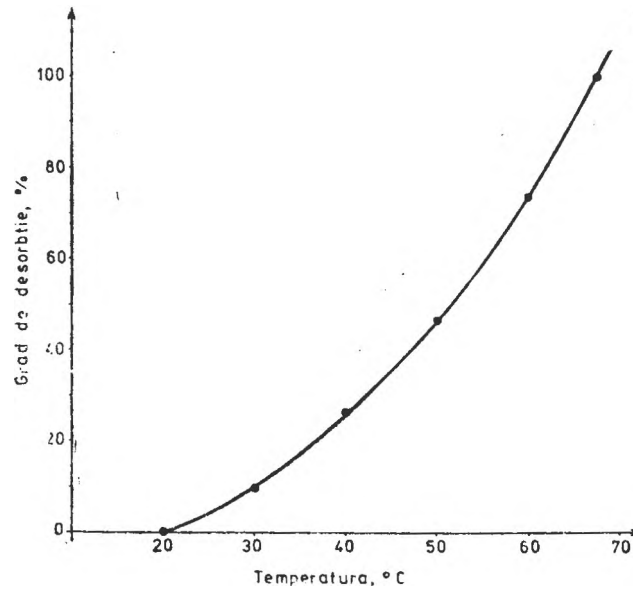

Fig. 2. Variația gradului de desorbție a SO_3 dintr-un absorbant format din 75% vol. NMP și 25% vol. apă.

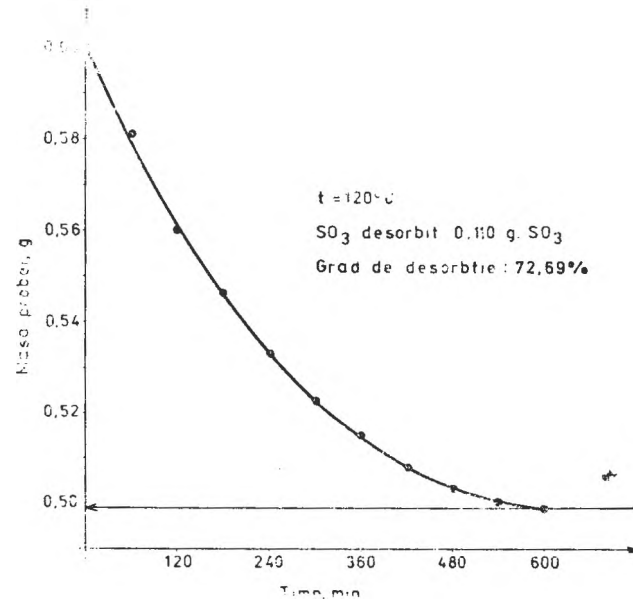

Fig. 3. Curba cinetică a desorbției SO_3 dintr-un absorbant format din 75% vol. NMP și 25% vol. apă.

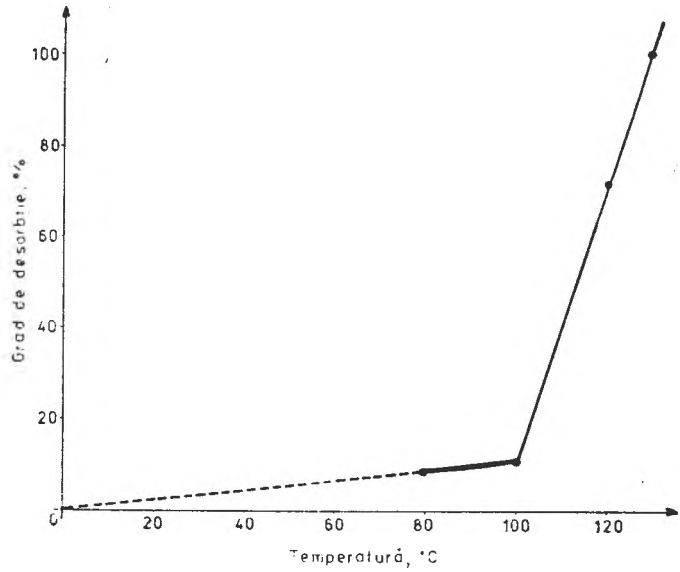

Fig. 4. Variaţia gradului de desorbţie a SO_3 din probe la care absorbantul este format din 50% vol. NMP şi 50% vol. EG.

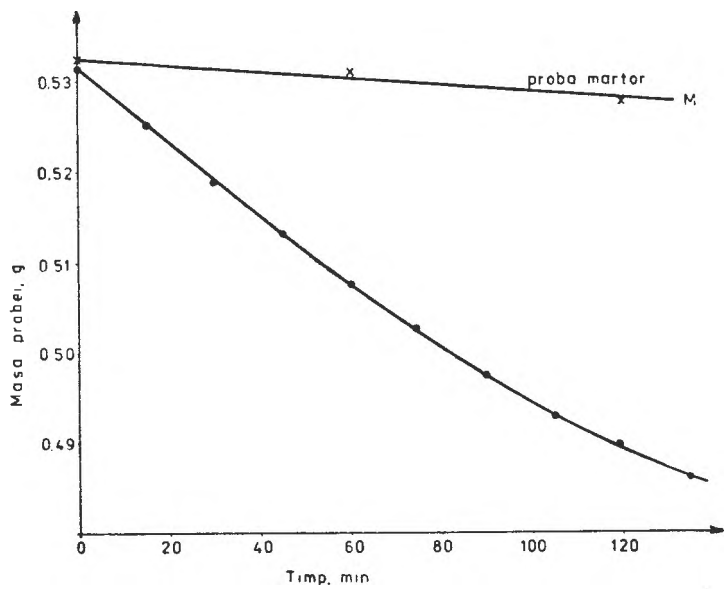

Fig. 5. Curba cinetică a desorbţiei SO_3 dintr-o probă cu 75% vol. NMP şi 25% vol. EG şi curba probei martor (M).

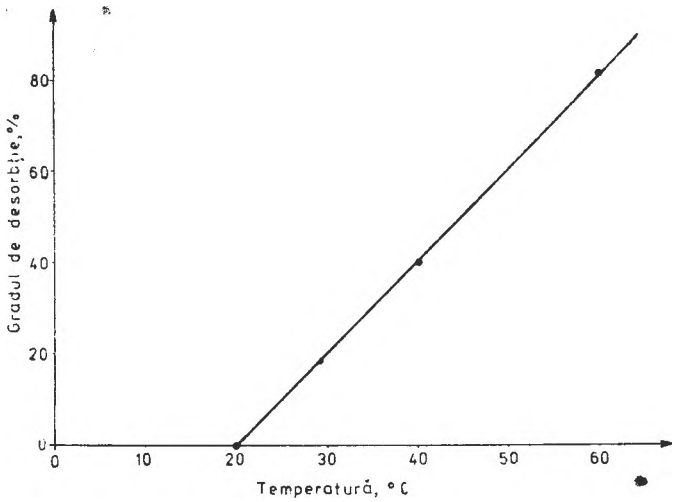

Fig. 6. Variația gradului de desorbție a SO_3 (%) în funcție de temperatură, utilizînd probe la care absorbantul este format din 75% vol. NMP și 25% vol. EG.

Dacă aceeași probă se supune desorbției la 80°C, eliminarea SO_3 se petrece cu viteză și mai mare (0,47 mg/min), fără ca pierderile de solvent să fie mai semnificative. Pentru a se evidenția mai bine diferența existentă între intensitatea desorbției la diferite temperaturi, s-a construit graficul din Figura 6 în care se dă variația gradului de desorbție a SO_3 (%), în funcție de temperatură (la 20°C desorbția nu are loc în măsură determinabilă).

Din grafic reiese că gradul de desorbție a SO_3 crește liniar cu ridicarea temperaturii de la 20 la 60°C. Deoarece gradul de desorbție la 60°C este de numai 81%, în cazul cînd se impune o desorbție de 100%, se recomandă să se lucreze la temperatura de 80°C, la care pierderile de solvent sînt încă nesemnificative, dar desorbția este practic totală.

Absorbantul format din 75% vol. EG și 25% vol. NMP, deși absoarbe bine SO_3, în scopuri industriale nu se recomandă, deoarece desorbția decurge numai peste 95°C și are loc prin descompunerea probei (proba se înnegrește, ceea ce indică o carbonizare). Curba cinetică de desorbție a unei astfel de probe este ilustrată de graficul din Figura 7. Se poate vedea că viteza de desorbție inițială este relativ mare (0,55 mg/min), în schimb are loc descompunerea și carbonizarea probei. Asemănător se comportă și probele în care drept absorbant a fost utilizat EG pur sau alcoolii grași cu C_{14}—C_{16} în moleculă.

Desorbția dioxidului de sulf s-a studiat prin aceeași metodologie care a fost descrisă la desorbția trioxidului de sulf, în schimb în acest caz s-au utilizat

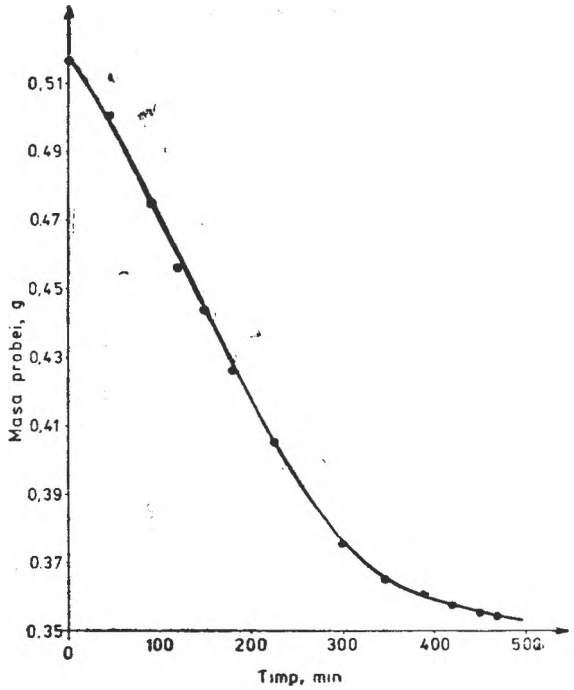

Fig. 7. Curba cinetică de desorbție a SO_2 dintr-o probă cu 75% vol. EG și 25% vol. NMP.

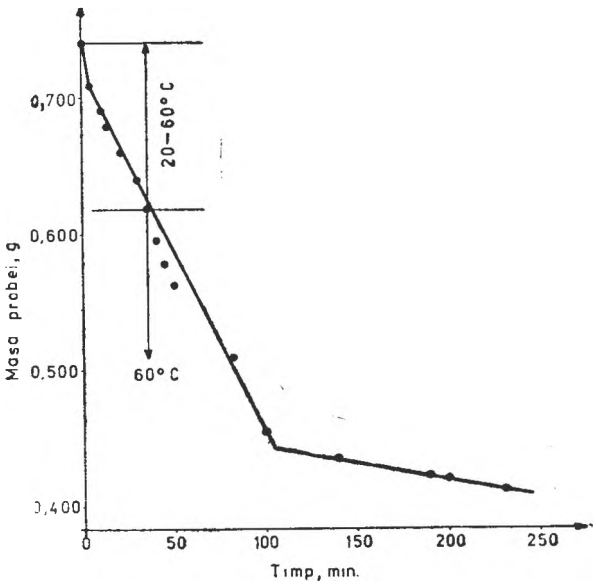

numai probe în care drept absorbant s-a utilizat numai NMP pură, care s-a dovedit a fi un absorbant nebănuit de eficace și în același timp prezintă avantajul că face posibilă desorbția rapidă la temperaturi coborîte (60—70 °C).

Rezultatele mai semnificative, obținute la desorbția SO_2 din soluții cu NMP sînt ilustrate în graficul din Figura 8. În timpul desorbției temperatura s-a mărit treptat pînă la 60 °C, unde s-a menținut apoi constantă pe toată durata experienței. Din grafic reiese că în timp de cca 90 minute desorbția SO_2 nelegat chimic, practic se termină. În condițiile unei încălziri mai rapide a probei (de ex.: încălzire directă cu bile de aluminosilicat) desorbția are loc cu viteză mare, ea fiind aproape spontană. De aceea trebuie create condițiile în care soluția (absorbitul) SO_2–NMP să vină în contact treptat, în doze relativ mici, cu suprafața încălzită, pentru a se preveni creșterile bruște de presiune în instalație, care ar putea cauza avarii grave.

Fig. 8. Curba cinetică de desorbție a SO_2 dintr-o probă cu NMP.

BIBIOGRAFIE

1. I. Vodnár, *Brevet de invenție* al R.S.R., București, Nr. 81993 (1983).
2. I. Vodnár, *Simpozion internațional organizat de Institutul de cercetări miniere.* Cluj-Napoca, vol. **2**, 55 (1979).
3. I. Vodnár, *Culegere de studii și cercetări economice,* vol **X**, 329 (1981), Cluj-Napoca.
4. J. Vodnár, 288-*th Event of the European Federation of Chemical Engineering* (Proceedings of the 4-th Conference on Applied Chemistry, Unit Operations and Processes), vol. **3**, 9 (1983), Veszprém (Hungary).
5. I. Vodnár, *Brevet de invenție* al R.S.R., Nr. 75628 (1981), București.
6. J. Vodnár, *Studia Univ. Babeș—Bolyai, Chemia,* 1985 (sub tipar).
7. J. Vodnár, C. Tohátan, V. Bozîntan, Gh. Ilia, Gh. Grebles, *Brevet de invenție al R.S.R.*, Nr. 81661 (1983), București.

STUDIA UNIV. BABEŞ—BOLYAI, CHEMIA, XXXI, 1, 1986

THE ABSORPTION OF SULFUR DIOXIDE IN AN ASCENDING TURBULENT LIQUID FILM[1]

III. Using saturated aqueous solution of calcium hydroxide as an absorbent

I. VODNAR*

Received: February 6, 1985

ABSTRACT. — The paper presents and discusses the results obtained by the absorption of sulfur dioxide from diluted gases (for instance that of the heat power plant), using aqueous solution of calcium hydroxide as an absorbent. The apparatus used enables to make absorption in an ascending turbulent liquid film. During the absorption the liquid phase was permanently recycled and mixed by a self-induced mixing. When the flow of calcium hydroxide was 500 ml/min, the coefficient of absorption had a value equal to 98%. On the base of experimental data it seems that the degree of absorption possibly can rise to 99%, or to a higher value, too.

The paper presents some results obtained by studying the absorption of sulfur dioxide from diluted gases (for instance that of the heat power plant), using aqueous solutions of calcium hydroxide as an absorbent. The apparatus [2] used enables to make absorption in an ascending turbulent liquid film. During the absorption the liquid phase was permanently recycled and mixed by a self-induced mixing (without a mechanical stirrer which requires high energy consumption and the use of some tight closing devices exposed to high wear). The apparatus was equipped with a one metre long glass tube for the formation of an ascending turbulent calcium hydroxide film (saturated aqueous solution), having the inner diameter equal to 18 mm, and the inner surface where the absorption takes place was 0,05652 m^2.

Experimental. Experiments were made in a micropilot apparatus which is a usable model of that mentioned in [2]. The ascending turbulent liquid film was formed on the inner surface of the pelliculizing tub. The used liquid film was continuous. The absorbent was used in a continuous flux and it was introduced with a peristaltic pump. The necessary sulfur dioxide was taken from a steel cylinder vessel and the air was ensured by an adequate compressor.

The sulfur dioxide content of the gas mixture was determined iodometrically and the absorbed sulfur dioxide by acid-base titration, too. Temperature varied between 20 and 35 °C. The saturated aqueous solution of calcium hydroxide as an absorbent was introduced in the apparatus continuously and the solution resulted by absorption was eliminated in the same way.

The used gas flow was 5—10 m^3/h and that of the absorbent varied from 60 to 700 ml/min.

Results and discussion. In the first series of experiments the dependence of the sulfur dioxide content of purified gas versus the absorbent flow (which was an aqueous solution of calcium hydroxide, containing 1,48 $Ca(OH)_2$/1000 ml) was studied. The temperature was 21 °C, the gas flow 10 m^3/h and the sulfur

---

[1] Part II, see [1].

* *University of Cluj-Napoca, Falculty Economic Sciences, Chemistry Department, 3400 Cluj-Napoca, Romania*

dioxide content of the used gas was 0,25 vol. %. The results obtained are illustrated in figure 1.

We can see that the sulfur dioxide content of purified gas decreases from 0,16 to 0,01 vol.% when the absorbent flow varies from 60 to 500 ml/min. This graph can be characterized by the following mathematic equation:

$$y = \frac{a}{x} \tag{1}$$

when a is constant.

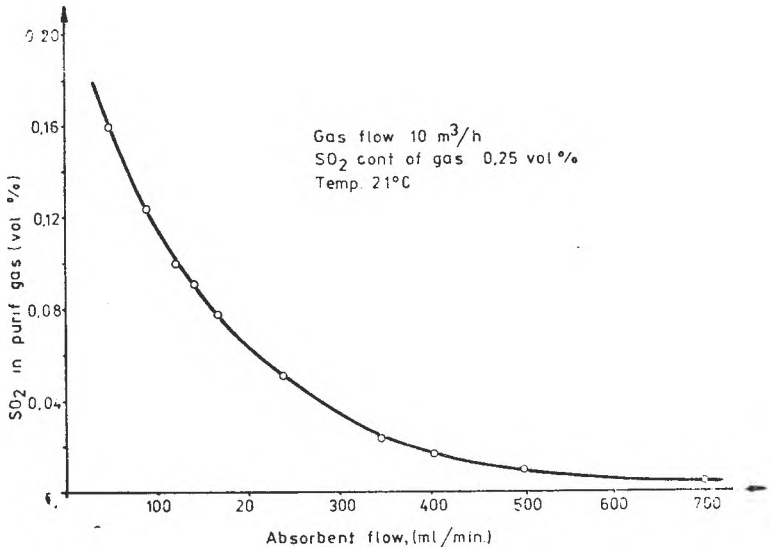

Fig. 1. Variation of sulfur dioxide content of purified gas (%) versus absorbent flow (ml/min).

In figure 2 we illustrated the influence of the gas flow versus the sulfur dioxide content of the purified gas, which as we can see, increases liniarly with the increas of the gas flow. When the gas flow varies from 4 to 10 m³/h, the sulfur dioxide content increases from 0,030 to 0,120 vol. %, if temperature is 21°C, initial sulfur dioxide content of the gas 0,25 vol.% and the flow of the saturated aqueous solution of calcium hydroxide as an absorbent is 88 ml/min. One can conclude that for a high purification of the residul gases, some higher flow of the absorbent must be used. This graph can be characterized mathematically by the equation:

$$y = ax + b \tag{2}$$

where a means the number of vol. % corresponding to a gas flow of one m³/h;

b — the quantity of SO_2 which cannot be absorbed in the used conditions of work.

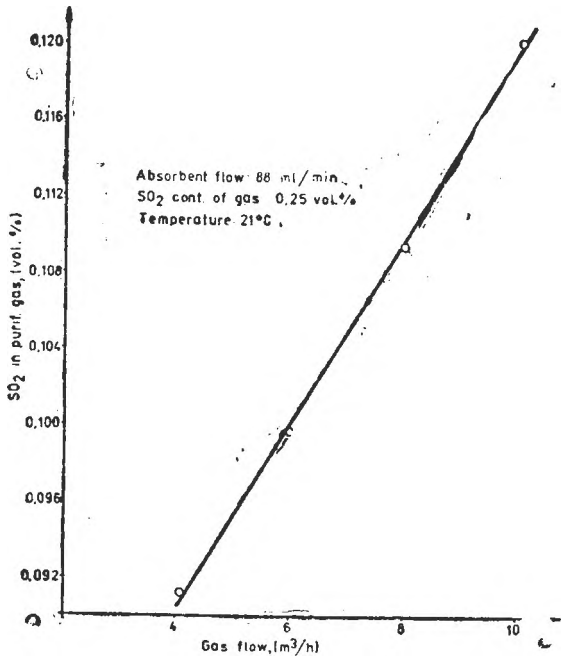

Fig. 2. Dependence between sulfur dioxide content of purified gas (%) and gas flow (m^3/h).

To verify the analytical determination concerning the sulfur dioxide content of the purified gases, the quantity of the absorbed sulfur dioxide was determined volumetrically, too. The results obtained show that the dependence between the consumption of N/10 HCl solution by the titration of calcium hydroxide solution delivered from the apparatus used during the experiment and the sulfur dioxide content of purified gases concur with that presented in Figure 1.

The most important data are illustrated in Figure 3 where the interdependence between the degree of absorption and the absorbent flow is given. The applied temperature was 21 °C, the gas flow 10 m^3/h and the sulfur dioxide constent of initial gas was 0,25 vol. %. The degree of absorption increases with the absorbent flow. Varying the absorbent flow from 88 to 500 ml/min, the degree of absorption increases from 51,4 to 96%, and if the absorbent flow attains the value of 700 ml/min, the degree of absorption is 98% (we must mention that the absorbent quantity is theoretically necessary to react with the sulfur dioxide contained by the gas is equal to 744 ml/min. So, it is possible that when such an absorbent flow is used, the degree of absorption should have a value nearly 100%). These results demonstrate the high efficiency of ascending turbulent liquid film. The graph of Figure 3 is characterized mathematically by the equation:

$$y = \frac{k \cdot x}{x + c} \tag{3}$$

where k and c are constants (see Figure 3).

The influence of tempeature on the quantity of sulfur dioxide absorbed is illustrated in Figure 4. The gas flow was 5 m^3/h, absorbent flow 371 ml/min and the sulfur dioxide content of gas was 0, 25 vol. %. This figure shows that when temperature rises from 20 to 35 °C, the absorbed quantity of sulfur dioxide increases from 34,9 to 35,1 g/h. That means the temperature has a weak influence on the sulfur dioxide absorption.

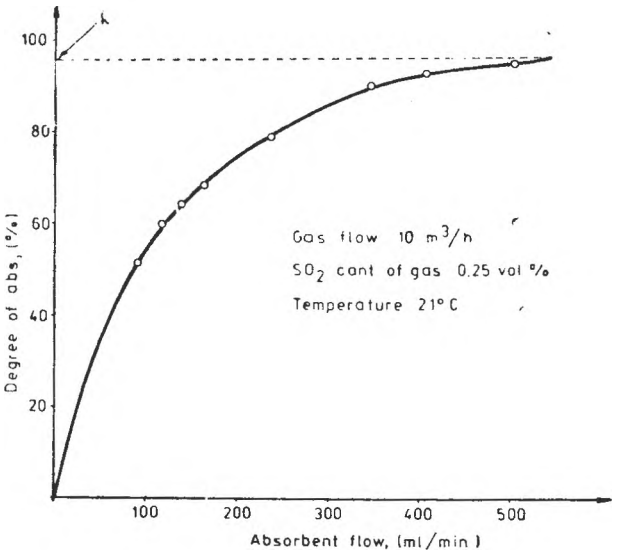

Fig. 3. Variation of degree of absorption (%) versus absorbent flow (ml/min).

The graph of figure 5 shows the influence of absorbent flow (ml/min) on coefficient of absorption (g $SO_2/m^2 \cdot h) \cdot 10^{-3}$. One can see that when the absorbent flow increases from 235 to 500 ml/min, the coefficient of absorption varies from 503 to 618 g $SO_2/m^2 \cdot h$. These results are among the best of those obtained in this field.

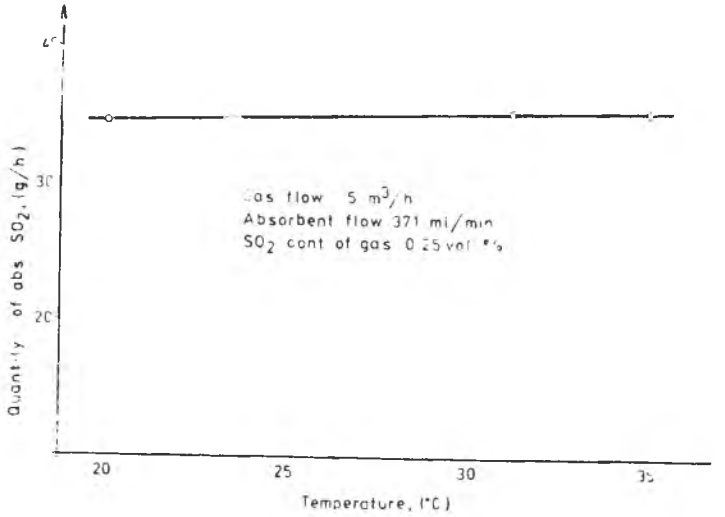

Fig. 4. Variation of absorbed quantity of sulfur dioxide (g/h) on temperature used (°C).

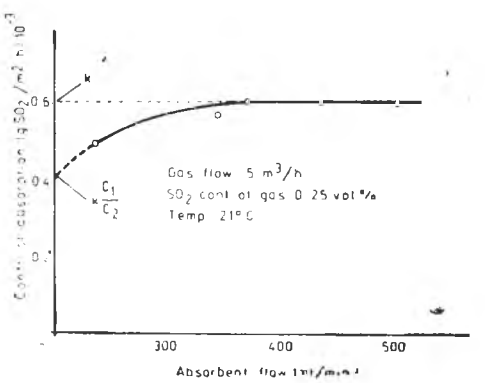

Fig. 5. Variation of absorbtion coefficient (g $SO_2/m^2 \cdot h$) versus absorbent flow (ml/min).

The graph of Figure 5 can be described mathematically by the equation:

$$y = k \cdot (x + c_1)/(x + c_2) \qquad (4)$$

where k, c_1 and c_2 are constants (see Figure 5).

The value of the coefficient of total mass transfer (K_g) was calculated by the method of W. M. Ramm [3], using the following experimental data: — initial SO_2 content of gas: 0,25 vol. % = 7,14 g/m³; — total gas flow: 5 m³/h (V_0 = 4,774 m³/h; — total initial pressure: 791,71 Hg mm; — degree of absorption: 98%; — absorbed quantity of SO_2: 0,618 kg/h; — initial partial pressure of SO_2: 1,979 Hg mm; — final partial pressure of SO_2: 0,0335 Hg mm; — motive power of absorption: 0,4775 Hg mm; — surface aria of absorption: 0,05652 m².

$$K_g = \frac{0{,}618}{0{,}05652 \times 0{,}4775} = 22{,}899 \left[\frac{\text{kg}}{\text{m}^2 \cdot \text{h} \cdot \text{Hg mm}}\right]$$

REFERENCES

1. J. Vodnár, *Studia Univ. Babeş–Bolyai, Chemia*, **30**, 59 (1985)
2. J. Vodnár, *Brevet de invenţie* al R.S.R., Nr. 81993 (1983).
3. W. M. Ramm, „Absorptionsprozesse in der Chemischen Industrie", VEB Verlag Technik, Berlin, 1953.

STUDIA UNIV. BABEŞ—BOLYAI, CHEMIA, XXXI, 1, 1986

DAS VERHALTEN VON AZOXYBENZOL UND SEINES UMLAGERUNGSPRODUKTS IN SAUREM MEDIUM

I. Herstellung und Characterisierung des Lösungsmittelsystems 20 vol.%Alkohol/80 vol. % Wassering Schwefel-oder Salzsäure

MARIA IONESCU* und HERMAN KOLCH**

Eingegangen am März 1985

ABSTRACT. — The Behaviour in Acid Medium of Azoxibenzene and its Transposition Product (I). Preparation and Characteristics of the Solvent System of 20% vol. Alcohol/80% vol Aqueous Sulphuric or Hydrochloric Acid. For the solvent Systems of 20% vol. Alcohol/80% vol Aqueous Sulphuric or Hidrochloric Acid a genuine solution preparation reproducible system has been devised, concurrently stating standard curves for determination of acid content in the measurement of density. Unlinear variation of the volume concentration with that of acid when mixing alcohol and sulphuric acid of higher concentration (over 50%), observed for the first time, is a new proof of the partial esterification that takes place in such a medium.

Nach der Untersuchung der photochemischen Umlagerung aromatischer Azoxyverbindungen in Monomerlösungen [1], bestand unsererseits Interesse, das Verhalten von Azoxybenzol und seines Umlagerungsprodukts in stark saurem alkoholischem Medium zu verfolgen.

Die von W a l l a c h 1880 erstmals beobachtete, durch konzentrierte Schwefelsäure katalysierte Umlagerung aromatischer Azoxyverbindungen in p-Hydroxyazoderivate hat bis in unsere Zeit das Interesse der Forscher wachgehalten. Bei der Bestimmung des Reaktionsmechanismus waren kinetische Messungen ausschlaggebend. Die Reaktionsgeschwindigkeiten wurden spektrophotometrisch, entweder in wässriger Schwefelsäure [2, 3], oder in organische Lösungsmittel enthaltenden Systemen [4,8] verfolgt, wobei gleichzeitig auch die pK-Werte der Azoxykörper bestimmt wurden. [2, 4, 9].

Das erstmals von J a f f é [10] bei der Untersuchung der Basizitäten substituierter Azobenzole verwendete Lösungsmittelsystem, bestehend aus 20 Vol—% Alkohol und 80 Vol—% wässriger Schwefelsäure, für das gleichzeitig eine neue Säurefunktion, H_0, aufgestellt wurde, weist gegenüber dem wässrigen System folgende Vorteile auf:

a) die Anwesenheit von Alkohol erleichtert das Studium vieler, in vollständig wässrigen Systemen schwerlöslicher Basen;

b) durch die Art der Lösungsmittelzubereitung gelingt es Lösungen gleichen reproduzierbaren Basenkonzentration bei verschiedenen Säuregehalten herzustellen.

* *Universität Cluj-Napoca, Fakultät für Chemie, 3400 Cluj-Napoca, Romania*

** *ICECHIM, Forschungszentrum für Plastmassen, Laboratorium Temeswar, Timişoara, Gării Strasse 25, Romania*

Um der starken Wärmeentwicklung beim Mischen der sauren wässrigen mit der alkoholischen Komponente, besonders bei hohen Säuregehalten, entgegenzuwirken und dadurch unter anderem eine ungewollte Umlagerung der im Alkohol gelösten Azoxyverbindung zu verhindern, haben Hahn und Jaffé [9] ein etwas umständliches Mischverfahren ausgearbeitet, wobei vier vorgekühlte Portionen wässriger Schwefelsäure steigender Konzentration der Reihe nach, unter Kühlung, der alkoholischen Lösung langsam zugefügt werden, um dann im Messkolben mit Schwefelsäure der letzten Konzentration aufgefüllt zu werden. Auch Kresge und Chen [11] mischten die beiden Komponenten unter Kühlung, obwohl sie nicht mit Azoxyverbindungen arbeiteten.

Unser Augenmerk richtete sich zunächst auf die Ausarbeitung eines reproduzierbaren Herstellungsverfahren und die genaue Charakterisierung des 20 Vol—% Alkohol enthaltenden stark sauren Lösungsmittelsystems.

Experimenteller Teil. a) *Herstellung der Lösungen:* Die Herstellung der $2 \cdot 10^{-5}$ molaren Lösungen von Azoxybenzol, bzw. p-Hydroxyazobenzol im Lösungsmittelsystem 20 Vol-% Alkohol/80 Vol-% wässrige Säure erfolgte nach einem eigenen Verfahren mittels der in Abb. 1 schematisch dargestellten Versuchsanordnung. In den Erlenmeyerkolben wurden 10 ml 10^{-4} m Stammlösung der zu untersuchenden Base in 95-%-igem Äthylalkohol und in den Scheidetrichter 35 ml wässrige Säurelösung eingeführt und etwa 5 Minuten abkühlen lassen, jedoch nicht unter den Frierpunkt

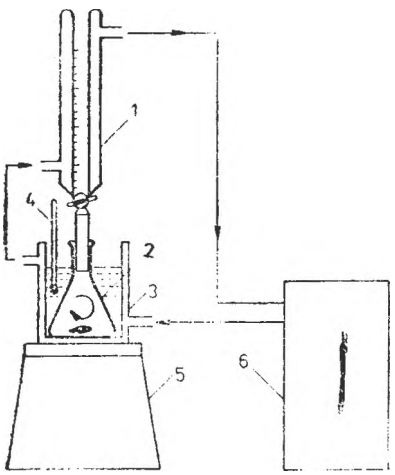

Abb. 1: Schema der bei der Herstellung der Lösungen verwendeten Apparatur: 1 — gradierte Scheidetrichter mit Kühlmantel; 2 — Erlenmeyer-Kolben (100 ml); 3 — doppelwandiges Gefäss aus Messingblech (400 ml); 4 — Thermometer; 5 — Magnetrührer; 6 — Kryostat (Typ MK—70, VEB Prüfgerätewerk Medingen, DDR)

des Säure/Wasser-Gemisches. (Der Frierpunkt wässriger Schwefelsäure ändert sich bekanntlich [13] sehr stark mit dem Wassergehalt und weist mehrere Maxima auf). Innerhalb von 10...15 Minuten wurde dann die Säure tropfenweise, unter energischen Rühren, der alkoholischen Basenlösung zugefügt und nachher der Inhalt des Mischgefässes in einen 50 ml-Messkolben überführt. Gespült wurde der Erlenmeyerkolben mit weiteren 5 ml Säure, die dann ebenfalls dem Messkolben zugefügt wurden. Nach Thermostatieren des Messkolbens auf 20 ± 0,2°C wurde mit Säure bis zur Marke aufgefüllt. Darauf wurde sofort in ein dunkelbraunes, mit Glasstopfen versehenes 50 ml — — Fläschchen umgeleert und dieses in den Thermostaten gestellt.

Die Bezugslösungen für die später vorzunehmenden spektrophotometrischen Messungen wurden nach dem gleichen Verfahren aus 95%-igem Alkohol und der entsprechenden Säure hergestellt.

Bei allen Lösungen wurde dieselbe Pipette und derselbe Messkolben verwendet. Im Falle der Azoxybenzol enthaltenden Lösungen wurde nur bei indirektem Licht gearbeitet, um die photochemische Umlagerung zu verhindern. Alkohol und die Säuren waren von analytischer Reinheit.

b) *Charakterisierung der Lösungen:* Es wurden nur die Bezugslösungen analysiert. Die Dichte wurde mit einem 25 ml — Pyknometer bei $20 \pm 0{,}2°$ gemessen.

Um die Volumenverkleinerung beim Mischen des Alkohols mit den wässrigen Säurelösungen zu bestimmen, wurde der 50 ml — Messkolben mit der fertigen Lösung, mit destilliertem Wasser, mit 10 ml Alkohol und leer gewogen. Mittels der pyknometrisch bestimmten Dichten wurden die Massenwerte in Volumenwerte verwandelt, wobei sich für den gefüllten Messkolben, bzw. für die 10 ml Alkohol Mittelwerte (aus 3 Messungen) von $V_0 = 49{,}87$ ml, bzw. $V_A = 9{,}98$ ml ergaben, während die Werte für die wässrigen Schwefel- und Salzsäurelösungen, V_g, zwischen 39,95 und 41,12 ml schwankten.

Der Säuregehalt der Lösungen wurde teilweise titrimetrisch mit 0,5 N NaOH-Lösung, in Gegenwart von Phenolphthalein, bestimmt. Die Lösungen wurden vor der Titrierung bis auf einen Säureghalt von etwa 1 Äquiv. H^+/l verdünnt, wobei ebenfalls die Anordnung aus Abb. 1, aber ohne Scheidetrichter, verwendet wurde. Je nach Säuregehalt wurden mittels Pipette zwischen 2 und 25 ml konzentrierter Lösung, unter Kühlung und energischen Rühren, langsam in den Kolben getropft, der soviel destilliertes Wasser enthielt, dass sich nach Zufügen der Säure eine Flüssigkeitsmenge von etwa 40 ml ergab. Nach Umgiessen in den 50 ml — Messkolben wurde das Mischgefäss zweimal mit je 5 ml destilliertem Wasser nachgespült und damit der bei 20°C thermostatierte Messkolben zur Marke aufgefüllt.

Der titrierte Säuregehalt wurde in Funktion der pyknometrisch gemessenen Dichte für beide Systeme (Salz- bzw. Schwefelsäure enthaltend) graphisch dargestellt. Die erhaltenen Kurven dienten der Bestimmung des Säuregehalts der restlichen Lösungen bekannter Dichte.

Ergebnisse und Diskussionen. Beim Mischen des Alkohols mit wässrigen Säurelösungen wird eine beträchtliche Wärmemenge frei, die jedoch durch das wirksame Kühlsystem der hier verwendeten Apparatur rasch abgeführt werden konnte, so dass auch lokale Erwärmungen beim Mischen der Flüssigkeiten ausgeschlossen waren. Dadurch konnte ein teilweises Entweichen der flüchtigen organischen Komponente, sowie der ungewollte Start der Wallach-Umlagerung im Falle der Azoxybenzollösungen weitgehend verhindert und sehr gut reproduzierbare Lösungen hergestellt werden.

Tafel 1 und 2 geben einen Überblick über die mit Schwefel-, bzw. Salzsäure hergestellten Lösungen. In der 3. Kolonne sind die durch Wägung ermittelten, in ml umgerechneten Mengen an wässriger Säure angegeben, die notwendig waren, um 10 ml Alkohol auf 50 ml aufzufüllen. Das Verhältnis $(V_A + V_S)/V_0$, zwischen der Summe der Volumina der alkoholischen und sauren Komponente und dem Inhalt des Messkolbens, als Mass der Volumenverkleinerung, wurde in Funktion der prozentuellen Konzentration der wässrigen Säurelösungen in Abb. 2 graphisch dargestellt. Wie ersichtlich, geht die beim Mischen von Alkohol mit reinem Wasser relativ hohe Volumenverkleinerung mit steigendem

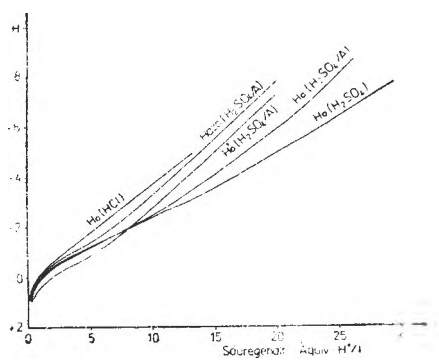

Abb. 2: Abhängigkeit der Volumenverkleinerung vom Säuregehalt beim Mischen wässriger Säure lösungen (H_2SO_4, HCl) mit Alkohol, in einem Verhältnis von 1 : 4 (V_S stellt das Volumen wässriger Säure dar, das notwendig ist, um $V_A = 10$ ml Alkohol auf $V_0 = 50$ ml aufzufüllen).

Tafel 1

Herstellung von 20 Vol-% Alkohol und 80 Vol-% wässrige Schwefelsäure enthaltenden Lösungen

H_2SO_4 — Ausgangslösungen			Hergestellte alkoholische Lösungen			
				Säuregehalt, in Äquiv. H^+/l		
D_4^{20}	Konz., %	V_S, ml*	D_4^{20}	reel	berechnet	reel/ber.
1,8364	97,00	41,12	1,6757	27,43 (t)	29,75	0,922
1,8355	96,00	41,10	1,6731	27,32	29,40	0,929
1,8337	95,00		1,6684	26,90	29,00	0,928
1,8145	90,02	40,59	1,6387	25,10	26,94	0,932
1,7787	85,01	40,28	1,5964	23,10 (t)	24,71	0,935
1,7274	80,02	40,10	1,5505	21,17	22,52	0,940
1,6745	75,45	40,11	1,5073	19,50 (t)	20,57	0,948
1,6692	75,00		1,5030	19,34	20,39	0,948
1,6104	69,99	40,10	1,4559	17,62	18,35	0,960
1,5533	65,00		1,4102	15,93 (t)	16,44	0,969
1,4981	59,98	40,14	1,3664	14,32	14,64	0,978
1,4453	55,00		1,3246	12,85	12,96	0,991
1,3952	50,01	40,19	1,2852	11,42 (t)	11,39	1,003
,3893	49,40		1,2805	11,20	11,20	1,000
1,3125	41,10		1,2203	8,81	8,82	0,999
1,3029	40,01	40,27	1,2128	8,51	8,52	0,999
1,2629	35,35	40,31	1,1814	7,32 (t)	7,31	1,001
1,2599	35,00		1,1791	7,19	7,22	0,996
1,2190	30,06	40,35	1,1470	6,00	6,00	1,000
1,2063	28,50		1,1371	5,62	5,63	0,998
1,1783	25,00	40,37	1,1150	4,85 (t)	4,83	1,004
1,1494	21,30		1,0924	4,02	4,02	1,000
1,1399	20,06	40,42	1,0850	3,76	3,75	1,003
1,0766	11,50		1,0352	2,00	2,02	(0,990)
1,0680	10,27		1,0283	1,78 (t)	1,80	(0,989)
1,0665	10,06	40,50	1,0271	1,72	1,75	(0,983)
1,0317	5,00		0,9997	0,83	0,85	(0,976)
0,9982	0	40,60	0,9735	0	0	—

* V_S stellt die Menge wässriger Säurelösung dar, die notwendig ist, um 10 ml Alkohol auf 50 ml aufzufüllen; (t) sind Werte durch Titration ermilttelt, der Rest mittels Eichkurve

Säuregehalt beträchtlich zurück. Im Falle der Salzsäre ist diese Änderung im untersuchten Konzentrationsbereich linear. Im Falle der Schwefelsäure besteht Linearität nur bis zu einer Konzentration von etwa 50%; bei 70 ... 75% durchläuft die Kurve ein Minimum, um dann ab 80% steil anzusteigen.

Die nichtlineare Änderung der Volumenverkleinerung mit dem Säuregehalt, beim Mischen von Alkohol mit Schwefelsäure, ist von keinem der Autoren, die mit diesem Lösungsmittelsystem gearbeitet haben [10—12], beobachtet worden und kann als indirekter Beweis für die Esterifizierungsreaktion gewertet werden. Kresge und Chen [11] konnten sowohl durch Titration, als auch durch Kernresonanzspektroskopie den Beweis erbringen, dass sich beim Mischen von Alkohol mit Schwefelsäure höherer Konzentration (ab 50%) saures Äthylsulfat bildet.

Um bei den acidimetrischen Bestimmungen die in den Lösungen tatsächlich vorliegenden Verhältnisse getreu wiedergeben zu können, musste verhindert werden, dass während der Titration der Halbester teilweise hydrolysiert. Des-

Tafel 2

Herstellung von 20 Vol-% Alkohol und 80 Vol-% Salzsäure enthaltenden Lösungen

HCl — Ausgangslösungen			Hergestellte alkoholische Lösungen			
D_4^{20}	Konz., %	V_S, ml*	D_4^{20}	Säuregehalt, in Äquiv. H^+/l		
				reel	berechnet	reel/ber.
1,1910	38,53	39,95	1,1150	10,07 (t)	10,08	0,999
1,1865	37,58	39,97	1,1118	9,79	9,80	0,999
1,1736	34,92	40,00	1,1024	9,00 (t)	9,02	0,998
1,1704	34,27		1,1001	8,79	8,83	0,995
1,1493	30,00	40,08	1,0850	7,60 (t)	7,60	1,000
1,1425	28,65		1,0800	7,20	7,22	0,997
1,1238	24,99	40,19	1,0663	6,20 (t)	6,21	0,998
1,1232	24,88		1,0658	6,17	6,18	0,998
1,1131	22,92		1,0586	5,62	5,64	0,996
1,0980	20,00	40,29	1,0475	4,85 (t)	4,86	0,998
1,0819	16,84		1,0356	4,03	4,04	0,998
1,0651	13,52		1,0233	3,22	3,20	(1,006)
1,0477	10,06	40,45	1,0102	2,34 (t)	2,34	1,000
1,0413	8,76		1,0057	2,04	2,03	1,005
1,0296	6,35		0,9968	1,47	1,46	(1,007)
1,0204	4,47		0,9900	1,01	1,02	(0,990)
0,9982	0	40,60	0,9735	0	0	—

* und (t) haben dieselbe Bedeutung wie in Tafel 1

halb wurden die Lösungen vor der Titration, unter Kühlung, stark verdünnt. Dass bei geringen Säuregehalten die Hydrolyse des sauren Schwefelsäureäthylesters vernachlässigbar klein ist [14], konnte auch in vorliegender Arbeit bestättigt werden: gleich und nach 24 Stunden durchgeführte Titrationen ergaben im Rahmen der erlaubten Fehlergrenze gleiche Werte.

In der 5. Kolonne der Tafeln 1 und 2 ist der Säuregehalt der hergestellten Lösungen in Äquiv.H^+/l wiedergegeben, wobei die mit (t) versehenen Werte durch Titration, die restlichen mittels Eichkurven Säuregehalt/Dichte bestimmt wurden. Kolonne 6 enthält den nach der Menge zugefügter wässrigen Säure (gemäss Kolonne 3) berechneten Säuregehalt der alkoholischen Lösungen. Das Verhältnis zwischen reelem und berechnetem Säuregehalt (letzte Kolonne) beträgt $1{,}000 \pm 0{,}005$*, solange keine Veresterung stattgefunden hat. Steigt der Säuregehalt der alkoholischen Schwefelsäurelösungen über 12 Äquiv.H^+/l, ist zwischen experimentellen und berechneten Werten keine Übereinstimmung mehr, wobei der Unterschied mit zunehmender Konzentration, als Folge der immer mehr begünstigten Veresterung, ständig grösser wird.

Es muss noch auf die Tatsache hingewiesen werden, dass die hier für alkoholische Säurelösungen ermittelten Dichten, trotz geringerer Messtemperatur (20 °C gegenüber 25 °C) etwas kleiner als die anderer Autoren [10, 11] sind, wobei der Unterschied gegenüber den von Kresge [11] mitgeteilten Werten etwas

* Bei Säuregehalten unter 3 Äquiv. H^+/l wirken sich die experimentellen Fehler nachteilig auf das Verhältnis aus.

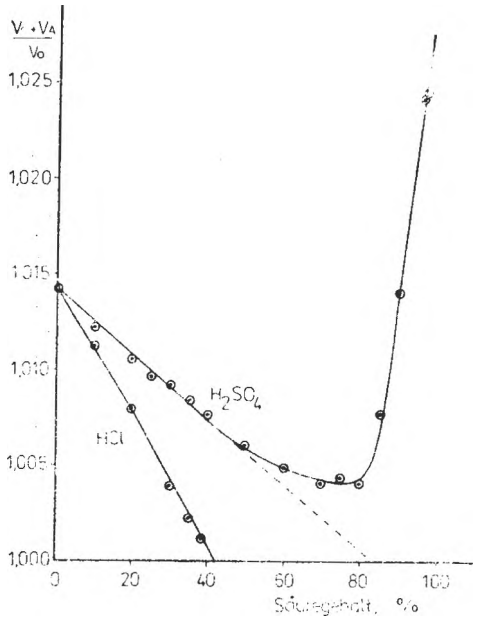

Abb 3: Der Verlauf der Säurefunktion in Abhängigkeit des Säuregehalts (in Äquiv. H^+/l) für Säureskalen folgender Systeme (Lösungsmittelsystem und Indikatoren): $H_0(HCl)$ — wässrige Salzsäure und Aniline [15]; $H_0(H_2SO_4)$ — wässrige Schwefelsäure und Aniline [15]; H_0 (H_2SO_4/A) — wässrige Schwefelsäure mit 20 Vol-% Alkohol und Aniline [11]; $H_0'(H_2SO_4/A)$ — wässrige Schwefelsäure mit 20 Vol-% Alkohol, Azobenzol-derivate und zwei Aniline [10]; $H_{azo}(H_2SO_4/A)$ — wässrige Schwefelsäure mit 20 Vol-% Alkohol und Azobenzolderivate [11].

grösser ist. Eine Erklärung dafür kann kann nur in der unterschiedlichen Arbeitsweise bei der Herstellung der Lösungen gesucht werden. Wahrscheinlich ist bei anderen Autoren durch ungenügende Kühlung und Arbeiten in offenen Gefässen beim Mischen der Komponenten ein Teil des Alkohols entwichen, was beim hier beschriebenen Verfahren praktisch ausgeschlossen war.

Angesichts der Tatsache, dass der Alkoholgehalt u.U. nicht genau der gleiche ist, stellt sich die berechtigte Frage, ob mit den von anderen Autoren für dieses Lösungsmittelsystem aufgestellten Säureskalen gearbeitet werden kann.

Um den Einfluss organischer Lösungsmittel, aber auch der verwendeten Indikatorbasen, auf den Verlauf der Säurefunktion in stark sauren Systemen besser erläutern zu können, wurden in Abb. 3 Säureskalen verschiedener Autoren [10, 11, 15] wiedergegeben. Am Beispiel der für schwefelsaure Lösungen, auf Anilinindikatoren gestützten Säureskalen mit [11] und ohne [15] Alkoholgehalt kann gezeigt werden, dass bei mittleren Säuregehalten (1 ... 10 Äquiv.H^+/l) die Anwesenheit von 20 Vol—% Alkohol die H_0-Werte praktisch nicht beeinflusst. Das dürfte auch im Falle anderer Indikatorklassen, wie z.B. der Azoderivate, zutreffen. Erst bei höheren Säuregehalten wirkt sich beim teilweisen Ersetzen des Wassers durch die organische Komponente die Verringerung der Wasseraktivität auf den Hydratationsgrad der Protonen aus und führt zu einem rascheren Anwachsen der Protonenaktivität [15—18]. Bei 20 Äquiv.H^+/l unterscheiden sich die beiden H_0-Säureskalen (mit, bzw. ohne 20 Vol-% Alkohol) um genau eine H—Einheit. Das ergibt für einen Alkoholgehaltsunterschied von 2% eine vernachlässigbare Differenz von 0,1 H-Einheiten. Um mehr als 2 Vol-%

alkohol dürften sich, trotz verschiedener Arbeitsweise, die von verschiedenen Autoren hergestellten Lösungen des selben Lösungsmittelsystems kaum unterscheiden, so dass einer Benützung der betreffenden Säureskalen nichts im Wege steht.

LITERATUR

1. M. Ionescu, H. Kolch, *Stud. Univ. Babeş—Bolyai, Chem.*, **24** (1), 62 (1979).
2. E. Buncel, B. T. Lawton, „Chem. and Ind". (London), **1963**, 1835; E. Buncel, B. T. Lawton, *Canad. J. Chem.*, **43**, 862 (1965).
3. E. Buncel, W. M. J. Strachan, R. J. Gillespie, R. Kapoor, *J. Chem. Soc.*, **1969**, 765; E. Buncel, W. M. J. Strachan, *Canad. J. Chem.*, **48**, 377 (1970); E. Buncel, A. Dolenko, „Tetrahedron Letters", **1971**, 113.
4. R. A. Cox, E. Buncel, *Canad. J. Chem.*, **51**, 3143 (1973).
5. S. Oae, T Maeda, *Tetrahedron*, **28**, 2127 (1972).
6. Chi-Sun Hahn, Kyu Wan Lee, H. H. Jaffé, *J. Amer. Chem. Soc.*, **89**, 4975 (1967).
7. J. Singh, P. Singh, J. L. Boivin, P. E. Gagnon, *Canad. J. Chem.*, **41**, 499 (1963).
8. L. C. Behr, E. C. Hendley, *J. Org. Chem.*, **31**, 2715 (1966); E. C. Hendley, D. Duffey, *J. Org. Chem.*, **35**, 3579 (1970).
9. Chi-Sun Hahn, H. H. Jaffé, *J. Amer. Chem. Soc.*, **84**, 949 (1962).
10. H. H. Jaffé, R. W. Gardner, *J. Amer. Chem. Soc.*, **80**, 319 (1958); Si Jung Yeh, H. H. Jaffé, *J. Amer. Chem. Soc.*, **81**, 3274 (1959).
11. A. J. Kresge, H. J. Chen, *J. Amer. Chem. Soc.*, **94**, 8192 (1972).
12. D. Dolman, R. Stewart, *Canad. J. Chem.*, **45**, 903 (1967).
13. Kirk-Othmer, *"Encyclopedia of Chemical Technology"*, 2. Aufl., vol. **19**, John Wiley and Sons, Inc., New York, 1969, S. 445.
14. J. L. Kurz, *J. Phys. Chem.*, **66**, 2239 (1962).
15. M. I. Vinnik, *Uspekhi Khimii*, **35**, 1922 (1966).
16. M. Ojeda, P. A. H. Wyatt, *J. Phys. Chem.*, **68**, 1857 (1964).
17. G. S. Doronin, E. S. Rudakov, N. S. Videshina, N. D. Selichkaia, *Zhur Prikl. Khim.*, **40**, 1464 (1967).
18. B. Nahlovsky, V. Chvalovsky, *Coll. Czech. Chem. Commun.*, **33**, 3122 (1968).

STUDIA UNIV. BABEŞ—BOLYAI, CHEMIA, XXXI, 1, 1986

PARTICULAR TYPES OF CONDUCTOMETRIC AC TITRATION CURVES

I. The Use of Silver Sensors[1]

CSABA MUZSNAY* and EDIT FORIZS**

Received: April 29, 1985

ABSTRACT. — The study of the previously proposed silver conductometric cells has been extended by using sensors with different cell constants and electrode constructions. Two kinds of dip-type sensors were used in titrations, such as ring- and spiral-form electrodes. Some typical conductometric titrations were carried out involving neutralizations and precipitations.

A peculiar behaviour of the spiral sensors has been detected, which has little value on the cell constant, as well as the interelectrodic distances. These titrations could be divided in two categories: 1) in the presence of the silver ions, in concentrations larger than 10^{-3} N, the shape of the titration curves differs from the classical one; 2) in the absence of common ions one can not observe differences with respect to the classical shape of the titration curves. Especially, the precipitation of silver chloride and silver iodide has been studied. The appearence of a minimum on the titration curves near the equivalence point (e.p.) and the high sharpness index of these curves can be brough into connection with the augmentation of the degree of polarization during titration.

Recently, considerable diversification of the conductometric sensors has taken place especially on the basis of the applied constructional principles, or by reason of the nature of the used electrode materials [1, 2]. The less precious metal electrodes exceled — depending on the studied systems — in considerable and specific degree of polarization, which up to the present has not been fully studied. The investigation of the previously proposed silver conductometric cells [3] has been extended by using sensors of various electrode constructions and different values of cell constants.

Experimental. *Conductance cells.* Two kinds of monoaxial dip-type conductometric Ag electrodes were used such as ring and spiral form electrodes (Fig. 1.).

The spiral sensors and the values of their constants differ from one another by the length of the spiral and the *speach* of the thread. The values of cell constants were the following: C= 0.55 cm^{-1} for the ring form electrodes and C = 0.012—0.68 cm^{-1} for the spiral electrodes. Over and above both platinized Pt and stainless steel combined with silver spirals were used as conductometric cells. The latter sensors differ from the normal silver spiral electrodes by substituting one of the silver spiral with inconel spiral into a special — biaxial — construction. Some of the characteristic data referring to the conductometric sensors are presented in Table 1.

Conductivity determinations. Both the measurements and the recordings of the conductance were made by the previously presented methods [3]. Volume corrections were made to the representation of the greater part of manually performed titration curves. In case of continuous recording,

---

[1] *An extended poster communication presented on the Euroanalysis V Conference, Cracowia, Poland, 28 Aug. 1984.*

* *University of Cluj-Napoca, Department of Inorganic and Analytical Chemistry, 3400 Cluj-Napoca, Romania*

** *Institute of Chemistry, 3400 Cluj-Napoca Romania*

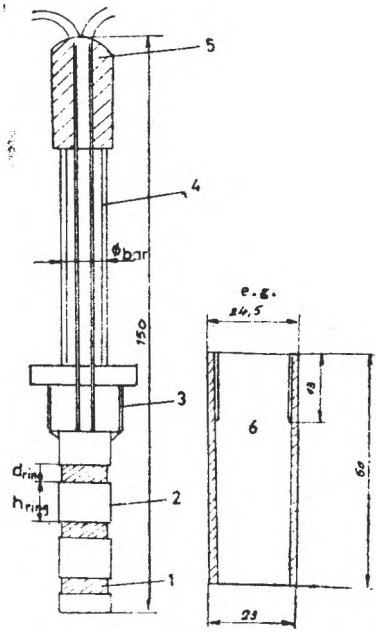

Fig. 1. Monoaxial conductometric ring form sensor with three Ag rings. 1. Silver rings, 2. Electrode body from plastic material, 3. Screw thread for bell protection, 4. Screened sheet, 5. Cable with double core, 6. Bell from thermoplastics on purpose to protection.

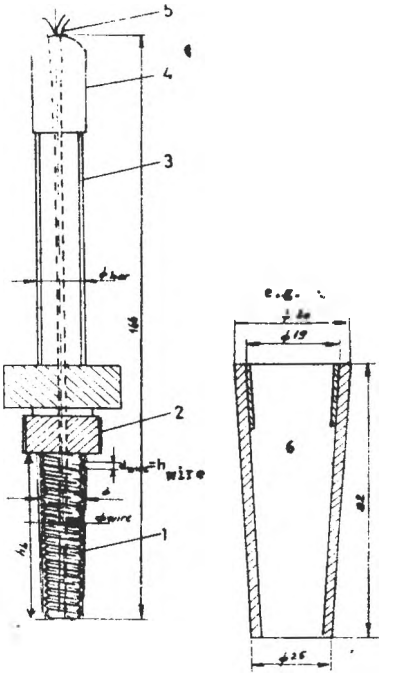

Fig. 2. Monoaxial conductometric silver spiral sensor. 1 Silver spiral, 2. Screw thread for bell protection, 3. Electrode body from plastic material, 4. Plastic covering, 5. Cable with double core, 6. Bell protection from thermoplastics.

the equivalence volume (V) was determined partly from the delivering rate of the titrant, partly from the running time of recorder up to e.p., (with recorder KUTESZ Type 175 adapted to the conductometer). The delivery of titrant with a fixed rate was carried out by means of automatic burette Radelkis Type OP—930/1. Titrations vere also carried out withot bell protection, especially in case of certain spiral sensors. The cell constants of spiral sensors without bell protection are modified to a small extent as compared to the values presented in Table 1.

TITRATION CURVES. Some typical conductometric titrations were carried out involving neutralizations and precipitations.

Titration curves with regular shapes. The titration curves of strong bases obtained with strong acids and the results of these titrations do not differ within the range of accepted experimental errors, neither do they differ from those obtained with the platinized Pt sensor, nor from those determined by classical volumetric methods (Fig. 3).

The titrations with precipitate formation could be divided in three categories: 1) Titration of electroactive silver species with precipitating ions (Figs. 4—11, 13); 2) Titration of precipitating anions with the electroactive silver ions (Fig. 12); 3) Titration with precipitate formation of electroinactive species.

The shape of these curves is the classical one when the ring form sensors are used, or when the third category of precipitate titration is effected with either of the sensors (Fig. 3—6).

Table 1

Charaeteristic data of the studied conductometric sensors

Nrs.	Type of sensors	Cell const. $cm^{-1} \cdot 10^2$	$\varnothing_{bar}$ mm	l_{bar}	$\varnothing_{wire}$ d_{ring}	h_{wire} h_{ring}	l_{bar}/h_{wire} nr. of spirals
1	Ag-spir	23.5	5	12	0.4	3	6
2	Ag-spir	26,8	5	19	0.4	3	6
3	Ag-spir	14.8	5	20	0.4	2	10
4	Ag-spir	18.2	5	20	0.4	2	10
5	Ag-spir	8.80	5	20	0.4	1	20
6	Ag-spir	3.86	5	20	0.4	1	20
13	Ag-spir	1.39	12	57	0.4	1.5	38
15	Ag-spir	1.27	12	57	0.4	1.5	38
7/4	Ag-spir	1.98	12	57	0.2	1.5	38
12	Ag-ring	55.2	14	53	8(r)	6(r)	—
12	Inox ring	22.7	(tube)	40	(r)	5(r)	—
3	Pt-ring	54.2	7 (tube)	50	3(r)	9(r)	—
1	Inox- — Ag spir	1.75	$\frac{11}{7}$	16	$\frac{1}{0.4}$	2	$\frac{16}{16}$

Titration curves of irregular shapes. These types of titration curves (Figs. 7—13) were obtained only by means of the spiral silver sensors, chiefly in the first category, and also in a smaller deagree in the second one of the titrations with precipitate formation, too.

Precipitation of AgCl. The following figures — Fig. 4. and Figs. 6—12. — show the precipitation of Ag^+ ions with Cl^- ions using five dip types sensors (Pt ring, inox ring, silver ring, inox-silver spiral, and silver spiral). Accentuated minima appear using silver spiral sensors, when the concentration of Ag^+ ions is more than 1 mN (Figs. 8—9.). The conductivity jump becomes higher with the increase of concentration of Ag^+ ion and vanishes in solutions more diluted then 1 mN (Fig. 10). Fig. 11 shows an automatically recorded titration curve.

The titrations made in reverse order ($AgNO_3$ as titrant) are characterised by smaller conductometric jumps than that previously obtained (Fig. 12.).

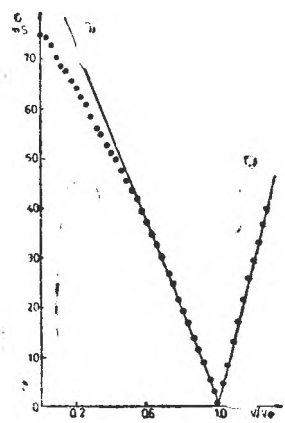

Fig. 3. Titration of 10 mN $Ba(OH)_2$ with 0.10 N sulphuric acid using the silver spiral sensor No. 7/4. The theoretical equivalence volume: 35.0 ml.

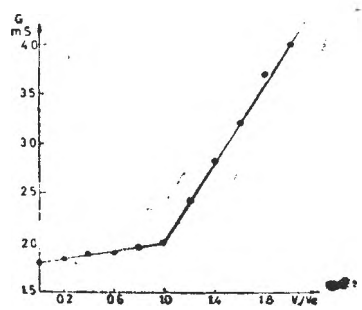

Fig. 4. Titration of 10 mN $AgNO_3$ with 0.10 N KCl using the Pt sensor No. 3. The theoretical equivalence volume: 5.00 ml.

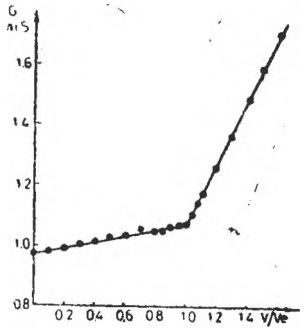

Fig. 5. Titration of 5 mN $AgNO_3$ with 0.10 N KCl using the silver ring sensor No. 12. The theoretical V_e: 5.00 ml.

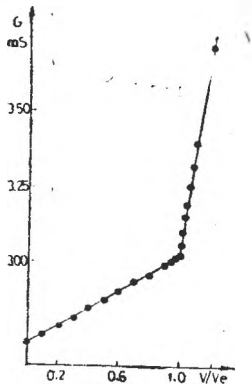

Fig. 6. Titration of 5 mN $AgNO_3$ with 0.10 N KI using the inox sensor No. 12. The the oretical equivalence volume: 5.00 ml.

Precipitation of AgI. The precipitation of Ag^+ ions with I^- ions was also made with five types of electrodes. It appears a smaller and less definite minimum than that obtained by the AgCl precipitation in the same manner. By repeating a great number of titrations, the conductivity jumps gradually decrease (Fig. 13a, 13b). After washing the spiral sensor with a 0.2 M KCN solution, instead of a minimum a plateau appeared, namely in the left vicinity of e.p. the conductivity did not change practically (Fig. 13c.).

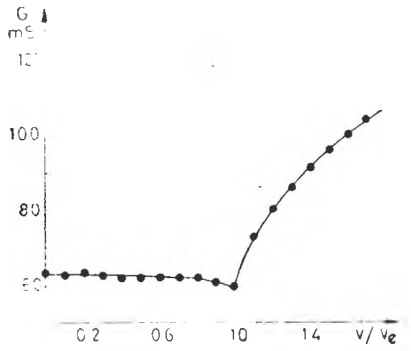

Fig. 7. Titration of 10 mN $AgNO_3$ with 1 N KCl using the Ag-inox sensor. The theoretical equivalence volume: 5.00 ml.

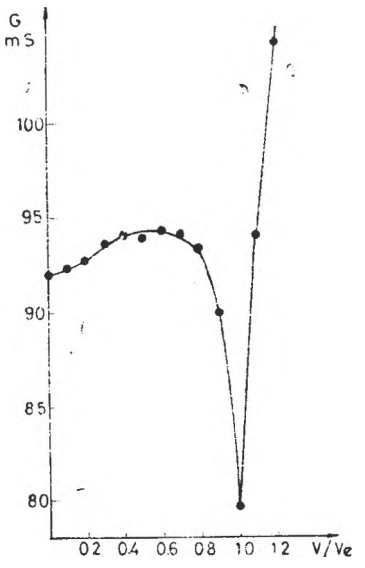

Fig. 8. Titration of 10 mN $AgNO_3$ with 0.10 N KCl using the silver spiral sensor No. 13. The theoretical V_e: 10.00 ml.

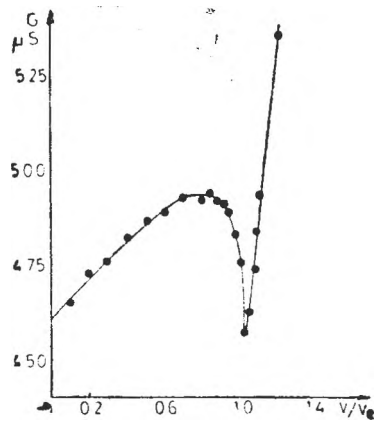

Fig. 9. The titration of a diluted (0.05 N) $AgNO_3$ solution with 0.10 N KCl solution using the silver spiral sensor No. 3. The theoretical equivalence volume is 5.00 ml.

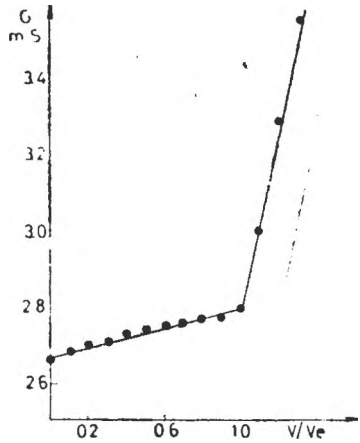

Fig. 10. Titration of more diluted $AgNO_3$ (1 mN) with 0.01 N KCl using the silver spiral sensor No. 5. The theoretical V_e: 1.00 ml.

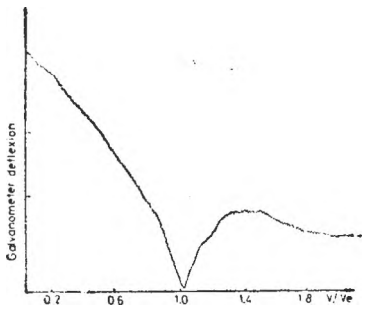

Fig. 11. Automatically recorded titration of 0.05 N $AgNO_3$ with 1N KCl using the silver spiral sensor No. 2.; V_e: 5.00 ml.

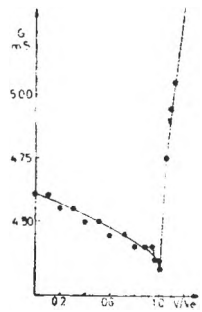

Fig. 12. Titration of 5 mN KCl solution with 0.10 N $AgNO_3$ using Ag spiral sensor (No. 3). The theoretical V_e: 5.00 ml.

The reverse order titrations in these cases had not definite and reproducible minimum. Small differences can be observed in comparison with the shape of the classical conductometric titration curves.

Discussion. In the titrations with minima, the conductance variations before e.p. have a nonlinear character. The graphically determined minimum of the titration curves coincides with e.p. Within the range of accepted experimental errors the e.p. obtained by means of the sensors „without peculiar comportments" was comparable with that of the studied spiral sensors (Table 2). In the case of the AgCl precipitations, the value of conductance minimum is fixed

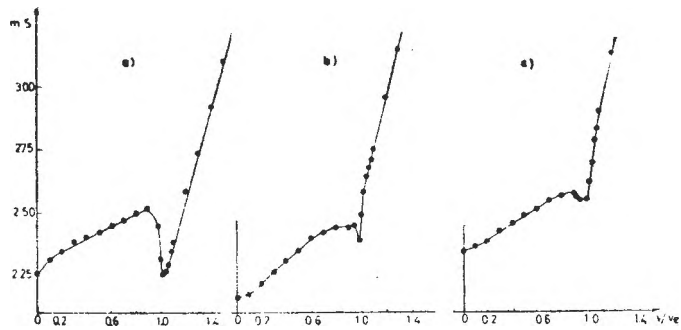

Fig. 13. Titration of 5 mN $AgNO_3$ solution with 0.10 N KCl using the Ag spiral sensor No. 2. Theoretical equivalence volumes: 5.00 ml. a) first titration, b) second titration, c) titration after the washing of sensor with 0.2 M KCN solution.

with an increased precision as compared to the determination of e.p. with conductometric sensors of linear character. The minimum of conductance, in case of AgI separation, can be fixed in some instances with smaller precision as compared to the AgCl precipitation.

Table 2

Results of titration obtained with spiral silver electrodes

Titrant	Titrand	V_e (ml) theoretical	V_e (ml) experimental			s%	Nr. of sensor
$AgNO_3$ 0.1 n.	KCl $5 \cdot 19^{-3}$ n.	5.00	5.00; 4.99	5.01;	5.01;	<0.1%	3
$AgNO_3$ 0.1 n.	KCl $5 \cdot 10^{-3}$ n	5.00	5.00; 5.00	4.90;	5.00;	<1%	12
$AgNO_3$ 0.1 n.	$(Et)_4NI$ $5 \cdot 10^{-3}$	4.90	4.90;	4.80;	4.90	1.16%	2
KCl 0.1 n.	$AgNO_3$ 0.01 n.	10.00	10.00; 10.0	10.0;	10.0;	0.0%	13
KCl 0.1 n.	$AgNO_3$ $5 \cdot 10^{-3}$	5.00	5.00;	5.10;	5.00;	<1%	3,4
		5.00	5.10;	5.00;	5.10		

Interpretation of particular form of titration curves. The behaviour of electrodes under a.c. conditions can be characterized by the polarization impedance (Z_p), and the phase angle (δ), but it can also be regarded as a system consisting of a polarization capacity C_p and a (parallel or series) polarization rezistance (R_p) [4—6]. The polarization impedance of semicell (Fig. 14) has an ohmical and an overvoltage component ($Z_{p,\Omega}$ and $Z_{p,\eta}$); $Z_p = Z_{p,\Omega} + Z_{p,\eta}$. The ohmical component corresponds to the adherent (or not adherent) layer of the precipitate formed near the electrode and has a high value in e.p. (complete precipitation). $Z_{p,\Omega}$ is dependent on the state of electrode surface and it can be modified by pretreatments of electrodes. The Ag/AgI surface is more sensible in this re-

gion than the Ag/AgCl one. The value of the overvoltage component is also concentration dependent. When the concentration of electroactive species is diminished, then $Z_{p,\eta}$ increases suddenly. In like manner does the degree of polarization increase. The cell impedance ($Z_{el} = Z_c + Z_p$) is a sum of the electrolyte impedance (Z_c) and the polarization impedance of both electrodes ($Z_p = Z_{1p} + Z_{2p}$).

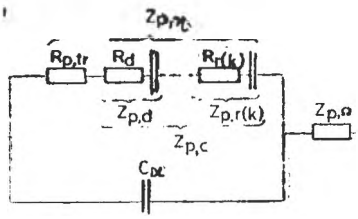

Fig. 14. Equivalent circuit of semicell. Indexes tr, d, r(k), and c refer to the following types of overvoltages: transfer, diffusion, reaction (kinetic), and concentration overvoltage.

The effect of the polarization impedance becomes perceptible in the behaviour of the conductometric cell, when the ratio $Z_p \cdot 100/Z_e$ is higher than 1—5% and varies suddenly during titration. This condition is satisfied especially in the titration of Ag^+ ions with X^- ions, presuming that the concentration of titrand is larger than 10^{-3}N. At smaller concentrations Z_e increases to such a degree that the numerical value of the ratio remains small, and does not vary in the course of titration. With the augmentation of titrand concentration, ratio Z_p/Z_e becomes greater and more variable than in more dilute solutions because of Z_e diminution. In these processes the concentration of titrand is determinant during titration, and the value of solubility product constants of the precipitate has not a considerable influence. The polarization rezistance counts much in the diminution of cell conductance. The appearence of minimum on the titration curve near e.p. can be brought into connection with the augmentation of the polarization degree during titration.

The cell construction and constants likewise determine the formation of titration curves with minimum. In the case of the spiral sensors with the smallest cell constant value, the distance between the neighbouring spirals (h_{wire}) is small, and that is why the contribution of the polarization impedance to the cell impedance, as compared to the impedance of electrolyte—which is found between the spirals —, enhances.

REFERENCES

1. O. Klug, *Magy. Kém. Lapja*, **39**, (5), 189 (1984).
2. B. A. Lopatin, O. Klug, „A konduktometrias és osszcillometriás elemzések" in series: *A kémia újabb eredményei*, V, **56**, Akad. Kiadó, Budapest, 1983.
3. Cs. Muzsnay, *Studia Univ. Babeş-Bolyai, Ser. Chem*, **22**, (1), 68 (1977).
4. K. Vetter, "Elektrochemische Kinetik" Springer Verl., Berlin, 1961.
5. T. Erdey-Grúz, "Kinetics of Electrode Processes", Akad. Kiadó, Budapest, 1972.
6. Cs. Muzsnay, *Conductometrie în curent continuu. Conductometria soluţiilor apoase de electrolit*, Thesis, Cluj-Napoca, 1978.

STUDIA UNIV. BABEŞ—BOLYAI, CHEMIA, XXXI, 1, 1986

ANALIZA GAZ-GROMATOGRAFICĂ A PRODUŞILOR REZULTAŢI ÎN PROCESUL REDUCERII CATALITICE A ANHIDRIDEI MALEICE

IONEL HOPÂRTEAN*, NICU DULĂMITĂ*, MARIA VAGAONESCU*

Intrat în redacţie la 23 mai 1985;

ABSTRACT. — Gas Chromatographic Determination of the Products Obtained by Catalytic Reduction of Maleic Anhydride. A new gas chromatographic method of maleic anhydride, using 2.7 XE as liquid phase on chromosorb GAW and dimethylformamide, as internal standard, has been developed. Using the calibration curve, γ-butirolactone was determined on a column packed with 20% on siliconic oil 550 on silanizated Chromosorb W by using phenyl-ethyl acetate as internal standard.

În procesul de fabricaţie al γ-butirolactonei, prin reducerea catalitică a anhidridei maleice, se formează ca produşi secundari anhidridă şi acid succinic. Analiza cantitativă a amestecurilor policomponente care conţin acizi şi anhidride corespunzătoare lor, alături de alţi compuşi organici, nu se poate efectua prin gaz-cromatografie datorită anhidrificării acizilor dicarboxilici la temperatura din coloana analitică.

Separarea şi dozarea componentelor din amestcul care conţine γ-butirolactonă (γ—BL) anhidridă succinică (AnS), acid succinic (AS) şi anhidridă maleică (AnM) în diferite concentraţii, s-a efectuat prin metoda gaz-cromatografică utilizînd ca fază staţionară 2,7%XE—60 suportată pe Cromosorb—GAW—DMCS şi ca standard intern dimetilformamidă (DMF), după ce în prealabil acidul succinic s-a derivatizat prin esterificare cu diazoetan [1—4]. Folosind o coloană analitică cu umplutură formată din 20% ulei siliconic 550 pe Cromosorb W silanizat şi standardul intern fenilacetatul de etil (FAE), pe baza curbei de etalonare, se dozează rapid γ-butirolactona.

Partea experimentală. În cursul analizei gaz-cromatografice la temperatura aplicată în coloana analitică are loc anhidrificarea acidului succinic din probele care conţin şi anhidridă sucinică. Pentru a evita acest fenomen s-a studiat posibilitatea derivatizării acidului succinic, în prezenţa anhidridei sale, prin esterificare cu diferiţi reactanţi. Cu metanol în dioxan, metanol şi trifluorură de bor sau în diazometan se esterifică atît anhidrida cît şi acidul succinic. Folosind diazoetan se esterifică numai acidul succinic [1, 2]. În proba luată în lucru se adaugă 10 cm^3 soluţie eterică de diazoetan, după care amestecul format se refluxează circa 15 minute şi apoi se elimină eterul prin distilare la presiune scăzută cînd rămîne în blaz un lichid uleios format din succinat de dietil (SDE) şi restul componenţilor. 1.1. *Sisteme binare:* 1.1.1. γ-BL 51% şi AnS 49%; 1.1.2. γ-BL 93% şi AnS 7%; 1.1.3. γ—BL 90% şi AS 10%; 1.1.4. AnM 50% şi AnS 50%. Din acestea se cîntăresc cîte a, g la care se adaugă b, g fenilacetat de etil (FAE) şi se dizolvă într-un cm^3 acetonă. 1.2. *Sisteme ternare.* Sînt formate din γ—BL, AnS şi AS în diferite proporţii, iar AS se derivatizează prin esterificare cu diazoetan şi apoi din lichidul uleios se iau a, g la care se adaugă b, g dimetilformamidă. 1.3. *Soluţii de γ—BL.* Se prepară soluţii de diferite concentraţii de γ—BL în toluen (10, 30, 53, 75 şi 90%) la care se adaugă cîte b_S, g fenilacetat de etil 40%. 1.4. *Analiza gaz-cromato-*

* *Universitatea din Cluj-Napoca, Facultatea de tehnologie chimică, Catedra de chimie fizică, organică şi tehnologică, 3400 Cluj-Napoca, România*

grafică. Analiza probelor 1.1. și 1.3. s-a efectuat pe un gaz cromatograf model 18.3—4 echipat cu detector de conductibilitate termică operat la 250 °C (temperatura în evaporator 270 °C, iar în coloana analitică 130—160 °C) și gaz purtător azot la un debit de 40 cm³/min. Folosind detector de ionizare în flacără s-au analizat probele 1.2. în regim de temperatură programată, (viteză de încălzire 8 °C/min. de la 130 pînă la 185 °C) la un debit de 20 cm³ azot/min. în coloana analitică. Pentru separarea componenților din probele studiate s-au testat diferite faze staționare și suporturi introduse în coloane de oțel cu diametru de 4 mm, ale căror caracteristici sînt prezentate în Tabelul 1. Umplutura nr. 7 din Tabelul 1 este potrivită în cazul separării componenților din probele 1.1 și 1.2, iar umplutura nr. 8 pentru cei din probele 1.3.

Tabel 1

Faze staționare și suporturi testate

Umplutura coloanei	Granulație suport (mesh)	Lung. col., (m)	γ—BL	AnS	AS	AnM
20% Carbowax 20M/Cromosorb W	60—80	2	+	+	—	+
Idem	60—80	4	+	+	—	+
15% Carbowax 20M/Cromosorb DMCS	60—80	2	+	+	—	+
20% Carbowax 20M/Firebrick	80—100	2	—	—	+	—
Porapak Q	50—80	4	—	—	+	—
10SE—30/Cromosorb silanizat	120—140	2	+	+	+[a]	+
2,7 XE—60/Cromosorb GAW—DMCS	60—80	4	+	+	+[a]	+
20% ulei siliconic 550/Cromosorb W, silanizat	80—100	1	+	+	+[a]	+

a = AS s-a determinat ca SDE

Compoziția în procente de masă a probelor s-a determinat prin metoda standardizării interne, folosind ca standard FAE pentru probele 1.1 și 1.3, iar DMF pentru probele 1.2. Se măsoară suprafețele vîrfurilor cromatografice prin metoda triunghiului. Toate măsurătorile sînt calculate ca medie a cinci determinări.

Rezultate și discuții. Cantitatea, în procente de masă, din fiecare component conținută în proba analizată se calculează folosind relația :

$$\%C = \frac{b_c}{a} \cdot 100 = \frac{b_s \cdot A_c \cdot 100}{A_s \cdot F_c \cdot a}$$

în care : b_c — reprezintă masa dintr-un anumit component, în g ; a — masa probei analizate, în g ; b_s — masa standardului, în g ; A_c — aria componentului c, în cm² ; A_s — aria standardului ales, în cm² ; F_c — factorul de corecție pentru răspunsul detectorului termic.

În Tabelul 2 se prezintă timpii de retenție, erorile de analiză și factorii de corecție la analiza sistemelor binare, iar în Fig. 1 cromatograma probei 1.1.1. Din analiza acestor date experimentale rezultă că se poate stabili compoziția unor sisteme binare cu o eroare care variază între limitele —0,3 și +0,4%, folosind ca standard FAE.

Standardul din Tabelul 3 s-a preparat prin amestecarea unor mase cunoscute de componenți puri (sistemul ternar 1.2) și DMF. Din cromatograme se determina ariile componenților, apoi se calculează procentele de masă și procentele de supră-

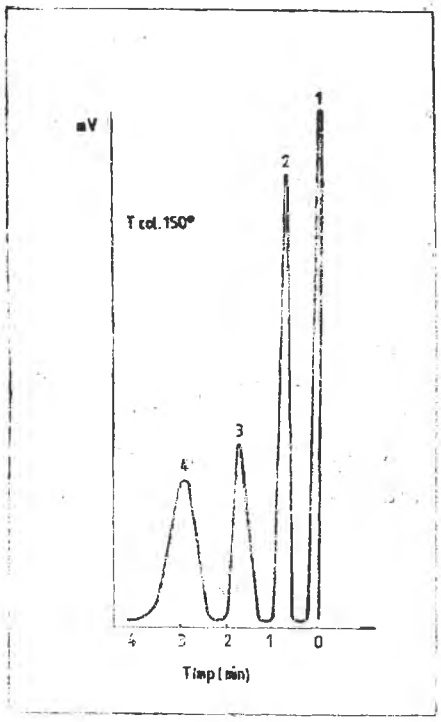

Fig. 1. Cromatograma sistemului binar 1.1.1.
1 — acetonă; 2 — γ—BL; 3 — AnS; 4 — FAE

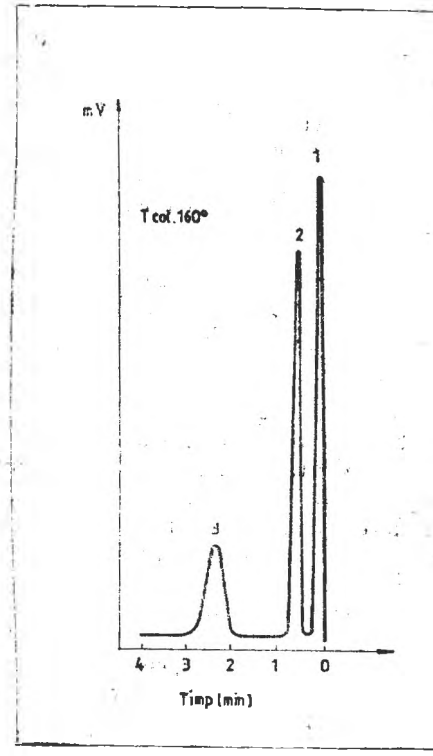

Fig. 2. Cromatograma soluției de γ—BL
1 — toluen; 2 — γ—BL; 3 — FAE

Tabel 2

Rezultatele analizei sistemelor binare 1.1

Nr. probei	Componenți	Timp retenție, min.	Masa, g		Eroare %	F
			Luat	Găsit		
1.1.1.	γ—BL	0,7	0,1040	0,1044	+0,4	1,019
	AnS	1,7	0,1002	0,1005	+0,3	1,013
1.1.2.	γ—BL	0,7	0,1990	0,1975	—0,1	1,019
	AnS	1,7	1,1040	0,1037	—0,3	1,013
1.1.3.	γ—BL	1,6[a]	0,9940	0,9920	—0,2	1,019
	AS	3,2	0,1048	0,1051	+0,3	1,067[b]
1.1.4.	AnM	0,6[c]	0,1028	0,1031	+0,3	0,949
	AnS	2,1	0,1025	0,1029	+0,4	1,013

temperatura coloanei analitice: a — 130° C; c — 140°C b = Fc al SDE

Tabel 3

Rezultatele analizei sistemului sintetic 1.2

Componenți	Timp retenție, (min.)	Masa comp.		Aria vîrf, cm²	% arie	Arie	F_c
		g	%			% masă	
DMF	6,0	0,1862	23,19	1,43	10,09	0,062	1,00
SDE	16,8	0,2086	25,98	7,00	49,23	0,269	4,34
γ—BL	20,4	0,3042	37,89	4,02	28,27	0,106	1,71
AnS	35,1	0,1038	12,93	1,76	12,41	0,136	2,19
Total	—	0,8028	99,99	14,21	100,0	—	—

față pentru fiecare component. Se împart ariile componenților cu masele procentuale corespunzătoare aflîndu-se valoarea factorului de corecție. Utilizînd metodologia indicată în Tabelul 2 sau factorii de corecție se determină compoziția, în procente de masă, a unei probe necunoscute. Datorită răspunsurilor diferite ale detectorului suprafețele procentuale diferă mult de masele procentuale, ceea ce justifică folosirea standardului.

Tabel 4

Compoziția unui sistem necunoscut 1.2

Componenți	Aria vîrf (cm²)	% arie	Arie / F_c	% masă
SDE	8,95	47,30	2,06	26,89
γ—BL	8,16	43,13	4,77	62,27
AnS	1,81	9,57	0,83	10,84
Total	18,92	100,0	7,66	100,0

Dacă se cromatografiază cîteva standarde Fig. 2 pentru soluțiile de γ—BL apoi se calculează raportul ariilor component/standard (notat cu y) și se reprezintă grafic în funcție de raportul maselor component/standard (notat cu x) se obține o dreaptă a cărei pantă este tocmai factorul de corecție. Pentru ecuația dreptei de forma : $y = A_0 + A_1 x$, se determină prin metoda celor mai mici patrate $A_0 = -0{,}089$ și $A_1 = 1{,}0063$ și se verifică statistic dacă ordonata la origine este zero. Cu ajutorul testului t s-a calculat dispersia ordonatei la origine $s_{A_0} = 0{,}0649$. Atunci t calculat va fi :

$$t_{calc} = \frac{|A_0|}{s_{A_0}} = \frac{0{,}089}{0{,}0649} = 1{,}37$$

Pentru $P = 95\%$, $k = 4$, t — tabelat are valoarea 2,78, deci mai mare decît t — calculat. Aceasta dovedește că cele două valori (0 și —0,089) nu diferă statistic și deci ordonata la origine este egală cu zero.

Analizînd soluţii de γ — BL brută şi luînd factorul de corecţie, identic cu panta dreptei, se dozează γ—BL cu erori de 0,4% masă.

Concluzii. Se prezintă o metodă gaz-cromatografică pentru analiza produşilor rezultaţi în procesul de fabricaţie al γ— butirolactonei din anhidridă maleică.

Pentru a realiza separarea componenţilor din produsul brut, după ce în prealabil acidul succinic s-a derivatizat prin esterificare cu diazoetan, s-au propus două faze staţionare suportate: 2,7% XE—60 pe Chromosorb GAW—DMCS şi 20% ulei siliconic 550 pe Chromosorb W silanizat. Folosind ca standard intern dimetilformamida sau fenilacetatul de etil se dozează rapid γ — butirolactona din produsul brut cu erori de ±0,4% masă.

BIBLIOGRAFIE

1. G. N. Freidlin, R. G. Nestorova, O. I. Sirobokova, A. A. Aramov, *J. Anal. Chem.*, **27**, 2067 (1972).
2. R. G. Nestorova, A. A. Aramov, G. N. Freidlin, D. I. Sirobokova, *Zh. Anal. Khim.*, **33**, 2416 (1978).
3. K. Anwers, E. Cauer, *Liebigs Ann., Chem.* **470**, 298 (1929).
4. A. I. Kosta, *„Obsciei praktikum po organiceskoi Khimii"*, Ed. Mir, 1965, p. 515, 535.

STUDIA UNIV. BABEŞ—BOLYAI, CHEMIA, XXXI, 1, 1986

NEW ACIDO-COMPLEXES OF COBALT(III) WITH GLYOXIME

GHEORGHE MARCU*, CSABA VÁRHELYI*, MAGDA SOMAY*, DANA ITUL* and ÉVA PÉTER*

Received: August 26, 1985

ABSTRACT. — The formation of the anionic chelates: $[Co(Glyox.H)_2X_2]^-$ and $[Co(Glyox.H)_2Y_2]^-$ (X = CN, NCS, Y = SO_3^{2-}, $S_2O_3^{2-}$) was proved by the oxidation of the components in aqueous alcoholic solutions. 23 new complex salts were insolated by means of double decomposition reactions. The anation of $NH_4[Co(Glyox.H)_2(SO_3)(H_2O)]$ with organic amines leads to the formation of $NH_4[Co(Glyox.H)_2(SO_3)(amine)]$. Some structural and thermal stability problems (Co—X, Co—Y bondings) were discussed on the basis of IR spectra and derivatographic measurements. Some physico-chemical properties of the new complexes were compared with those of the analogous derivatives of dimethyl-glyoxime and methyl-isopropylglyoxime.

Introduction. The simplest aliphatic α-dioxime, glyoxime ($C_2H_4N_2O_2$) forms easily from glyoxal and hydroxylamine hydrochloride in aqueous solution. Some physico-chemical properties of this substance (dipolemoment in dioxane [1], isotopic shifts in the i.r. spectra of the deuterized products [2], acidity and protonation constant [3]) were studied by comparison to those of higher homologues. The basicity of the N-atom of aliphatic α-dioximes, the N—H bond by protonation and the $M—\overset{+}{N}$ — bond by formation of M (Diox. $H)_2$ — type complexes were observed to increase from the glyoxime to the higher homologues of the aliphatic α-dioximes (e.g. methylglyoxime, dimethylglyoxime, diethylglyoxime etc.) due to the inductive effect of the alkyl groups. The reaction of glyoxal with $NH_2OH \cdot HCl$ leads to the formation of the anti (α) — isomeric modification, as shown by neutron diffraction measurements [4]. As compared with the other aliphatic dioximes, the above mentioned chelating agent was only a little studied from co-ordination chemical point of view. The [M(Glyox. $H)_2$] (M = Ni, Pd and Pt) was obtained and its structure determined by means of x-ray meansurements [5—7]. The Ni(Glyox. $H)_2$ was proposed for detection of nickel [8] and for the spectrophotometric determination of cobalt (II) in basic media [9].

Results and discussion. We have observed that this dioxime is also able to synthesize various mixed chelates $[Co(Glyox.\ H)_2X_2]^{2-}$, $[Co(Glyox.\ H)_2(amine)X]$ and $[Co(Glyox.H)_2(amine)_2]^+$ by means of oxidation of a mixture of Co(II) — salts, glyoxime and monodentate ligands (e.g. Cl^-, Br^-, I^-, NCS^-, amine, phosphine etc.) and by substitution reactions from the aquo- and halogeno-derivatives, respectively. The sodium salts of the dicyano- and dithiocyanato-acids can be obtained with the oxidation of the components by air bubbling in aqueous solution. The $H[Co(Glyox.\ H)_2(CN)_2]$ and $H(Co(Glyox.H)_2$

* *University of Cluj-Napoca, Faculty of Chemical Technology, Department of Inorganic and Analytical Chemicstry, 3400 Cluj-Napoca, Romania*

$(NCS)_2$] form well defined crystalline salts with monovalent transition metal cations and metal-amines.

Table 1

New complex salts of the type Cation $[Co(Glyox.H)_2(CN)_2]$

Formula	Mol. wt. calcd.	Aspect	Analysis	
			Calcd.	Found
trans-$[Co(en)_2Cl_2] \cdot A$	535.1	sparkling, irregular green plates	Co 22.02 C 22.44 H 4.15	21.94 23,85 4.88
trans-$[Co(en)_2Br_2] \cdot A \cdot H_2O$	642.1	bright green sparkling thin plates	Co 18,32 H_2O 2,83 H 3.77	18.55 2.80 4.01
$[Co(DH)_2(NH_3)_2] \cdot A$	608.3	gold yellow thin plates	Co 19.38 C 33.14 H 4.30	18.98 33.64 4.38
$[Co(DH)_2(pyridine)_2] \cdot A \cdot 2H_2O$	768.5	gold yellow sparkling irregular plates	Co 15.34 H_2O 4.68 H 4.46 C 38.39	15.43 4.85 4.50 39.00
$[Co(DH)_2(aniline)_2] \cdot A \cdot H_2O$	778.5	brown irregular plates	Co 15.14 H_2O 2.31 C 40.12 H 4.66	15.16 2.50 40.26 4.41
$[Co(DH)_2(o\text{-toluidine})_2] \cdot A \cdot 2H_2O$	824.5	yellow-brown hexagonal plates	Co 14.30 H_2O 4.37	14.80 4.10
$[Co(DH)_2(p\text{-toluidine})_2] \cdot A$	788.5	yellow-brown plates	Co 14.95	14.75
$K[Co(Glyox.H)_2(CN)_2] \cdot H_2O$	342.2	long, orange sparkling prisms	Co 17.22	17.10

A = $[Co(C_2H_3N_2O_2)_2(CN)_2]^-$

Table 2

New complex salts of the type Cation $[Co(Glyox.H)_2(NCS)_2]$

Formula	Mol. wt. calcd.	Aspect	Analysis	
			Calcd.	Found
trans-$[Co(en)_2Cl_2] \cdot B$	599.3	light brown prisms	Co 19.67 S 10.70	19.40 10.48
$[Co(DH)_2(aniline)_2] \cdot B$	824.6	brown hexagonal plates	Co 14.30 S 7.71	14.28 7.48
$[Co(DH)_2(\alpha\text{-naphtylamine})_2] \cdot B$	924.7	short brown prisms	Co 12.73	12.60
$[Co(DH)_2(thiourea)_2] \cdot B$	790.6	brown microcryst.	Co 14.91 S 16.22	15.17 16.06
$K[Co(Glyox.H)_2(NCS)_2]$	388.4	brown prisms	Co 15.18	15.03

B = $[Co(C_2H_3N_2O_2)_2(NCS)_2]^-$

The free acids can also be isolated from aqueous solutions with an excess of H_2SO_4.

The above mentioned oxidation reaction in the presence of non complexing anions (e.g. SO_4^{2-}, NO_3^-, $CH_3—COO^-$) leads to obtaining the diaquo-complex: $[Co(Glyox.H)_2(H_2O)_2]^+$.

The anation of this derivative with stoechiometric amount of Na_2SO_3 (1 : 2), $Na_2S_2O_3$ (1 :2) and $(NH_4)_2SO_3$ (1 : 1) leads to the formation of sulfito — and thiosulfato-complexes:

$[Co(Glyox.H)_2(SO_3)_2]^{3-}$, $[Co(Glyox.H)_2(S_2O_3)_2]^{3-}$ and $[Co(Glyox.H)_2(H_2O)(SO_3]^-$

The latter mixed complex can be used as starting material for other anation reactions with aromatic and heterocyclic amines.

$$[Co(Glyox.H)(H_2O)(SO_3)]^- + \text{amine} = [Co(Glyox.H)_2\ (\text{amine})(SO_3)]^- + H_2O$$

Some new products of this type are characterized in Table 3.

Table 3

New complex salts of the type $NH_4[Co(Glyox.H)_2(SO_3)(amine)]$

Formula	Mol. wt. calcd.	Aspect	Analysis	
			Calcd.	Found
$NH_4[Co(Glyox.H)_2(SO_3)-$ (α-naphtylamine)] · $2H_2O$	510.4	irregular redbrown prisms	Co 11.55 S 6.28 H_2O 7.05	12.02 6.10 7.27
$NH_4[Co(Glyox.H)_2(SO_3)-$ (p-anisidine)] · $1.5H_2O$	481.3	brown plates	Co 12.25 H_2O 5.61	12.41 5.80
$NH_4[Co(Glyox.H)_2(SO_3)-$ (p-Cl-aniline)] · $2H_2O$	494.8	irregular brown cryst.	Co 11.89 H_2O 7.28	11.94 7.75
$NH_4[Co(Glyox.H)_2(SO_3)-$ (pyridine)] · H_2O	428.3	short, brown prisms	Co 13.76 S 7.49 H_2O 4.20	13.50 7.10 4.05
$NH_4[Co(Glyox.H)_2(SO_3)-$ (aniline)] · $2H_2O$	460.3	brown prisms	Co 12.80 S 6.96 H_2O 7.82	12.70 7.13 7.99

From the aqueous solutions of $Na_3[Co(Glyox.H)_2(SO_3)_2]$ and $Na_3[Co\ (Glyox.\ H)_2(S_2O_3)_2]$ some new metal-amine salts were isolated by double decomposition reactions with hexamines of Co(III) and Cr(III).

It is worth mentioning that the mono- and divalent metal (II, III) amines are unable for this purpose.

The sulfito- and thiosulfato-bis-glyoximino-complexes decompose in acidic media and SO_2 is evolved. From the thiosulfatocomplexes elementary sulfur is also deposited.

The physico-chemical properties of the glyoximino-derivatives are similar to those of the sulfito- and thiosulfato- Co(III) complexes of dimethylglyoxime, nyoxime and benzyldioxime. Some differences appear in the solubility, thermal stability and spectral data.

Table 4

New complex salts of the type $Cation_3$ $[Co(Glyox.H)_2(SO_3)_2]$ **and** $Cation_3$ $[Co(Glyox.H)_2(S_2O_3)_2]$

Formula	Mol. wt. calcd.	Aspect	Analysis		
				Calcd.	Found
$[Co(NH_3)_6] \cdot C \cdot 3H_2O$	608.4	yellow short prisms	Co	19.37	19.25
			H_2O	8.88	9.04
$[Co(NH_3)_6] \cdot D \cdot 3.5H_2O$	681.5	yellow-brown microcryst.	Co	17.30	17.38
			S	18.82	19.20
			H_2O	9.25	9.35
$[Co(NH_3)_5(H_2O)]C \cdot 2H_2O$	591.3	dark yellow short irregular prisms	Co	20.39	20.05
			H_2O	6.09	5.88
$[Co(NH_3)_5(H_2O)] \cdot D \cdot 2H_2O$	655	yellow-brown prisms	Co	17.98	17.70
			S	19.57	19.16
			H_2O	5.49	5.60
cis-$[Co(en)_2(NH_3)_2]C \cdot 3H_2O$	660.4	bright yellow microcryst.	Co	17.85	18.06
			H_2O	8.18	7.85
cis-$[Co(en)_2(NH_3)_2]D \cdot 3H_2O$	724.4	brown plates	Co	16.26	16.16
			H_2O	7.46	7.58
			S	17.70	18.00
$[Cr(urea)_6]C \cdot 6H_2O$	913.6	short green-yellow prisms	C	13.13	13.49
			H	4.63	4.39
			H_2O	11.83	11.36
$[Cr(urea)_6]D \cdot 4H_2O$	941.7	yellow prisms	H_2O	7.65	7.80
			C	12.76	12.36
			H	4.40	4.30
$[Co(en)_3]C \cdot 6H_2O$	740.5	orange plates	Co	15.91	15.42
			S	8.66	8.40
			H_2O	14.60	14.74
$[Co(en)_2(o\text{-phen})]C \cdot 5H_2O$	842.6	yellow-orange microcryst.	Co	13.99	13.78
			H_2O	14.24	14.20

C = $[Co(C_2H_3N_2O_2)_2(SO_3)_2]^{3-}$; D = $[Co(C_2H_3N_2O_2)_2(S_2O_3)_2]^{3-}$

The *IR spectra* show that two intramolecular O—H. O hydrogen bridges stabilize the coplanar $Co(Glyox.H)_2$ system, i.e. the „trans" geometric configuration of the complex studied

(νO—H: 2300—2400 cm^{-1}, δO—H..O: 1700—1800 cm^{-1}).

From the four IR and Raman active vibration frequencies of the sulfito-ligand, with a pyramidal structure and a C_{3v} symmetry, the ν_1 (S—O) vibrations appear at 1090—1130 cm^{-1} (s) and the ν_3 (S—O) ones at 960—980 cm^{-1}. The thiosulfato-group has also a C_{3v} symmetry with six IR and Raman active vibration frequencies. The most important of these, ν_2(S—O), ν_4(S—O), appear at 1010—1020 cm^{-1} (s) and at 1140—1180 cm^{-1} (s), respectively. By co-ordination to metal ions through the sulfur atom (in our cases Co—SO_3 and $CoSSO_3$), the νS—O valence frequencies are shifted to higher wave number values in both cases. (The shift in the opposite direction is characteristic to a M—O—S—O coordination.

The $\nu C{=}N$ frequencies of the co-ordinated NCS— group appear at 2080 cm^{-1} and this phenomenon pleads for a cobalt-isothio-cyanate — bonding (Co—NCS). The $\nu C{=}N$ frequencies of the CN-ligand at 2130—2140 cm^{-1} are in agreement with a Co—CN co-ordination through the carbon donor atom. By the free, ionic CN^- these frequencies can be observed at 2080 cm^{-1}.

The *thermal decomposition* of some $NH_4[Co(Glyox.H)_2(SO_3)(amine)]nH_2O$ —type complexes was studied by derivatography. The TG and DTA curves of $NH_4[Co(Glyox.\ H)_2(SO_3)(Py)] \cdot H_2O$ and $NH_4(Co(Glyox.\ H)_2(aniline)(SO_3)] \cdot 2H_2O$ are presented in Figs. 1 and 2.

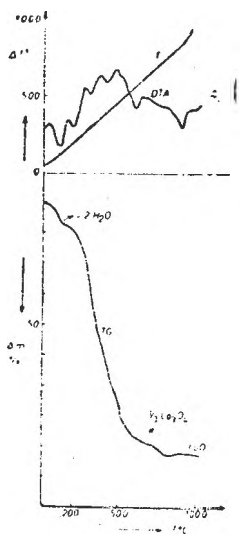

Fig. 1. TG and DTA curves of $NH_4[Co(Gylox.H)_2(SO_3)(Py)]\ H_2O$

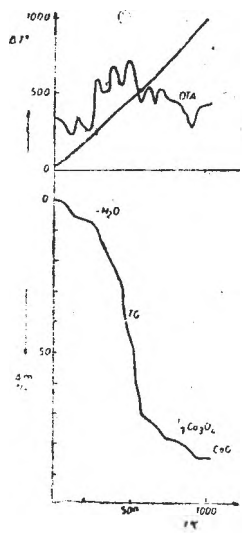

Fig. 2. TG and DTA curves of $NH_4[Co(Glyox.H)_2(SO_3)(aniline)]\ 2H_2O$

The substances studied are crystallohydrates. The loss of the crystallization water molecules occurs between 80 and 130°C. On the TG curves one or two the weight loss stops, corresponding to the end of the dehydration processes, and the same number of endothermal peaks on the DTA curves appears. After the dehydration processes, another endothermal reaction occurs (160—180°C), which can be considered as deamination, but it does not lead to a well defined intermediate product as in the case of the diamine derivatives $(Co(DH)_2(amine)_2]X \rightarrow$ $\rightarrow [Co(DH)_2(amine)X] +$ amine). The further decomposition stages are complex exothermal reactions, presumably with the participation of the atmospheric oxygen and imply the destruction of the whole co-ordination sphere (230—300, 330—480°).

Experimental. The sulfito-, thiosulfato-, ciano- and thiocyanatocomplexes were obtained on an analogous way described in our previous papers for dimethylglyoxime, — nyoxime — and benzyldioxime derivatives [10, 11].

Working conditions by the derivatographic measurements: heating rate: 10°/min. Sample weight: 100 mg, atmosphere: static air.

REFERENCES

1. C. Pigenet, J. Armand, H. Lumbroso, *Bull. soc. chim. France*, **1970**, 2124.
2. E. Borello, M. Colombo, *Ric. sci. (Roma)*, **25**, 2899 (1955; *C.A.* **51**, 14 557 (1957).
3. N. A. Plechanov, V. M. Peshkova, *Vestnik Moskovskogo Gas. Univ., Ser. Khimia*, **1974**, 492.
4. M. Calleri, G. Ferraris, D. Vitterbo, *Acta Cryst.*, **20**, 73 (1966).
5. M. Calleri, G. Ferraris, D. Vitterbo, *Acta Cryst.*, **22**, 468 (1967).
6. M. Calleri, G. Ferraris, D. Vitterbo, *Inorg. chim. Acta*, **1**, 297 (1967).
7. G. Ferraris, D. Vitterbo, *Inorg. chim. Acta*, **25**, 2066 (1973).
8. S. Kuse, S. Motomizu, K. Toei, *J. Chem. Soc.*, Japan, Chem. and Ind. Chem., **8**, 1611 (1973).
9. Masuda Nobosuka, Kajiwara Meisetsu, *Bunseki Kagaku*, **17**, 1352 (1968); C.A. **70**, 63 856 (1969).
10. Cs. Várhelyi, M. Somay, G. Ádámosy, *Rev. Roumaine Chim.*, **24**, 423 (1979).
11. J. Zsakó, Cs. Várhelyi, G. Liptay, *J. Thermal Anal.*, in press.

STUDIA UNIV. BABEŞ—BOLYAI, CHEMIA, XXXI, 1, 1986

PROTOLYTIC EQUILIBRIA IN MONOLAYERS OF BIOLOGICAL SIGNIFICANCE

EMIL CHIFU*, MARIA TOMOAIA-COTIŞEL*, AURORA MOCANU*, LIDIA ANDREI* and JÁNOS ZSAKÓ*

Received: November 29, 1985

ABSTRACT. — The influence of subphase pH ($3 \leqslant pH \leqslant 9$) on collapse pressure is studied, in the case of stearic acid, zeaxanthin and astaxanthin monolayers spread at aqueous solution/air interface. The paper also deals with, protolytic equilibria, and apparent surface acidity constants, K_a, are derived from the experimental collapse pressure *vs.* pH curves, by using a perfect solution approximation. The obtained pK_a values are 5.63; 6.84 and 6.66, respectively. The results are discussed in terms of molecular structure.

Introduction. The monolayer properties of non-ionic surfactants are influenced by the subphase pH, leading sometimes to important changes in the value of collapse pressure [1—4]. The latter is assigned to transformation of the uncharged monolayer into an ionic one, due to deprotonation of the surfactant in alkaline media, or to its protonation in the acid region. In some cases even equilibrium constants have been reported for these protolytic processes [1, 2]

In the present paper deprotonation of three biosurfactants, *viz.* stearic acid, zeaxanthin and astaxanthin, is investigated by studying their monolayer properties on aqueous subphases of different pH values, in the range 3—9, and apparent surface acidity constants are derived for them.

Surface acidity constants. The surfactant molecules may often receive a proton from an acid, or give one away to an appropriate base. Let us consider the ionization of insoluble surfactant molecule HX in a monolayer spread at aqueous solution/air interface:

$$\underset{(1)}{HX} + \underset{(0)}{H_2O} \rightleftharpoons \underset{(3)}{H_3O^+} + \underset{(2)}{X^-} \tag{1}$$

The equilibrium constant of reaction (1) can be given as

$$K = \frac{a_2^M a_3^M}{a_1^M a_0^M} \tag{2}$$

where a_i^M stands for equilibrium activity of the molecular species i in monolayer (the value of i is indicated in Eq. (1) for each molecular species, under the corresponding formula).

* *University of Cluj-Napoca, Department of Physical Chemistry, 3400 Cluj-Napoca, Romania*

As shown in an earlier paper of ours [1], the equilibrium constant obeys by the following equation:

$$RT \ln K = -\Delta G^{\circ M} - \pi \Delta A' \tag{3}$$

where $\Delta G^{\circ M}$ stands for variation of the standard Gibbs free energy in reaction (1), π is the surface pressure, and

$$\Delta A' = A_2' + A_3' - A_1' - A_0'$$

A_i' being the molar area of species i.

Since species H_2O and H_3O^+ are present in both the monolayer and bulk subphase, the thermodynamic equilibrium between these phases implies the equality of their chemical potentials. Consequently, both a_0^M and a_3^M will be determined by composition of the subphase. This allows us to define, in this heterogeneous system, an apparent surface acidity constant

$$K_a = \frac{a_2^M a_3^B}{a_1^M} \tag{4}$$

obeying by relation

$$RT \ln K_a = RT \ln a_0^B - \Delta G' - \pi(A_2' - A_1') \tag{5}$$

In Eqs. (4) and (5), a_i^B stands for activity of species i in the bulk subphase, $\Delta G'$ is variation of the standard Gibbs free energy corresponding to the transfer of a proton from surfactant molecule HX in the monolayer to a water molecule in the bulk subphase.

If the subphase is a dilute solution, a_0^B is practically constant. Since in the case of surfactant molecules the proton transfer cannot essentially modify the molecular area, in first approximation the last right hand side term of Eq. (5) can be neglected. Thus, K_a practically depends on temperature only.

By adopting the rational activity scale for monolayer, and the practical one for the bulk subphase, as well as by presuming both phases to be perfect solutions, the apparent surface acidity constant becomes

$$K_a = \frac{x_2^M [H]^B}{x_1^M} \tag{6}$$

where x_i^M stands for the molar fraction of i in monolayer and $[H]^B$ for the molar concentration of H_3O^+ in the bulk subphase.

Due to the protolytic equilibrium, the monolayer can be considered as a mixed phase containing two surfactant species, viz. HX and X^-, as well as H_2O and H_3O^+, according to Eq. (1). Since in the bulk subphase $x_3^B \ll x_0^B$, and one cannot expect to be otherwise in the monolayer, x_3^M can be neglected before the other molar fractions, at least as first approximation. Thus, one can adopt

$$x_0^M + x_1^M + x_2^M = 1 \tag{7}$$

From Eqs. (6) and (7) one obtains:

$$x_1^M = \frac{[H]^B}{K_a + [H]^B}(1 - x_0^M) \text{ and } x_2^M = \frac{K_a}{K_a + [H]^B}(1 - x_0^M) \tag{8}$$

Upon compression of the monolayers, a new phase eventually appears — the collapsed bulk phase. By presuming a metastable thermodynamic equilibrium [5] between the monolayer and the "freshly collapsed" bulk phase, the collapse pressure, π_c, depends on monolayer composition [6]. In perfect solution approximation, the equilibrium condition for the surface mixture of surfactants 1 and 2 can be written as [1]

$$x_1^M \frac{\exp[(\pi_c - \pi_1)A_1/kT]}{1 - \exp(-\pi_1 A_0/kT)} + x_2^M \frac{\exp[(\pi_c - \pi_2)A_2/kT]}{1 - \exp(-\pi_2 A_0/kT)} = 1 \tag{9}$$

where π_c, π_1 and π_2 stand for the collapse pressure of the mixture and the collapse pressure of the „pure" monolayers containing surfactant 1 or 2, respectively. A_0, A_1, A_2 stand for molecular area of water and of the surfactant species, respectively.

On the other hand, the equilibrium between the monolayer and the subphase enables us to obtain x_0^M in the perfect solution approximation, as function of the surface pressure. Upon collapse pressure, π_c it will be [1]

$$x_0^M = \exp(-\pi_c A_0/kT) \tag{10}$$

In the case of the protolytic equilibrium (1), composition of the monolayer, and consequently the collapse pressure, will depend on the subphase pH. By taking into account Eqs. (8) and (10), the equilibrium condition (9) becomes:

$$\frac{1 - \exp(-\pi_c A_0/kT)}{K_a + [H]^B}\left\{[H]^B \frac{\exp[(\pi_c - \pi_1)A_1/kT]}{1 - \exp(-\pi_1 A_0/kT)} + K_a \frac{\exp[(\pi_c - \pi_2)A_2/kT]}{1 - \exp(-\pi_2 A_0/kT)}\right\} = 1 \tag{11}$$

where π_1 and π_2 can be obtained as limiting values of the collapse pressure at low and high pH values, respectively.

Eq. (11) allows us to derive apparent surface acidity constants from experimental collapse pressure *vs* subphase pH curves.

Experimental. *Film Forming Materials.* The studied surfactants were: stearic (octadecanoic) acid (p.a., Schuchardt), zeaxanthin (3,3'-dihydroxy-β-carotene) and astaxanthin (3,3'-dihydroxy-4,4'-dioxo-β-carotene), the last two carotenoid pigments of all-*trans* configuration (Hoffmann La Roche).

Spreading Solvents. For stearic acid pure benzene, in the case of zeaxanthin benzene containing 2—3% absolute ethanol and with astaxanthin benzene containing 4—8% chloroform were used.

Subphases. Bidistilled water, containing various electrolytes, was used as subphase for monolayers. The subphase pH was adjusted by means of NaOH (pH: 9), borate buffers (pH: 7.6—9), phosphate buffers (pH: 6—9), citrate buffers (pH: 3—7) and HCl (pH: 3).

Recording of the Compression Isotherms. The surface pressure *vs* mean molecular area curves were recorded by using the Wilhelmy method. The waiting time allowed for evaporation of the spreading solvent was of 2—30 min. The monolayers were compressed manually and the surface pressures were recorded discontinuously, at room temperature (22 ± 2°C). The compression rate employed were in the range 0.5—2.5 Å²/molecule.min in the case of stearic acid and 2—4 Å²/molecule.min with carotenoid pigments.

Results and Discussion. The compression isotherms were recorded at different pH values, while the collapse pressure and the collapse molecular area were derived from each curve as values corresponding to the sudden slope change of the isotherm at high surface pressures, indicated by arrows on Figure 1.

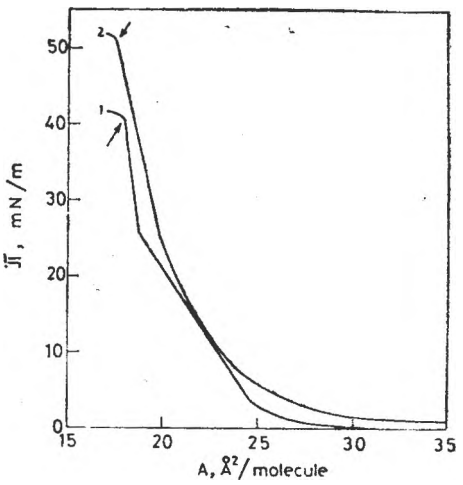

Fig. 1. Compression isotherms of stearic acid and deriving of collapse pressure and collapse molecular area (see arrows) 1 — — pH = 3 ;2 — pH = 8.

In the case of all the studied surfactants, the collapse pressure increased with increasing pH, but in a well defined pH region only, and it showed a constant value out of this region, *viz.* a lower one at the acid side, characterizing the protonated species, and a higher one at the alkaline side, corresponding to deprotonated molecular species. In Figure 1 the compression isotherms of stearic acid are given for these extreme conditions, allowing us to derive surface characteristics π_1, A_1 for the protonated species and π_2, A_2 for the deprotonated ones. These surface characteristics are presented in Table 1.

Table 1

Collapse pressure and collapse molecular area of the neutral molecules and of their anion-

Biosurfactant	HX		X^-	
	Π_1 (mN/m),	A_1(Å²)	Π_2 (mN/m),	A_2(Å²)
Steanc acid	40.8	18.0	51.0	17.6
Zeaxanthin	44.8	30.0	50.3	30.0
Astaxanthin	45.0	24.0	51.0	21.0

The surface collapse pressure *vs* pH curves of the studied surfactants are given in Figure 2. The experimental points represent a mean value, obtained from at least 10 isotherms recorded at the same pH. The shape of the curves is consistent with the hypothesis of a protolytic equilibrium. In the acid region the surfactant forms a „pure" monolayer, containing only protonated — that is neutral — molecules, the collapse pressure is constant, equal to π_1. In the S-shaped portion of the curve, the monolayer becomes mixed, due to ionization of the surfactant, i.e., beside protonated molecules, it also contains deprotonated ones. In the alkaline region the collapse pressure attains its maximum value, π_2, when the surfactant is completely ionized, and the monolayer becomes again a „pure" one, formed by anions X^-. It is worth mentioning that the higher value of π_2, as compared to π_1, might be due to appearance of an electric double layer with participation of anions X^- and the corresponding counterions coming from the subphase.

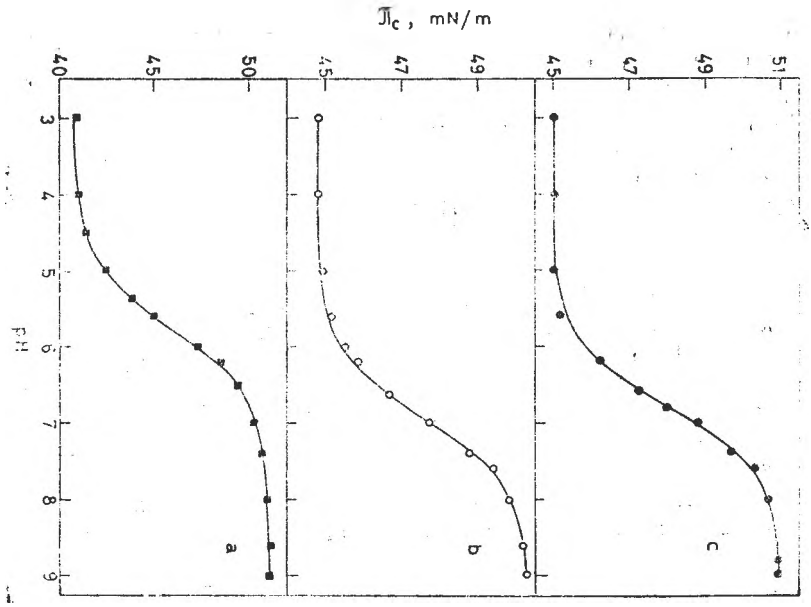

Fig. 2. Collapse pressure *vs* pH curves.
a — Stearic acid; b — Zeaxanthin; c — Astaxanthin.
The full line curves were calculated by means of Eq. (11)
and by using the surface characteristics given in
Table 1 and K_a values in Table 2.

From the experimental π_c values obtained for intermediate pH's, apparent surface acidity constants were derived, by using Eq. (11). In these calculations the π_1, π_2, A_1 and A_2 values given in Table 1 were used, as well as the approximate value $A_0 = 10 Å^2$/molecule, for the water molecules. Deriving of K_a values was performed by means of a curve-fitting procedure. Eq. (11) was solved by presuming different K_a values. For each K_a the standard deviation of the experimental π_c values from the theoretical ones (obtained as the solution of Eq. (11)), was calculated. By performing a systematic variation of K_a, this standard deviation was minimized. The obtained K_a values are given in Table 2, together with corresponding minimum standard deviation Δ.

Tabele 1

Apparent surface acidity constants and minimum standard deviations of the collapse presssures from the theoretical ones

Biosurfactant	$K_a \cdot 10^7$ (moles·litre^{-1})	Δ (mN/m)
Stearic acid	23.4	0.24
Zeaxanthin	1.45	0.16
Astaxanthin	2.19	0.15

In the literature apparent surface acidity constants were reported for stearic acid only, viz. $K_a = 2.82 \times 10^{-6}$ on the basis of surface potential measurements [7], and 6.31×10^{-9} by measuring the collapse pressure [2] and by using a simplified variant of Eq. (11). As seen, our results are in agreement with the former value. The K_a values of the carotenoids, exhibited in Table 2, are consistent with each other, taking into account their molecular structure. Zeaxanthin, having on OH group only, is the weakest acid. Astaxanthin is a little stronger, due to the inductive effect of the neighbouring carbonyl group. The strongest is stearic acid, having the electron-withdrawing carbonyl linked directly to the OH group.

It is worth mentioning that the numerical value of K_a is almost with an order of magnitude smaller than the acidity constants of the inferior fatty acids in aqueous solutions. That could be accounted for by both the shift of the pH scale in monolayer as compared to the subphase, due to the surface potential [8] and/or the different structure of water in the monolayer as to that in the bulk phase. The diminution of the surface equilibrium constant might also be a real one. Thus, the acidity constant of stearylphosphonic acid adsorbed at oil/water interface seems to be 30 times smaller than that in the bulk [9], which might be assigned to the preferential accumulation of the neutral molecular species in the interface [10].

The protolytic equilibria in monolayers of biosurfactants, as fatty acids and carotenoid pigments, might play an important role in membrane phenomena occurring *in vivo*, e.g. in the electric properties of biomembranes, taking into account that they are ubiquitous as both structural and functional components of some natural membranes.

REFERENCES

1. Zsakó, J., Tomoaia-Cotişel, M., Mocanu, A., and Chifu, E., *J. Colloid Interface Sci.*, **110**, 317 (1986).
2. Joos, P., *Bull. Soc. Chim. Belges*, **80**, 277 (1971).
3. Porter, E. F., *J. Am Chem. Soc.*, **59**, 1883 (1937).
4. Myers, R. J., *J. Am. Chem. Soc.*, **57**, 2734 (1935).
5. Gaines, G. L., Jr., "Insoluble Monolayers at Liquid-Gas Interfaces", Wiley Interscience, New York, 1966.
6. Zsakó, J., Tomoaia-Cotişel, M., and Chifu, E., *J. Colloid Interface Sci.*, **102**, 186 (1984).
7. Betts, J. J., and Pethica, B. A., *Trans. Faraday Soc.*, **52**, 1581 (1956).
8. Davies, J. T., and Rideal, E. K., "Interfacial Phenomena", Acad. Press, New York, 1963.
9. Payens, T. A. J., "Proc. 2nd. Internat. Congr. of Surface Activity", vol. 1, Butterworth, London, 1957, p. 64.
10. Hiemenz, P. C., "Principles of Colloid and Surface Chemistry", Marcel Dekker, New York, 1977, p. 280.

STUDIA UNIV. BABEŞ—BOLYAI, CHEMIA, XXXI, 1, 1986

ELECTROSYNTHESIS OF PROPIONITRILE
I. Preliminary experiments

LIVIU ONICIU*, IOAN A. SILBERG, DAN A. LÖWY**, MARIA JITARU** and FLORENTINA CIOMOŞ****

Received: February 2, 1986

ABSTRACT. — The paper presents preliminary experiments concerning the conditions for the orientation of acrylonitrile electroreduction towards propionitrile by avoiding reductive dimerization reactions, which yield adiponitrile and methylglutaronitrile. The influence exerted upon the selectivity of propionitrile formation by the composition of the supporting electrolyte, the electrocatalytic properties of cathode and the flow speed in the electrochemical reactor were investigated. The results point to the option for undivided electrochemical reactors, fitted with couples of monopolar electrodes: Pb, Cu or Cd cathodes and stainless steel anode. The supporting electrolyte, containing mainly phosphate buffers, to which submicellar concentrations of cationic surfactants are added, is to be circulated in the reactor at $\geqslant 1$ m/s.

The electrochemical reduction of acrylonitrile (ACN) to propionitrile (PN) is part of the research program of our team, aiming at the implementation of electroorganic synthesis — an economically, energetically and ecologically advantageous alternative — in the Romanian chemical industry.

The paper reports preliminary results in determining the experimental conditions necessary for the orientation of ACN electroreduction towards the synthesis of PN, by avoiding reductive dimerizations, leading to adiponitrile (ADN) and methylglutaronitrile, as well as the cyanoethylation of water, yielding bis (cyanoethyl) ether (1—4). In order to determine the appropriate conditions for this synthesis, the influence of various parameters is to be investigated, including the nature and composition of the supporting electrolyte, the electrocatalytic properties of the cathode, as well as the circulation rate of the fluid in the electrochemical reactor.

The electrosynthesis of PN, a deceptively simple process of double electronation and double protonation of the polarized ACN molecule, can take place along several pathways (Fig. 1). The most probable are the mechanisms involving an alternation of E (electronation) and C (protonation) steps, or the simultaneous uptaking of one electron and one proton. We consider that EE processes (two simultaneous or successive electronations) followed by two C steps (simultaneous or successive protonations) are energetically unfavourable.

On metals with low hydrogen discharge overvoltage, the electroreduction of ACN might also proceed *via* a CC-mechanism (the electrohydrogenation of the activated olefine bond). However, in this case the proton discharge has to be carefully controlled, in order to ensure the complete *in situ* consumption of hydrogen.

* *University of Cluj-Napoca, Depatrment of Physical Chemistry, 3400 Cluj-Napoca, Romania*
** *ICECHIM—Institute of Chemical and Biochemical Energetics, Cluj-Napoca Research Group, 3400 Cluj-Napoca, Romania*

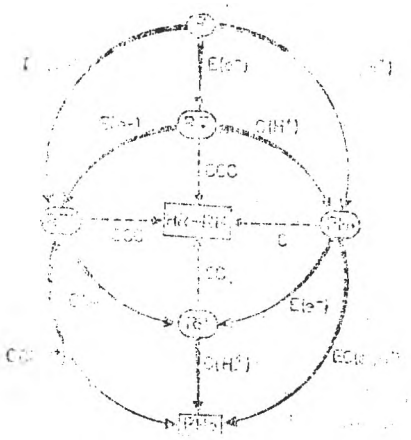

Fig. 1. The mechanism of the acrylonitrile (R) electroreduction to propionitrile (RH_2) and adiponitrile (HR—RH).

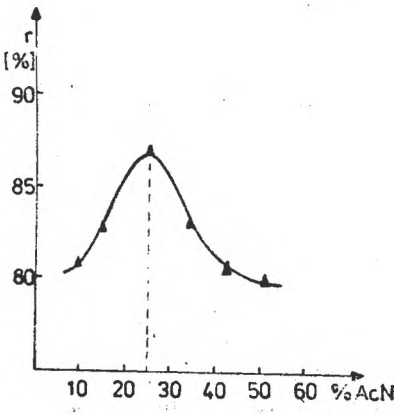

Fig. 2. Yield of propionitrile (r) *versus* the proportion of acrylonitrile in the electrolysis mixture.

Under certain conditions (4), all of the four intermediate species showed in Fig. 1 can undergo condensations with a molecule of ACN, leading to the main hydrodimer, ADN (represented as HR—RH in the center of Fig. 1).

In order to obtain PN with maximal yields it is recommended to have an approx. 25% proportion of ACN (see Fig. 2) in the dispersion subjected to electrolysis; this proportion ensures at the cathode a sufficient influx of ACN to counteract the hydrogen discharge, but is, at the same time, small enough to allow avoiding, under well-chosen conditions, the electrohydrodimerization leading to ADN (5).

Experimental. The experimental set-up (Fig. 3) consists of a pressfilter type, undivided electrochemical reactor (1), fitted with monopolar electrodes (2), a phase-separation vessel (3), heat — exchanger (4) and circulation pump (5). The electrode couple is connected to a stabilized direct current source (6). The following parameters were monitored: temperature (by means of the thermometer 7, immersed in the vessel 3), the cell voltage (voltmeter 8) and current intensity (ampermeter 9). The phosphate buffer (pH 7) supporting electrolyte also contains a cationic surfactant, which facilitates the access of ACN at the cathode by lowering the lyophilic character of the interface [6, 7].

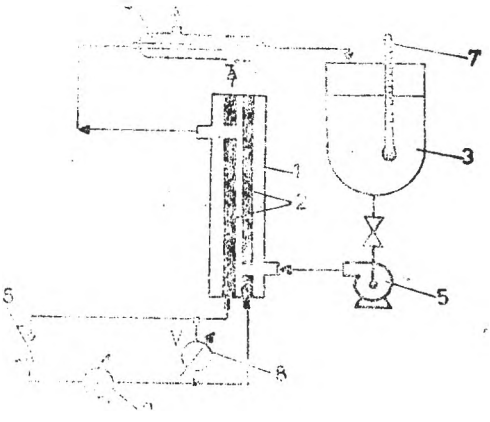

Fig. 3. Experimental set-up.

Results and Discussion. The products of ACN electroreduction obtained under the above mentioned conditions were analyzed by gas-chromatography with a M-9 type modular chromatograph (ITIM — Cluj-Napoca); the method was previously described (8).

The selectivity of PN formation (S) is defined as:

$$S = \frac{[PN]}{[PN] + [ACN]} \cdot 100$$

where [PN] and [ADN] stand for the concentrations of propionitrile and adiponitrile, respectively, in the organic phase.

The experimental data thus obtained pointed out that the selectivity of PN formation is increased as the surfactant concentration in the supporting electrolyte solution decreases. Thus, the selectivity reaches values over 90% when submicellar concentrations of the quaternary ammonium salts (QAS) are used (Fig. 4). Under the same conditions the Cd-stainless steel electrode couple yields only 60% selectivity.

Figure 4 also displays the concentration profile of the surfactant — the trimethylalkyl (C_{12}—C_{14})—ammonium chloride, manufactured by I.D. Timişoara under the trade name Romegal CM (henceforth abbreviated RCM). The decrease of RCM concentration in the aqueous phase takes place due to two processes: the partition of the surfactant between the aqueous and the organic phase (occurring immediately after the preparation of the electrolysis mixture) and its slow consumption during the electrosynthesis.

The data in Table I show that the selectivity of the electroreduction process is controlled by both the electrocatalytic properties of the cathode and the nature of the employed surfactant. By using the diallyldipropylammonium chloride (prepared by ICPAO-Mediaş) respectively a copolymer of dimethyl diallylammonium chloride and acrylamide („Penilit" — „Petru Poni" Institute, Jassy), the selectivities obtained on the Pb-stainles steel electrode couple are 6—7.5 times larger than those obtained with RCM. The selectivity seems to also be favorably influenced by increasing the flow speed in the reactor.

Conclusions. Prospectives. The preliminary investigations herewith reported concerning the electroreduction of ACN to PN bring in the forefront the

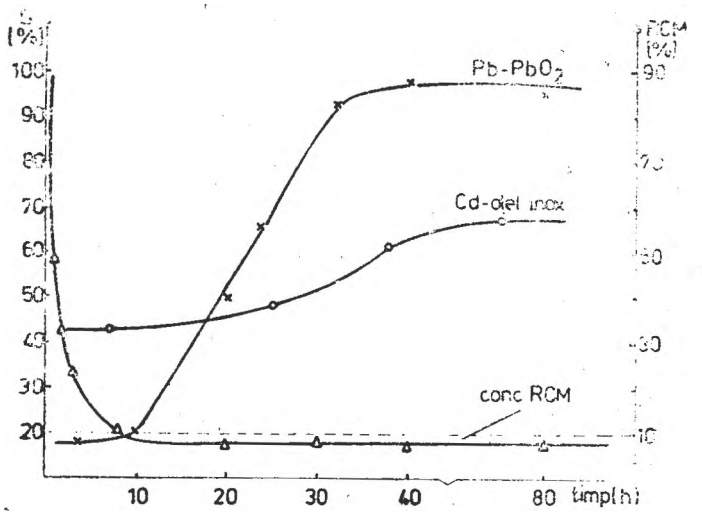

Fig. 4. Evolution of the selectivity for propionitrile formation (S) on Pb—PbO_2 and Cd-stain less steel electrode couples, *versus* the surfactant concentration in the aqueous phase (c_{RCM}).

Table 1

The influence of experimental parameters upon the selectivity of propionitrile selectivity

SURFACTANT USED	ELECTRODE COUPLE	S [%] 1 m/s	S [%] 0,2 m/s	EXPERIMENTAL CONDITIONS
Dimethyldialyl ammonium chloride	Pb-stainless steel	85,6	77,3	
	Pb-stainless steel	12,1	—	
	$Pb-PbO_2$	42,3	36,5	pH 7
Romegal CM*	Cd-stainless steel	60,9	48,4	$i \simeq 10$ mA/cm² $t = 25 \pm 1$°C
	Cu-stainless steel	62,8	60,3	concn. of the surfactant $\leqslant$ CMC
Ponilite*	Pb-stainless steel	91,7	84,9	

* See text

option for the use of undivided electrochemical reactor, with monopolar electrodes (stainless steel anodes, and copper, cadmium or lead cathodes). The supporting electrolyte, phosphate buffer, containing submicellar concentrations of QAS is to be circulated at rather high linear speed ($\geqslant$ 1 m/s).

Furthermore, the Cd-stainless steel and Cu-stainless steel electrode couples deserve more attention. Taking into account the low hydrogen discharge overvoltage on copper as well as its catalytical properties, the formation of PN on cathodes made of this metal might proceed not only by electroreduction but also by electrohydrogenation of the polarized ACN molecule. This pathway can be energetically more favorable if, as mentioned above, the requirement of total *in situ* consumption of the discharged hydrogen is met.

Experiments are now in progress investigating the influence of pH lowering, an acid medium increasing the availability of protons for the C steps, thus reducing the chances of the undesired reductive dimerizations.

REFERENCES

1. Oniciu, L., Silberg, I. A. and Ciomoş, F., *Rev. Chim.* Bucharest, **36** (5), 406 (1985).
2. Oniciu, L., Ciomoş F. and Silberg, I. A., *ibid.*, **36** (6), 503 (1985).
3. Oniciu, L., Silberg, I. A. and Ciomoş, F., *ibid.*, **36** (7), 628 (1985).
4. Oniciu, L., Silberg, I. A., Bâldea, I., Ciomoş, F., Jitaru, M., Löwy, D. A., Oprea, O. H. and Radu, L., "Kinetics of competing reactions of acrylonitrile electroreduction to adiponitrile and propionitrile" in: *Proceedings of the* 36th *Meeting of the International Society of Electrochemistry*, Salamanca, Spain, September 23—28, 1985, p. 13 010
5. *Badische Anilin und Soda Fabrik A.- G.*, Fr. Demande 2 004 052 (Cl. C 07 c), 21 Nov. 1969; *C. A.* **72**, 128 147 g (1970).
6. Oniciu, L., Löwy, D. A., Silberg, I. A., Anghel, D. F., Ciomoş, F. and Jitaru M., "Electroanalytical methods for determination of cationic surfactants involved in adiponitrile electrosynthesis", in: *Proceedings of the second Symposium of Applied Electrochemistry*, Timişoara, 4—5 October 1985, Tome I, p. 207.
7. Oniciu, L., Löwy, D. A., Silberg, I. A. and Anghel, D. F., *Analusis* **14**, 456 (1986).
8. Löwy, D. A., Silberg, I. A. and Oniciu, L., *Rev. Chim.*, Bucharest, **36** (4), 354 (1985).

STUDIA UNIV. BABEŞ—BOLYAI, CHEMIA, XXXI, 1, 1986

POTASSIUM BIS—(BORO—11—TUNGSTO) URANATE

MARIANA RUSU* and ALEXANDRU V. BOTAR*

Received: April 30, 1986; accepted: Spril 30. 1986

ABSTRACT. — The authors present their investigations on potassium salt of bis-(boro-11-tungsto) uranate heteropolyanion. The chemical composition and individuality of this heteropolycompound, as well as the coordination number of uranium in this compound have been determined. It has been found that compound $K_{14}[U(BW_{11}O_{39})_2] \cdot 25H_2O$ contains twenty-five water molecules of zeolitic nature and their elimination up to 500°C entails no alteration in the structure of this compound.

The unsaturated heteropolytungstates of UL_2—type, where $L = PW_{11}O_{39}^{7-}$, $SiW_{11}O_{39}^{8-}$, $P_2W_{17}O_{61}^{10-}$, $As_2W_{17}O_{61}^{10-}$ are obtained after partial degradation of the saturated anions at pH = 6—7 by adding potassium hydrocarbonate, in the presence of the U(IV) metallic ion [1—3]. The potassium salt of $U(BW_{11}O_{39})_2^{14-}$ heteropolyanion has been obtained by a direct reaction between $Na_2WO_4 \cdot 2H_2O$, H_3BO_3 and $U(CH_3COO)_4$.

Experimentnl. *Synthesis of potassium salt.* The synthesis of potassium salt of $[U(BW_{11}O_{39})_2]^{14-}$ heteropolyanion was obtained by the following method: a solution containing 10 g (0.303 mol) H_3BO_3 was added to a solution containing 100 g (0.162 mol) $Na_2WO_4 \cdot 2H_2O$. The pH of 6—6.5 was adjusted by CH_3COOOH conc. Then the solution was heated to 70°C. To this, a solution containing 7 g (0.015 mol) $U(CH_3COO)_4$ was added stepwise, under continuing stirring. The U(IV) salt was obtained by reducing a U(VI) salt using the Jones method [4]. The mixture was refluxed for 30 min. to 80—90°C. The solution was finally cooled down to 5°C, filtered and 50 g KCl was added to it. Dark-brown microcrystals were yielded after having kept the mixture at this 5°C temperature for 48 hrs., which were subsequently purified by repeated re-crystallization from distilled water (70°C and pH = 6 — 6.5).

Chemical analysis: The potassium salt of $[U(BW_{11}O_{39})_2]^{14-}$ heteropolyanion was chemically analysed acording to the general procedure [5]. Uranium was photocolorimetrically analysed with Arsenazo III [6]. The amount of tungsten was determined by precipitation with cinchonine, followed by an ignition to WO_3 at 800° [7]. Boron was determined by treatment with glycerol solution, then the released acid was titrated with 0.1 M NaOH solution [8]. Potassium was determined by stirring with tetraphenylborate [9]. The water content was stated thermogravimetrically. The chemical analysis results are given in Table 1.

Compound	K		U		B		W		H_2O	
	calcn.	found	calcn.	found	calcn.	found	calcn.	found	calcn.	found
$K_{14}[U(BW_{11}O_{39})_2] \cdot 25H_2O$	8,40	8,28	3,61	3,68	0,33	0,31	61,68	61,95	6,66	6,87

UV electronic spectrum. The chemical individuality of $K_{14}[U(BW_{11}O_{39})_2] \cdot 25H_2O$ heteropolycompound was checked by recording the UV electronic spectrum on aqueous solutions of the synthesized compund (Fig. 1.), with a $5 \cdot 10^{-6}$M concentration in heteropolycompound (Fig. 1). The spectrum was recorded by a "Specord—UV—VISS" spectrophotometer.

* *University of Cluj-Napoca, Faculty of Chemistry, 3400 Cluj-Napoca, Romania*

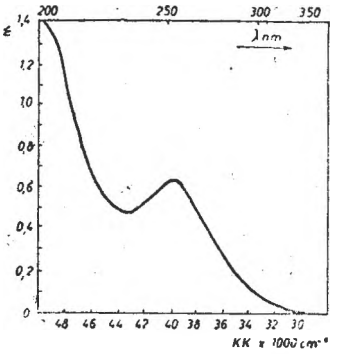

Fig. 1. UV spectrum of compound $K_{14}U(BW_{11}O_{39}) \cdot 25H_2O$

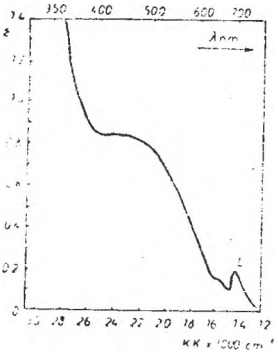

Fig. 2. *In visible* electronic absortion spectrum of compound $K_{14}U(BW_{11}O_{39})_2 \cdot 25HHO$

The in visible *electronic spectrum.* The oxidation state of uranium in the obtained compound was ascertained by using the absorption spectrum *in visible* domain on a solution of $5 \cdot 10^{-3}$ M compound concentration (Fig. 2). The electronic absorption spectrum *in visible* was also recorded by a "Specord UV—VISS" spectrophotometer.

IR spectrum. The IR spectrum of solid $K_{14}[U(BW_{11}O_{39})_2] \cdot 25H_2O$ heteropolycompound was recorded by a "UR—10—Zeiss Jena" spectrophotometer, using the KBr pellets technique. The spectral analysis data are shown in Table 2.

Compound	$\bar{\nu}$ cm^{-1}	Assigning
$K_{14}[U(BW_{11}O_{39})_2] \cdot 25H_2O$	750	W-O-W (ν_{asim}); W=O (V)
	810	W-O-W (ν_{asim}); W=O (V)
	960	W-O-W (ν_{asim}); W=O (V)
	1120	U-O (V)
	1240	B-O (V)
	1640	H-O-H (V)

Thermal analysis. The thermal analysis was determined in 40—600° temperature range. The measurements were performed by an OD—102 Paulik—Erdelyi derivatograph without maintaining isothermal conditions, imparting a 4 °C/minute heating rate and a 100 mg balance sensitivity, sample weight being 800 mg. The thermograph of compound $K_{10}[U(BW_{11}O_{39})_2] \cdot 25H_2O$ is plotted in Figure 3.

Results and Discussion. The newly-obtained heteropolycompound has the formula: $K_{14}[U(BW_{11}O_{39})_2] \cdot 25H_2O$, in good agreement with the experimental data. This compound is formed according to the following equations:

$$22Na_2WO_4 + 2H_3BO_3 + U(CH_3COO)_4 + 26CH_3COOH =$$

$$= Na_{14}[U(BW_{11}O_{39})_2] \cdot 25H_2O + 30CH_3COONa + 16H_2O$$

$$Na_{14}[U(BW_{11}O_{39})_2] + 14KCl = K_{14}[U(BW_{11}O_{39})_2 + 14NaCl$$

The UV spectrum of the aqueous solution of compound $K_{14}[U(BW_{11}O_{39})_2]$ exhibits an absorption band with a peak at 40.000—38.500 cm^{-1}, what is assigned to a charge transfer from oxigen to tungsten atoms, i.e. to a $p_\pi - d_\pi$ electron

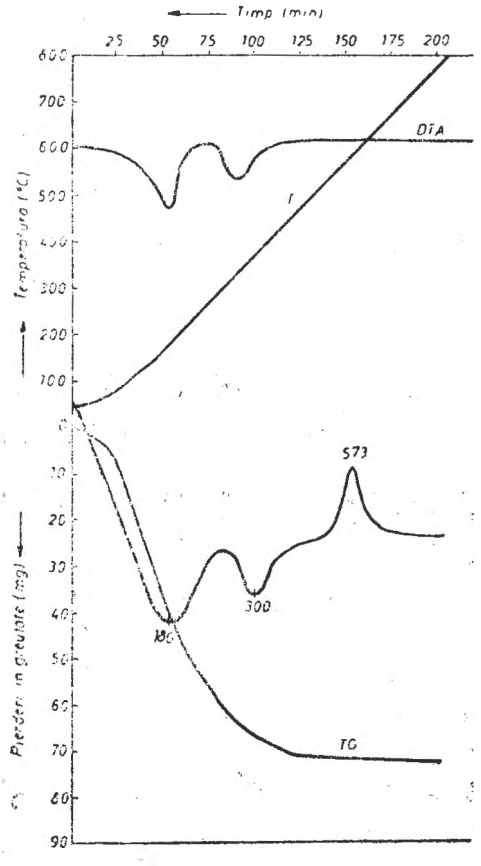

Fig. 3. Thermograph plot of compound $K_{14}U(BW_{11}O_{39})_2 \cdot 25_{22}O$

transfer [10]. This band is specific to the 1:1:11 heteropolyanions type.

By studying the electronic absorption spectrum of compound $K_{14}[U(BW_{11}O_{39})_2]$ *in visible*, we observed the presence of an L band at 14.490 cm^{-1} and a broad absorption band at 25.000—20.000 cm^{-1} what is, entailed by the charge transfer from U(IV) to W(VI). These two bands suggest an octahedral configuration of the U(IV) central ion [11].

The IR spectrum of compund $K_{14}[U(BW_{11}O_{39})_2] \cdot 25H_2O$ displays three absorption bands from 700—1000 cm^{-1}, which are due to stretching vibration of the W—O bonds. The absorption band maxima are found at 760.875 and 960 cm^{-1}; absorption bands in the above mentioned range are characteristic of heteropolytungstates, particularly of the 1:1:11 series and allow to indentify this compounds on the basis of IR spectra [12]. The three absorption bands located at 1120.1240 and 1640 cm^{-1} seen in the IR spectrum are due to B—O, U—O and H—O—H bond stretching vibration, respectively. The broad absorption band situated between 3600 and 3400 cm^{-1} is also indicative of the HOH bond stretching vibration.

The thermal dehydration process of $K_{14}[U(BW_{11}O_{39})_2] \cdot 25H_2O$ heteropolycompound, shown in Fig. 3., starts at 40°C and evolves in two stages:

1) Between 40—170°, sixteen hydration water molecules are eliminated, as evidenced by the endothermal effect at 165° and a weight loss of 4.25%;
2) Between 170—420°, nine other water molecules are eliminated, as shown by the endothermal effect at 360° and the weight loss of 2.61%.

The overall weight loss up to this temperature, calculated by addition of the weight losses in the two stages, is 6.86% and corresponds to 25 crystallization water molecules of zeolite nature. The elimination of these does not affect the parent structural lattice.

Destruction of the complex and the formation of a new phase is evidenced by the exothermal peak at 573°. The stability of the anhydrous compound ranges between 420—500°.

The study of electronic absorption spectra in UV, visible and IR ranges on $K_{14}[U(BW_{11}O_{})_2] \cdot 25H_2O$ heteropolycompound shows that this compound belongs to 1 : 1 : 11 heteropolycompound series and suggests an octahedral configuration of the U(IV) central ion.

REFERENCES

1. M. Rusu, *Teză de doctorat*, „Univ. Babeş-Bolyai" Cluj-Napoca.
2. Gh. Marcu, M. Rusu and L. Ocheşel, *Rev. Roumaine de Chimie*, **22**, 849 (1977).
3. Gh. Marcu, M. Rusu and M. Oneaga, *Studia Univ. Babeş-Bolyai, Chemia* **2**, 51 (1979).
4. J. H. Kennedy, **24**, *Analyt Chem.* **32**, 150 (1960).
5. V. E. Simmons, Ph. D. Thesis, Boston University, 1963.
6. B. V. Savvin, *Talanta*, **8**, 673 (1961).
7. A. I. Vogel, "A Textbook of Quantitative Inorganic Analysis" 2-nd ed., London, 1951 p. 418.
8. C. Gh. Macarovici, „Analiza chimică cantitativă anorganică", Ed. did. şi ped., Bucureşti (1979), p. 174.
9. M. Kohler, *Z. analyt. Chem. B.*, **138**, 9 (1953).
10. M. T. Pope, *Inorg. Chem.*, **2**, 662 (1970).
11. K. W. Bagnal, J.C.S. Dalton, **1973** 2682.
12. C. M. Flynn, Jr. and M. I. Pope, *Inorg. Chem.*, **10**, 2745 (1971).

CRONICA

Participări la manifestări ştiinţifice internaţionale

● Dr. Luminiţa Silaghi — Dumitrescu a participat la „Cel de al 7-lea Simpozion European de Spectroscopia Polimerilor" organizat la Dresda (R.D.G.) între 15—18 oct. 1985, prezentînd lucrările: *Spectroscopic Criteria to Distinguish Polymeric and Molecular Structures in Metallic and Organo-Metallic Derivatives of Dithiophosphorous Ligands*, I. Silaghi-Dumitrescu R. Grecu, L. Silaghi-Dumitrescu, R. Constantinescu, C. Silvestru şi I. Haiduc; *Spectroscopic Arguments for Polimerization of Organotin Diorgano-Phosphinates*, C. Silvestru, R. Grecu, R. Constantinescu, L. Silaghi-Dumitrescu şi I. Haiduc.

● Conf. dr. Emil Cordoş a participat la „Sedinţa de lucru a grupului C.A.E.R. pentru confecţionarea aparaturii de cercetări ştiinţifice, Wroclaw, 26—29 martie 1985, (Polonia).

● Prof. dr. Gheorghe Marcu a luat parte ca membru al delegaţiei române la „*A XIV-a* Consfătuire a academiilor de ştiinţe din ţările socialiste" organizată între 23—28 septembrie 1985 în Varşovia.

Organizări de sesiuni ştiinţifice

● „Sesiunea anuală de comunicări ştiinţifice a cadrelor didactice de la Facultatea de tehnologie chimică" a fost organizată în 13—14 decembrie 1985 şi s-au prezentat 26 de lucrări. Conferinţa plenară a fost ţinută de conf. dr. Emil Cordoş cu titlul „Reconsiderarea conceptiilor constructive în aparatura de analiză instrumentală, în urma asocierii cu mijloace de calcul".

Publicări de tratate, cărţi şi cursuri universitare

● I. Haiduc, J.J. Zuckerman, *Basic Organometallic Chemistry*, Ed. Walter de Gruyter, Berlin, New-York, 1985, 488 pag.

I. Haiduc, M. Curtui, Jovanca Haiduc, I. Silaghi-Dumitrescu, *Solvent extraction of uranium, thorium and rare earth with dialkyldithiophosphoric acids* în „Chemical Aspects of Nuclear Methods of Analysis", "Proceedings of the Final Research Co-ordination Meeting", organized by J.A.E.A, Hamamatsu, Japan, 2—5 oct. 1981, Viena, 1985, pag. 10—172.

E. Cordoş, L. Kékedy-Nagy, *Lucrări practice de analiză instrumentală*, Edit. Univ. Cluj-Napoca, 1985, pag. 133.

I. Hopârtean, *Produse de sinteză organică fină*, Edit. Univ. Cluj-Napoca, 1984, 172 pag.

Lucrări ştiinţifice apărute în reviste de specialitate din ţară şi străinătate

S. Agachi, L. Oniciu, "Optimized Operation of a Fuell Cell", *The 36-th Meeting of the International Society of Electrochemistry, Salamanca, Spain, September* 23—28, 1985 p. 291.

I. Bâldea, V. Fărcăşan, I. Olteanu, "Kinetics of the Jacobson Reaction", *Rev. Roumaine Chim.*, **30**, 385 (1985).

E. Chifu, J. Zsakó, M. Tomoaia-Cotişel, A. Mocanu, M. Sălăjan, J. Demeter-Vodnár, J. Albu, „Filme interfaciale de interes biologic", *A III-a Conferinţă Naţională de Biofizică*, U.S.S.M., Iaşi, 1985, pp. 16—23.

C. Anghel, V. C. Anghel, L. Kékedy-Nagy, „Procesul de purificare a saramurii de clorură de magneziu (Consideraţii)", *Rev. Chim. (Bucureşti)*, **36**, (3), 326 (1985).

L. Literat, „Studii de microscopie electronică asupra unor refractare cu rol de suporturi catalitice", *Materiale de Construcţii (Bucureşti)*, **15**, (2), 87 (1985).

S. Mager, „Formulele de proiecţie Fischer şi semnificaţia lor în chimia organică", *Rev. fiz. chim.*, **22**, (5), 197 (1985).

S. Mager, „Selectivitatea şi specificitatea în reacţiile compuşilor organici", *Rev. fiz. chim.*, **22** (9), 389 (1985).

F. Makkay, E. Herman, „Folosirea mijloacelor audio-vizuale la lecţiile de chimie", *Rev. fiz. chim.*, **22** (1), 26 (1985).

R. Vătulescu, T. Budiu, „Gh. Marcu, J. Pal, „Heteropolytungstates with Ti(IV) and Ni(II)", Part III—V., III. "The absorption spectra of the heteropolyanions Ni(II) undecatungsto-

titanate (IV) and Ni(II) pentatungstotitanate (IV)", Part. IV. "The thermal behaviour of the potassium salt of the Ni(II) undecatungstotitanate (IV) anion", Part V. "The thermal behaviour of sodium and potassium salt of the Ni(II)-pentatungstotitanate (IV) anion"., *Rev. Roumaine Chim.*, **30**, 823 (1985); *ibid.*, **30**, 831 (1985); *ibid.* **30**, 1025 (1985).

Cs. Muzsnay, „Modele ale structurii de echilibru complex al apei lichide redate prin diferite grade de complexitate. Funcțiile termodinamice de bază ale proceselor elementare", *A III-a Conferință Națională de Biofizică*, U.S.S.M., Iași, 1985 pp. 197—203.

L. Oniciu, E. M. Rus, P. Ilea, V. Voina, D. Constantin, „Electrozi de nichel pentru acumulatoare alcaline", *Rev. Chim. (București)*, **36**, 340 (1985).

L. Oniciu, E. M. Rus, D. Constantin, V. Voina, P. Ilea, „Electrozi de cadmiu sinterizați utilizați în acumulatoare alcaline Ni—Cd", *Rev. Chim. (București)*, **36**, 836 (1985).

L. Oniciu, I. A. Silberg, F. Ciomoș, „Electrosinteza adiponitrilului I. Căi de obținere a adiponitrilului, mecanismul reacției de electrohidrodimerizare a acrilonitrilului la adiponitril", *Rev. Chim. (București)*, **34**, 406 (1985).

V. Danciu, I. A. Silberg, L. Oniciu, Metodă spectrofotometrică de determinare a gradului de reducere electrochimică a acidului p-nitrobenzoic la acid p-amino-benzoic", *Rev. Chim. (București)*, **36**, 243 (1985).

L. Oniciu, I. A. Silberg, F. Ciomoș, „Electrosinteza adiponitrilului. III. Aspecte tehnologice", *Rev. Chim. (București)*, **36**, 628 (1985).

D.A. Löwy, I. A. Silberg, L. Oniciu" ,1,1'-Oxi-bis (2,3,3, 3-tetraclorpropan)-ul, agent sinergetic pentru pesticide", *Rev. Chim. (București)*, **36** 33 (1985).

D.A. Löwy, I. A. Silberg, L. Oniciu, „Metode gazcromatografice de separare a produșilor de electroreducere a acrilonitrilului", *Rev. Chim. (București)*, **36**, 354 (1985).

D.A. Löwy, I. A. Silberg, L. Oniciu, O. H. Oprea, Modificarea chimică a polietilenei I Studiul polimerului funcționalizat prin spectrometrie IR", *Mater. Plast. (București)*, **22**, 111 (1985).

L. Oniciu, F. Ciomoș, I. A. Silberg, „Electrosinteza adiponitrilului II. Influența condițiilor experimentale asupra selectivității electrosintezei adiponitrilului", *Rev. Chim. (București)*, **36**, 503 (1985).

L. Oniciu, „Vistas in the Electrochemical Energy Conversion and Organic Electrosynthesis", în: *Lucrările celui de al 2-lea Simpozion de electrochimie aplicată, Timișoara*, 4—5 octombrie, 1985, I, p. 156.

L. Oniciu, V. Danciu, K. Mester, „Electrolytic Reduction of the Nitrobenzene to p-Aminophenol", *Ibid.*, I., p. 187.

L. Oniciu, Cs. Bolla, D.L. Boboș, G. Taralungă, P. Ilea, „Method for Preparing Non-Aqueous Electrolytes", *Ibid.*, I., p. 195.

L. Oniciu, J. A. Silberg, I. Bâldea, F. Ciomoș, D. A. Löwy, M. Jitaru, O. H. Oprea, "Contributions to the Mechanism of Acrylonitrile Electrohydrodimerization", *Ibid.*, I, p. 201.

L. Oniciu D. A. Löwy, I. A. Silberg, D. F. Anghel, F. Ciomoș, M. Jitaru, „Electroanalytical Method for Determination of Cationic Surfactants Involved in Adiponitrile Electrosynthesis", *Ibid.*, I, p. 207.

L. Oniciu, E. M. Rus, M. Schenker, D. Constantin, V. Voina, „Studium der Oxydation von Schwefelverbindungen bei der elektrochemischen Ablagerung von Antimon", *Ibid.*, I, p. 216.

L. Oniciu, Cs. Bolla, G. Țaralungă, L. Boboș, "Preparation of Manganese dioxide Containing Cathodic Material for Lithium Batteries with Nonaqueous Electrolytes", *Ibid.*, I, p. 216.

L. Oniciu, A. Topan, L. Mureșan, D. Ghertoiu, A. Pântea, "Effect of Addition on the Quality of the Cathode Deposit in the Electrolytic Refining of Lead", *Ibid.*, p. 231.

L. Oniciu, I. A. Silberg, I. Bâldea, F. Ciomoș, M. Jitaru, D. A. Löwy, O. H. Oprea, L. Radu, "Kinetics of Competing Reactions in the Electroreduction of Acrylonitrile to Adiponitrile and Propionitrile", in "*The 36-th Meeting of the International Society of Electrochemistry*", Salamanca, Spain, September 23—28, 1985, p. 107.

L. Oniciu, I. A. Silberg, V. Danciu, M. Olea, S. Bran, "Kinetics and Mechanism of p,p'Diaminodihenzyl Electrosynthesis", *Ibid.*, p. 182.

I. Silaghi-Dumitrescu, I. Haiduc, "The Electronic Structure and Bonding in the Thiophosphonyl Cation PS^+", *Phosphorus and Sulfur*, **22**, 85 (1985).

J. F. Nixon, P. B. Hitchcok, *I.* Silaghi-Dumitrescu, I. Haiduc, "The Crystal and Molecular Structure of a Versatile Bidentate Ligand: tetraphenyldithiodiimidodiphosphinate, $Ph_2(S)P—NH—P(S)Ph_2$", *Inorg. Chim. Acta*, **96**, 77 (1985).

M. Tomoaia-Cotișel, J. Zsakó, E. Chifu, P. J. Quinn, "Mixed Monolayers of 1,2-Distearoyl Digalactosyl Glycerol and Astaxanthin", *Structure, Function and Metabolism of Plant Lipids*, Elsevier Science Publishers, B. V. pp 421—424 (1984).

M. Tomoaia – Cotişel, E. Chifu, J. Zsakó, "Mixed Monolayers of Egg Lecithin and Carotenoids", *Colloids and Surfaces*, **14**, 239 (1985).

M. Tomoaia – Cotişel, E. Chifu, J. Zsakó, "The Structure of Some Lecithin Monolayers at the Air/Water Interface", *Water and Ions in Biological Systems*, A. Pullman, V. Vasilescu and L. Packer, eds., Plenum Press, New York and London, pp. 243–250 (1985).

I. Gănescu, Cs. Várhelyi, G. Brînzan, "Bestimmung des 1,4-Dihydrazinophtalazins mit Reineckesalzanaloga", *Archiv Pharm.* (Weinheim). **318**, 30 (1985).

I. Gănescu, N. Calu, G. Brînzan, Cs. Várhelyi, "New Substitution products of $K_3[Cr(NCS)_6]$ with Chinaldine", *Rev. Roumaine Chim.*, **30**, 309 (1985).

Cs. Várhelyi, F. Mánok, J. Horák, E. Grünwald, "On the Dioximine Complexes of Transition Metals, LXXI. Quantitative Determination of Nickel with 1,2-Cyclo-Octanedione Dioxime", *Chem. Analit.* (Warsaw), **30**, (11) 11 (1985).

Cs. Várhelyi, J. Zsakó, G. Liptay, M. Somay "On the Dioximine Complexes of Transition Metals, LXVII. New Sulfito-Bis-Dimethylglyoximino-cobalt (III) – Complexes and Their Thermal Decomposition", *Rev. Roumaine Chim.*, **30**, 695 (1985).

J. Zsakó, M. Tomoaia-Cotişel, I. Stan, V. Coman, V. Tămaş, E. Chifu, „Colapsul unor straturi de carotenoide la interfaţa aer/apă". *A III-a Conferinţă Naţională de Biofizică*, U.S.S.M., Iaşi, pp. 63–68 (1985).

J. Zsakó, Cs. Várhelyi, B. Csegedi, E. Kékedy, "Kinetic Analysis of Thermogravimetric Data, XXIII. Thermal Decomposition of Some $[Co(py)_4(NCS)_2]$ Type Complexes", *Thermochim. Acta*, **83**, 181 (1985).

J. Zsakó, "Influence of the Subphase Liquid Activity on the Equilibrium Collapse Curves of Insoluble Mixed Monolayers", *J. Colloid Interface Sci*, **106**, 51 (1985).

J. Zsakó, "Kinetic Analysis of Thermogravimetric Data", *Thermal Analysis*, Ed. by Z.D. Zivkovic, Collection of Papers, Bor, Yugoslavia, pp. 167–237 (1984).

Brevete

L. Kékedy, E. Jakab, F. Kormos, Electrod de referinţă, *Brevet R.S.R.* nr. 81 981 din 12 ian. 1983.

I. Pop, C. Naşcu, A. Palmariuc. M. Ionescu, Gh. Marcu, M. Pop, Puşcaş, Procedeu de metalizare chimică a copolimerului A.B.S., *Brevet R.S.R.* nr. 87 605 din 26 martie 1985.

S. Mager, F. Jugrestean, I. Cristea, E. Vargha, Procedeu de preparare a acidului malonic, *Brevet R.S.R.* nr. 86 542 din 16 ian. 1985.

S. Mager, F. Jugrestan, R. Tăranu, I. Hopîrtean, Procedeu de obţinere a fenilmalonatului de dietil, *Brevet R.S.R.* nr. 87 987 din 10 aprilie 1985.

M. Diudea, S. Fodor, V. Fărcăşan, D. Breazu, S. Mager, Procedeu de obţinere a tioglicolatului de amoniu, *Brevet R.S.R.* nr. 88 237 din 1985

I. Cristea, V. Fărcăşan, I. Panea, Procedeu pentru obţinerea 1–(4-hidroxi-6-metil-2-pirimidinil)-3-metil-pirazolonei, *Brevet R.S.R.* nr. 89 139 din 30 octombrie 1985.

L. Oniciu, O. H. Oprea, D. A. Löwy, I. A. Silberg, Procedeu de obţinere a unor membrane schimbătoare de ioni, *Brevet R.S.R.* nr. 87 994 din 25 aprilie 1985.

L. Oniciu, D. A. Löwy, O. H. Oprea, J. A. Silberg, A. Horváth, *Brevet R.S.R.* nr. 88 088 din 25 aprilie 1985.

L. Oniciu, I. A. Silberg, F. Ciomoş, M. Jitaru, P. Popescu, D. A. Löwy O. H. Oprea, Procedeu de preparare a adiponitrilului, *Brevet R.S.R.* nr. 88 417 din 15 mai 1985.

Premii

Prin Ordinul M.E.I. nr. 5641 din 15 iunie 1985 s-a acordat titlul de *Profesor universitar evidenţiat* profesorului Gheorghe Marcu

Susţineri de teze de doctorat

Muntean Mihail, *Îmbunătăţirea proceselor de fabricare a sodei* (caustice) *calcinate amoniacale*, conducător ştiinţific prof. dr. Marcu Gheroghe (12 februarie 1985).

Kulcsár Géza-Iosif, *Studiul adsorpției unor complecși pe electrod de mercur*, conducător științific prof. dr. Kékedy Ladislau (22 martie 1985).

Albu Iosif, *Tensiunea interfacială în procese de extracție lichid-lichid*, conducător științific prof. dr. Emil Chifu (5 iunie 1985).

Mirică Nicolae, *Intensificarea proceselor de electrod prin deplasarea relativă electrod-electrolit la oxidarea electrochimică a manganatului de potasiu la permanganat de potasiu*, conducător științific prof. dr. doc. șt. Liviu Oniciu (5 iulie 1985).

Smarandache Victoria, *Contribuții la sinteza merelilului și a unor fenotiazine cu posibilă acțiune antivirotică*, conducător științific prof. dr. Valer Fărcășan (2 decembrei 1985).

Lingner Harald, *Studiul formării precipitatelor ($CaSO_4$, $SrSO_4$, $BaSO_4$). Influența forței ionice și a solventului.*, conducător științific prof. dr. doc. șt. Candin Liteanu (17 decembrie 1985).

Hobai Ștefan-Virgil, *Studiu statistic asupra selectivității informaționale a sistemelor analitice pe bază de MLB în funcție de unii parametri fizico-chimici*, conducător științific prof. dr. doc. șt. Candin Liteanu (21 decembreie 1985).

RECENZII

Colin A. Vincent et al. **Modern Batteries. An Introduction to Electrochemical Power Sources,** Edward Arnold, 1984, 264 pp.

"Modern Batteries" is the fruit of co-operation between Scottish and Italian scientists, which started about 20 years ago in the laboratories of H.A. Laitinen (University of Illinois) where, at that time, B. Scrosati and C.A. Vincent worked together. A few years later, within the frames of a joint research project with Consiglio Nazionale delle Ricerche (Center on Electrode Processes at Milan) they were joined by F. Bonino and M. Lazzari. This program was sponsored by English (Engineering Research Council and British Council) and Italian (Consiglio Nazionale delle Ricerche) scientific bodies.

The work consists of 8 sections, an appendix, a glossary and an alphabetical index. The presentation of the topics covered, with a terse historical restrospective and consideratıcns regarding the different sorts of electrochemical power sources and their applications form the object of section 1, followed by a presentation of the theoretical bases (electrical double layer, potential, thermodynamics of the galvanic sources, kinetic aspects and performances) dealt with in section 2.

Sections 3 and 4 are devoted to the conventional systems (primary and secondary) and section 5 presents unconventional primary and secondary batteries, with lithium anodes and various cathodic depolarizing agents. The hot batteries in different alternatives are treated in section 6, whereas the 7-th section describes the batteries having the essential components (electrodes and electrolytes) in solid state. The 8-th section is reserved for hybrid electrochemical power sources (metal-air, metal-halogen and metal-hydrogen).

The appendix contains recommendations for optimal use and recharge of the batteries and a table with values of electrical parameters and conversion factors. A useful and relatively complete glossary of usual terms in electrochemical conversion of energy, and a functional index complete the book.

A special mention for the large number of figures (199) which illustrate very suggestively the various sections of this book, written in a pleasant, fluent style, at a level accessible for the reader possessing a medium level of knowledge in chemistry and physics. A special attention was paid to an attractive and diversified presentaţion of the aspects connected with the galvanic sources technology, and of their multiple validations, from the microconsumer to the macroconsumer, from the cardiac pacemaker to the peak-levelling storage station for thermoelectrical power plants, from the conventional, aqueous systems, characterized by a secular tradition (only apparently, because vestiges of electrochemical energy conversion are known ever since the time of the Parthians populating Mesopotamia, more than two thousand years ago), up to the unconventional systems, making use of non-aqueous solutions, solid electrolytes, alkali metal anodes, etc. In connection with the latter sort of systems, a point is made of the contribution of materials science and of the technological progress in general, the absence of which would have made inconceivable their evolution and development.

The essential features of this book lie in the high density of scientific and technological information, in the pertinent commentaries accompanying the presentation of various electrochemical power sources and their technological alternatives, in stressing their destination/destinations and in the critical evaluation of the variants and models manufactured on a large or small scale.

The general impression is positive, and the book can be used, with much profit, by specialists in electrochemical energy conversion, by researchers and students, thanks to the modern information and the lucid evaluations regarding the described power sorces.

L. ONICIU

Surfactants, edited by Th. F. Tadros, Academic Press, London, New York, 1984.

The book is the result of the residential school perfectioning courses on surfactants, sponsored by the Royal Society of Chemistry of Great Britain, held at Bristol University between July 18—22, 1983. The scientific content of the course was devised by the Editor.

The interest in such scientific meetings lies in that surfactants — surface-active substances — are widely used in all fields of the chemical industry, such as: detergents, paints and dyestuffs, plastics, pesticides, cosmetics, pharmaceuticals etc. It is to also be

mentioned that surfactants hold a primary rôle in oil industry, or, sometimes they are employed for environmental protection. Too, they are essential in the processes of yielding foams and emulsions, of wetting and adhesion, detergency and lubrication, of mass transfer and liquid evaporation control, in detecting traces of film-forming substances.

The material included in the book was carefully chosen and it covers a wide range of surfactant applications, providing valuable information (arranged in thirteen chapters) for the specialists dealing with surfactants and their applications.

The first four chapters constitute, perhaps, the fundamental basis of the physical chemistry of surface-active substances and supplies the reader with ample references for more detailed information on the various topics. The book starts with an introductory chapter by R.H. Ottewill which gives a brief account of the various classes of surface-active reagents and their solution properties. This is followed with a chapter by A. Couper on the fundamental aspects of surfactant solutions, with particular attention to the thermodynamics of micellization and adsorption in interfaces. Chapter 3, by R.G. Laughlin, dwells upon phase equilibria and mesophases in surfactant systems. The structural aspects of micellar systems are dealt with in Chapter 4, worked out by B. Lindman; special attention is paid to the dynamic features of surfactant micelles using self-diffusion studies.

Chapters 5 to 9 deal with some basic principles involved in the application of surface-active reagents in disperse systems. Chapter 5, by J. T. Overbeek, P. L. de Bruyn and F. Verhoeckx, lays the foundation for the fundamentals of microemulsion formation and stability, some recent thermodynamic theories being briefly reviewed. Chapter 6, by J. W. Goodwin, deals with the structure and rheologic characteristics of the surfactant concentrated systems. Chapter 7, by R. Aveyard, deals with the subject of adsorption of surfactants at the air/liquid, liquid/liquid, and solid/liquid interfaces, which is the clue in understanding how surfactants function as stabilizers for emulsions, foams and suspensions. Chapter 8, by B. Vincent, deals with the rôle of surfactants in the formation and stability of emulsions and foams. Chapter 9, worked out by the Editor, gives an account of the rôle of surfactants in suspension preparation and in the control of their physical stability. A brief account is then given of the influence of surfactants on the flow behaviour of suspensions.

In Chapter 10 T. D. Blake gives an account on the rôle of surfactants in wetting phenomena, in the spreading of liquids on solid surfaces etc.

The last three chapters of the book illustrate some of the applications of surfactants in complex industrial processes and biological systems. Thus, Chapter 11, by E. L. Neustadter, highlights the rôle played by surfactants in enhanced oil recovery. Chapter 12, by R. I. Hancock, gives a comprehensive review of the various types of non-ionic surfactants, particular attention lying with macromolecular surfactants. In fine, chapter 13, by the Editor, gives some examples of the application of surfactants to biological systems, pointing to the rôle of surfactants in micellar solubilization, in liposome systems, in application of pesticides and herbicides by spraying etc.

Due to the wide application of surfactants in various fields of the science and technology, it is essential that the physical chemistry of such substances is adequately and thoroughly understood, respectively their uncommon properties and their phase behaviour. Also, the proper understanding of the basic phenomena involved in the use of surfactants for preparation of emulsions and suspensions, in foams and microemulsions, in wetting and adhesion processes etc., is of vital importance to the end of obtaining right compositions and controlling stability of the systems involved.

All in all, the book reviews the physical chemistry of surfactants, their behaviour at interfaces and their rôle in wetting processes and dispersions. The *problematique* is completed with carefully chosen subjects designed to illustrate a wide range of the application of surfactants.

MARIA TOMOAIA-COTIȘEL

D. N. Kursanov, Z. N. Parnes, M. I. Kalinin and N. M. Loim, **Ionic Hydrogenation And Related Reactions. Soviet Scientific Reviews Supp lement Series: Chemistry**, Published by OPA Ltd. Amsterdam for Harwood Academic Publishers, 1985, 252 pp.

The first volume in the series which is entitled ,,Soviet Scientific Reviews Supplement Series: Chemistry" represents a very promising attempt to inform the international scientific community about the last news in the field of chemistry in which the soviet scientists have significant contributions. The inaugural volume of the series is devoted to a new original method for the reduction of double bonds that has received the name

„ionic hydrogenation". The authors of the monograph belong to a well known research group of the famous Nesmeyanov Institute of Organo-Element Compounds, Moscow.

It should be noted that the monograph not only considers the work of Soviet authors, but also provides complete coverage of the world literature on the problem under consideration. Most of the 472 references mentioned at the end of each of the eight chapters of the book, refer to papers published after 1970.

By comparison with all of the methods of hydrogenation previously used, that are based on the ability of the substrate to coordinate with the catalyst (catalytic hydrogenation) or the electron affinity of the substrate (hydrogenation by metals or complex hydrides) the new method, „ionic hydrogenation", is based on the ability of the substrate to add a proton. The carbenium ion, so formed, leads by the addition of a hydride ion to the hydrogenation product. Because the substrate is attacked in the first step by an electrophilic reagent, a proton, this method may be called „Electrophilic ionic hydrogenation".

In the field of the reactions applied to compounds with multiple carbon-carbon bonds (alkenes, alkynes, aromatic hydrocarbons, cap. 1), C=O bonds (aldehydes, ketones, quinones, acids, cap. 4), carbon-nitrogen bonds (azomethines, oximes, nitriles, cap. 5) or nitro and azoderivatives (cap. 5), a different kind of selectivity, by comparison with the one known in the case of other hydrogenation methods, was observed. The selectivity of the reaction is not changed if the hydride-ion donor is replaced by two reagents, one of which furnishes electrons (a metal, such as zinc) while the second is an acid, acting as a proton donor. The ionic hydrogenation is able to achieve the selective hydrogenation of internal olefinic double bonds with three substituents, without involving mono and disubstituted olefins. Excellent results have also been obtained in the synthesis of steroids. In the field of heterocyclic compounds the method offers great advantages, mostly in the case of the reduction of thiophenes to tetrahydrothiophenes. The reaction occurs without the danger of the formation of side products which accompanies the usual catalytic reaction. The chapter devoted to heterocyclic compounds deals also, with benzothiophens, furans, indoles.

In most of the cases, the ionic hydrogenation takes place in the presence of the trifluoroacetic acid as proton donor and of the trietylsilane which represents the donor of the hydride ion.

Beyond the selectivity advantage, the ionic hydrogenation proceeds at moderate temperature (usually 20—50°) and at a low acidity of the mediu, which prevents the disadvantage of secondary reactions (isomerisations, polymerisation). Besides, the reaction produces high yields.

The investigation of the reaction mechanism constitutes the subject of the third chapter where the kinetic aspects of the reaction are presented. The role of the intermediate carbenium ion, of the proton supplier and of the hydride ion donor are also discussed. The same chapter deals also with some important aspects of the utilisation of some compounds labeled with deuterium, respectively in the investigation of the reaction mechanism.

Chapter 6 of the monographs presents the problem of the mobility of the hydrogen bonded to different elements (halogens, metals, silicon, carbon in different organic compounds), as hydride ion.

Chapter 7 deals with catalytic ionic hydrogenation of alkenes, cycloalkenes and of compounds with C=O and C=N bonds.

The last chapter of the monograph (cap. 8) takes into consideration the transfer of alkyl groups from tetraalkylsilanes to the carbenium ion, in the conditions of the ionic hydrogenation. Of great utility is also the appendix of the book, which presents significant examples of preparative syntheses (including those of practical importance) based on the ionic hydrogenation reaction.

A special mention deserves the excellent graphic presentation of the book.

Taking into account all the aspects of the monographs, one can certainly maintain his value and his scrientific interest for a large number of scientists working in the field of organic chemistry.

SORIN MAGER

Chromatography '84. *Proceedings of the Advances in Liquid Chromatography*, Szeged, Hungary, September 10—14, 1984. Symposia Biologica Hungarica 31, Edited by H. Kalász and L. S. Ettre, Akadémiai Kiadó, Budapest, 1986.

The volume includes about 54 scientific papers divided into five chapters: General topics, Stationary phases for chromatography and their interaction, Drugs, metabolites, biologicaly active compounds, Separation of amino acids, polypeptides and nucleotides and Separation of substances of various classes.

The first part „General topics in chromatography" includes 7 papers, for example: „Description of chromatographic analysis by

means of the teoretical model" by Veress et al. In this paper a mathematical model for the chromatographic separation process is reported.

In the second part ,,Stationary phase for chromatography and their interaction" 12 papers are included. Some of the papers treat problems concerning: ,,The synthesis and performance of a chemically bonded sulfur heterocyclic stationary phase for HPLC" by Colmsjö et al.; ,,Cyclodextrin polymers as stationary phases in LC" by Szilasi et al.; ,,The preparation of RP silica" by Welsch et al. Another series of papers treats problems concerning the properties of the stationary phases, for example: steric effects of substituents in normal-phase, temperature dependence of the retention time and resolution, the comparison of the properties of C_{18} films bonding, and others.

The final part of the volume includes 35 papers with interesting aplications in HPLC as: drugs, metabolites, biologically active compounds, endogenous substances, amino acids, polypeptides, nucleotides and separation of substances of various classes.

The high level scientific content as well as the special graphical presentation of the volume are due to authors and to editors, as well as to the high reputation of the publishing house.

The paper included in this volume are extremely important from a theoretical and practical point of view for analytical chemists as well as for biochimists.

S. GOCAN

KÉKEDY LÁSZLÓ, **Térfogatos analitikai kémia (Titrimetria)** (Volumetric analytical Chemistry (Titrimetry), Dacia Publ., Cluj-Napoca, 1986.

Professor Kékedy exposes in eight chapters the main problems of the classical titrimetric analysis: basic concepts and classification of the analytical procedures, preparation of the measuring solutions, titration curves, etc. An important part of the book deals with the determination of the equivalence point by visual and instrumental methods (potentiometric, conductometric, amperometric, thermometric, fotometric, etc.). The various titrations as the acide-base, redox, chelatometric and other titrimetric methods based on complex formation and precipitation are presented and discussed critically in a modern point of view.

A separated chapter (No. 9.) is devoted to processing of the experimental data using modern statistical methods.

On the basis of the theoretical considerations the book helps the reader to orientate in resolving various analytical problems. The laboratory exercises chosen reflect the main characteristics of the procedures described and are useful for different practical purposes. The comprehensive bibliography from the last 2—3 decades ensures the reader an easy and fast orientation in different titrimetric problems.

The material is treated in a light, concise style easy to understand for students of various faculties (chemistry, biology, pharmacy, agronomy, chemical engineering, etc.), chemists and researchers in many fields of the natural sciences.

F. MÁNOK and CS. VÁRHELYI

Catalytic Materials, Relationship between Structure and Reactivity, Edited by Thadeus E. Whyte, Jr., Ralph A. Dalla Betta. Eric G. Derouane and R. T. K. Baker, American Chemical Society Symposium Series no. 248, 1985, 451 pp.

The American Chemical Society (ACS) initiative o fover a decade ago (1974) to create a rapid information access route to the scientific novelties and achievements, debated at the specialized symposia, found its embodiment in the ACS Symposium Series. The 248-th volume of this series comprises a well-outlined, topics-oriented selection of the papers presented at the ACS Symposium on Catalysts held the 13—16 th June 1983, under the sponsorship of the Chemical Engineering and Industrial Chemistry Section in San Francisco, California (USA).

It is well-known that the spectacular progresses in the field of catalysis during the last years are mostly due to the unparalleled development of investigation methods of great precision, which gave access to the finest details of the investigated objects, thus yielding very many new insights into the catalysts structure and texture, and into the cathalytic act itself, as a part of the evolution of various systems.

A first-rate contribution in this direction stems from the spectroscopic methods and techniques, and from the electron microscopy. It is in this area of top interest that originates very much of the recent theoretical, experimental, and methodological information contained in the 451 pages of this book.

The volume is divided into 23 chapters grouped in three thematic sections: spectroscopy, zeolites characterization, and microscopy and other new methods.

A number of eight reports are grouped in the first section, dealing with new information on heterogeneous catalysis, obtained *via* spectroscopic techniques. The discussion covers such topics as the thermal decomposition of iron pentacarbonyl on titanium dioxide in the formation of Fe/TiO_2 catalysts; the interaction ethylene-Ru (001) investigated by secondary ion mass spectrometry (SIMS); the X-ray photoelectron spectroscopy (XPS) of Co catalysts; the modification of surface reactivity by structured deposition of metal films; fine structure of X-ray absorption lines; the Mössbauer effect and the reactivity of hydrothermally treated and heteropolyacid promoted catalysts; applications of high resolution ^{13}C NMR and magic-angle spinning (NMR) (MASNMR); the part played by oxygen ions in the partial oxidation of hydrocarbons, as reflected by activity measurements and electron paramagnetic resonance (erroneously designated in the chapter title as „proton electron resonance").

The second section, devoted to the studies oriented towards the structure characterization and catalytic activity of zeolites consists of 6 reports with distinct view-points and methods in explaining the catalytic activity of this type of compounds. A presentation is given of the prospectives and impact of quanto-mechanical calculations in describing and characterizing the zeolites; preparation and characterization of aluminium-deficient zeolites; the distribution of aluminium in zeolites and the factors affecting the synthesis of pentasilzeolites. Two of these studies are based on the combined physical techniques of characterizing the acidity and basicity of zeolites and the structure-selectivity relationship in the case of the xylene isomerization and toluene selective disproportionation.

The last section (microscopy and other new methods) comprises 9 report from the field of quantitative electron microscopy and of other new non-conventional methods applied to the study of catalysts and of heterogeneous catalytical systems.

A first group among these studies deal with the performances of conventional transmission-, (TEM), and scanning electron microscopy, in the characterization of catalysts. The selected topics include the analytical electron microscopy of catalyst particles, single-particle diffraction, and topographic imaging of small metallic particles on catalyst supports, the use of scanning electron microscopy in investigating the surface and the small particles, as well as the probing of surface details by heavy atom method.

From the category of other new investigation methods, papers are presented, concerning the possibilities of nuclear magnetic resonance (NMR), photoacoustic spectroscopy, photothermal IR- and tunneling spectroscopy. All describe new techniques implemented in the study of catalyst surfaces. The section is concluded by a study on the correlation between reactivity and the size of the supported palladium particles.

An index of authors and subjects concludes the book.

The lecture of this book results in a thorough information on the actual problems of heterogeneous catalysis, as seen through the prospective of the modern, sophisticated investigation methods.

The book is of certain utility for researchers in the field of heterogeneous catalysis, as a guide in testing and characterizing industrial catalysts, for laboratory studies devoted to the improving of performances or creating new catalysts, and for the characterization of various catalytic systems. It also is of interest for research apparatus designers and for the fundamental research. The ample bibliographic quotations represent a precious source of information for further documentation on catalysis for researchers, teachers and students in physics, chemistry and chemical engineering.

LIVIU LITERAT

Municipiul Cluj-Napoca, Cd. nr. ÎNTREPRINDEREA POLIGRAFICĂ CLUJ, 446/1986

Revista ştiinţifică a Universităţii din Cluj-Napoca, **STUDIA UNIVERSITATIS BABEŞ-BOLYAI,** apare începînd cu anul 1986 în următoarele condiţii:

matematică — trimestrial

fizică — semestrial

chimie — semestrial

geologie-geografie — semestrial pentru geologie şi anual pentru geografie

biologie — semestrial

filozofie — semestrial

ştiinţe economice — semestrial

ştiinţe juridice — semestrial

istorie — semestrial

filologie — semestrial

STUDIA UNIVERSITATIS BABEŞ-BOLYAI, the scientific journal of the University of Cluj-Napoca, starting with 1986 is issued as follows:

mathematics: quaterly

physics: biannually

chemistry: biannually

geology-geography: biannualy on geology and yearly on geography

biology: biannually

philosophy: biannually

economic sciences: biannually

juridical sciences: biannually

history: biannually

philology: biannually

Abonamentele se fac la oficiile poștale, prin factorii poștali și prin difuzorii de presă, iar pentru străinătate prin „ROMPRESFILATELIA", sectorul export-import presă, P. O. Box 12—201, telex. 10376 prsfir, București, Calea Griviței nr. 64—66.

Lei 35